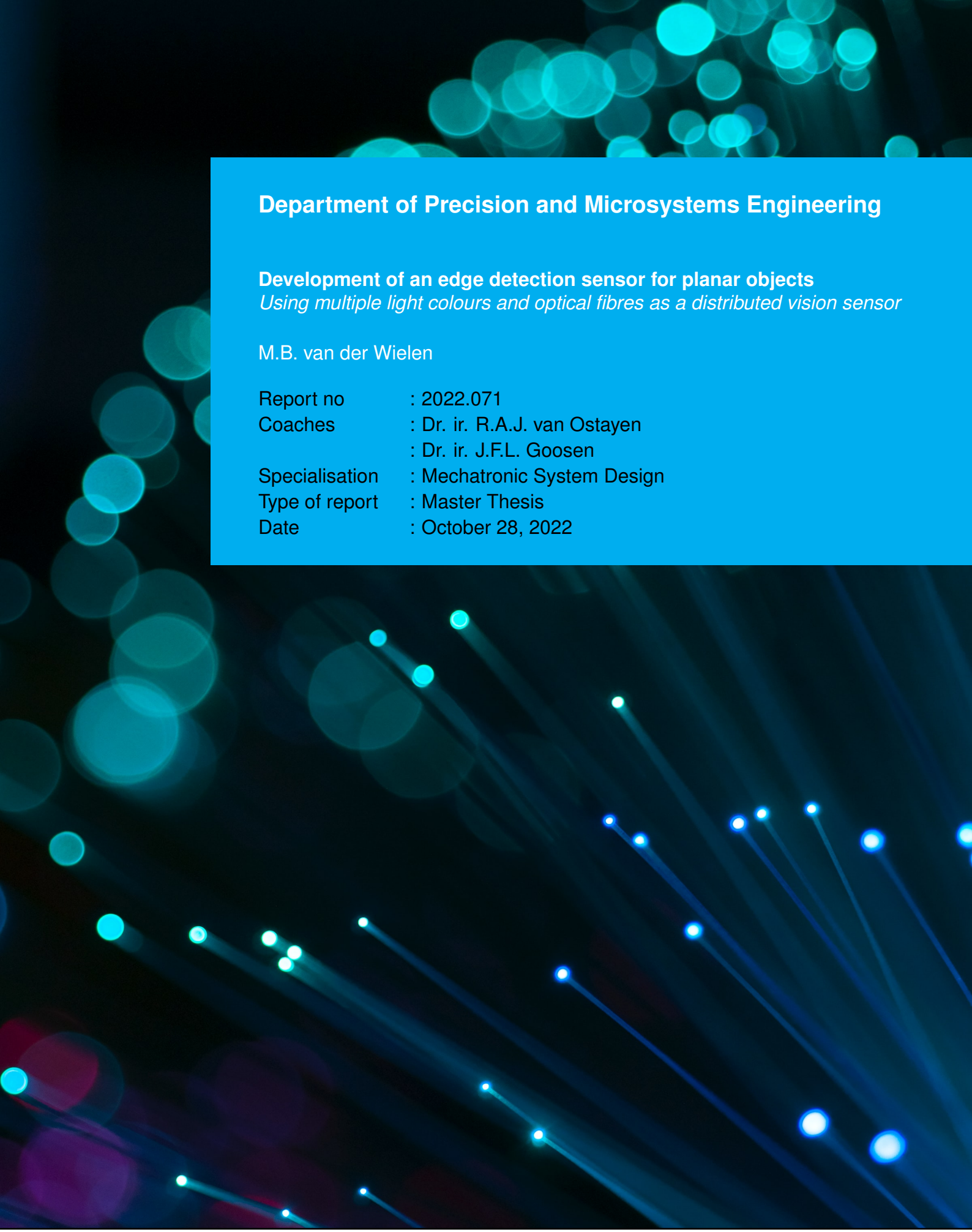

Department of Precision and Microsystems Engineering

Development of an edge detection sensor for planar objects

Using multiple light colours and optical fibres as a distributed vision sensor

M.B. van der Wielen

Report no	: 2022.071
Coaches	: Dr. ir. R.A.J. van Ostayen
	: Dr. ir. J.F.L. Goosen
Specialisation	: Mechatronic System Design
Type of report	: Master Thesis
Date	: October 28, 2022

TU Delft Delft University of Technology

Challenge the future

Development of an edge detection sensor for planar objects

Using multiple light colours and optical fibres as a distributed vision sensor

by

M.B. van der Wielen

to obtain the degree of Master of Science

at the Delft University of Technology,

to be defended publicly on Wednesday, November 9, 2022 at 13:00 CET.

Student number:	4478088	
Project duration:	June 15, 2021 – November 9, 2022	
Thesis committee:	Dr. ir. R. A. J. van Ostayen,	TU Delft, supervisor
	Dr. ir. J. F. L. Goosen,	TU Delft, supervisor
	Dr. G. J. Verbiest,	TU Delft

An electronic version of this thesis is available at `http://repository.tudelft.nl/`.

TU Delft

Abstract

The use of optical fibres as distributed vision sensor within a contactless handling system is discussed in this research. Different light colours are used to see if this can detect an object's edge position and orientation in a better way than using one light colour. A volume diffuser is implemented to expand the vision of the optical fibres. The described system in this research can be used in the photovoltaic industry where there is a desire in reducing the thickness of wafers to reduce production costs and even higher the efficiency of solar cells. The thickness of wafers is in the order of micrometres. The problem is that this thickness is limited because the breakage rate will increase if the thickness will be reduced. A system is designed to solve this issue. A contactless handling system ensures that the wafers will not make any contact with the system. This research looked at a contactless handling system that uses hexagonal air bearings as an actuator. The stresses within the transported objects will change. The stresses built up due to contact are eliminated, but the pressure differences on the object will cause some bending stresses. The question is to what extent these stresses are important.

The optical fibres are separated into two groups, transmitting- and receiving fibres. The fibres are placed alternately on the corner edges of the hexagonal air bearings. One building block is used in this research that consists of one receiving fibre surrounded by three transmitting fibres, with each emitting one primary light colour. If the transported object is positioned above a transmitting fibre, the light coming out of the fibre will reflect against the object. The receiving fibre will receive the reflected light. A camera will look at the end of the receiving fibre. If light is obtained out of the receiving fibre, the object is positioned somewhere above this fibre. If no light is obtained out of the receiving fibre, the object is not around the fibre. The volume diffuser causes that different light intensities can be measured out of the receiving fibre. The different intensities can be coupled to specific object positions. The experiments executed in this research have shown how the light obtained in the receiving fibre can be used for calculating object position and orientation.

Four experiments are executed in this research. The findings of each experiment are shown below, together with the figures of the most important results.

1. Experiment 1
   The first experiment showed a valid way to calculate the centre pixel coordinates of the three transmitting fibres and the receiving fibre in the centre. The pixel coordinates of the receiving fibre are used in the other experiments for measuring the RGB value. A coordinate system is introduced that will be used in the remainder of this research. This coordinate system can be seen in Figure 1.

2. Experiment 2
   The second experiment tested different kinds of diffusers. The Setacryl M2002 opal diffuser was chosen because of its high diffusivity and minimal blooming at higher light intensities. What can be concluded from the second experiment is that, for example, the red transmitting fibre not only emits red light but also green and blue light. So, if an object is floating above one transmitting fibre, all three primary light colours can be achieved in the receiving fibre.

3. Experiment 3
   The third experiment tested the influence of object displacements on the RGB value without light reflection. Two diffuser layers with a piece of material between them imitated the end concept. A decrease in RGB value was found after being constant for a certain distance. The RGB value dropped rapidly for the 0-degree object orientation from the line $y = -8$ and for the 90-degree object orientation from the line $x = -10$. The results of the displacements and the change in RGB value received by the receiving fibre can be seen in Figure 2.

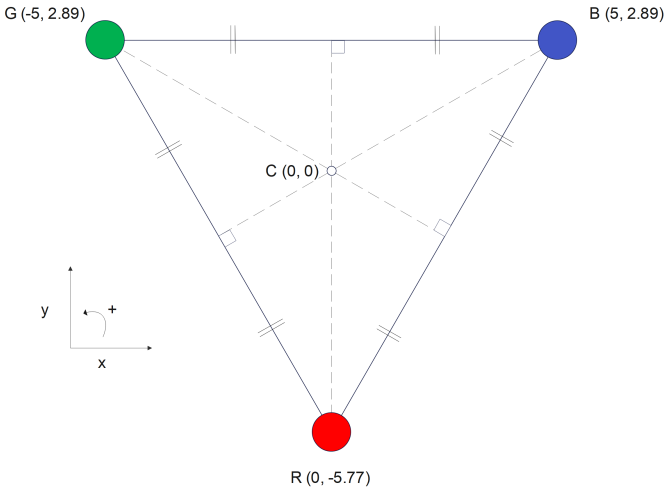

Figure 1: The used coordinate system in this research with the three transmitting fibres indicated with R, G and B. The origin, indicated with C, is the centre where the receiving fibre is located.

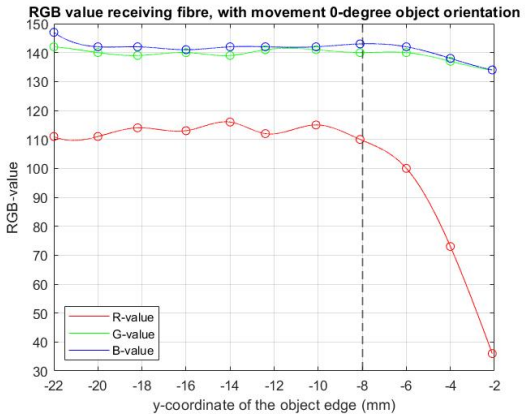

(a) Change in RGB value for a movement of 0-degree object orientation.

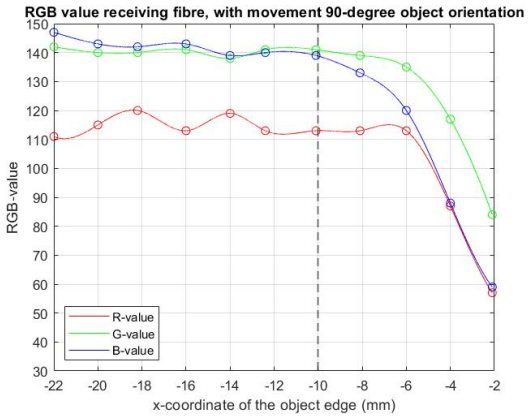

(b) Change in RGB value for a movement of 90-degree object orientation.

Figure 2: Change in RGB value for a movement of a 0-degree and a 90-degree object orientation without light reflection.

4. Experiment 4
   The fourth and last experiment investigated the final concept, where reflection was included. Results similar to those of experiment three were expected because of the design of the experiment, however, there was a clear difference. This was due to a large amount of backscattering that occurred within the volume diffuser. Another diffuser also showed a lot of backscattering. The Setacryl diffuser was chosen to continue with because the amount of backscattering did not differ a lot and the light from the Setacryl diffuser got more evenly diffused. A range was found where the RGB value changed. This range lies between the lines $y = -2$ and $y = 4$ for the 0-degree object orientation, and lies between the lines $x = -8$ and $x = 2$ for the 90-degree object orientation. The movements for this experiment are the opposite in comparison with experiment three. In Figure 3 and Figure 4 the transition area can be seen.

The experiments showed some results, but the results were not very logical. This was because a lot of disruptions were found in the LEDs. The red LED, for example, gave a lot of green and blue light. It was hard to distinguish different object orientations because some orientations could result in the same RGB value received in the receiving fibre.

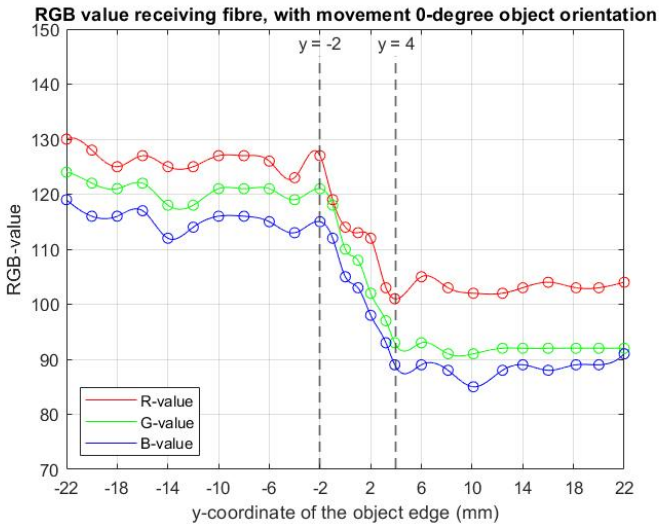

Figure 3: Graph of the RGB value course when a piece of material is travelling over the diffuser layer with a 0-degree angle.

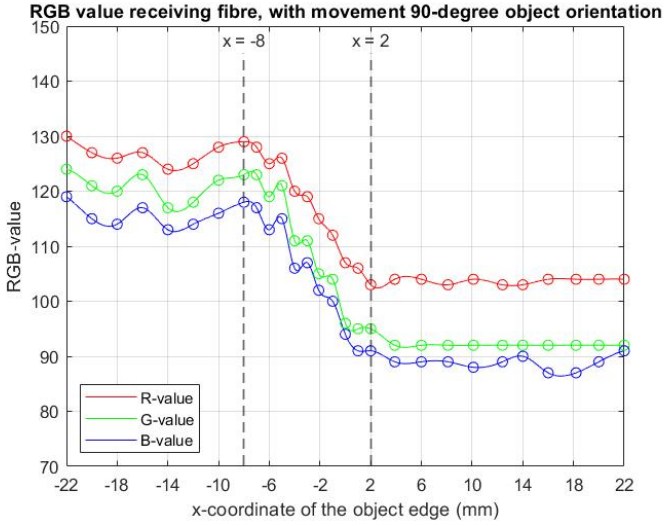

Figure 4: Graph of the RGB value course when a piece of material is travelling over the diffuser layer with a 90-degree angle.

Chapter 7 and chapter 8 did not give the results that were expected. That is why chapter 9 discussed and tested a model when the LEDs only emit one pure light colour. The influence of the red LED was investigated by sealing the other two light sources. The green and blue disruptions in the red light intensity graph were set to zero. The red light intensity graphs for horizontal and vertical movements were made. It was observed that for vertical movements, the transition range lies between the lines $y = -7$ and $y = 2$. For horizontal movements, the transition range lies between the lines $x = -4$ and $x = 4$. The red transition area for all four movements can be seen in Figure 5a. The green and blue LED light intensity course is set to be the same as the red LED light intensity course. The transition ranges of the green and blue LED can be seen in Figure 5b and Figure 5c. The green and blue transition ranges for horizontal and vertical movements can mathematically be found through interpolation. When the three transition ranges were combined, a total measurement range was found for vertical movements between the lines $y = -7$ and $y = 5$. For horizontal movements, this lies between the lines $x = -6$ and $x = 6$. These measurement ranges were also found when translated to the green and blue transition ranges. The six transition ranges that resulted from that are drawn in Figure 6. The overlapping area, which is indicated with the grey part, is the area where the object edge position and orientation can be measured if the object edge is crossing this area. The only thing that can be improved is to make the light intensity transition range wider. In that way, it is easier to distinguish all possible object orientations.

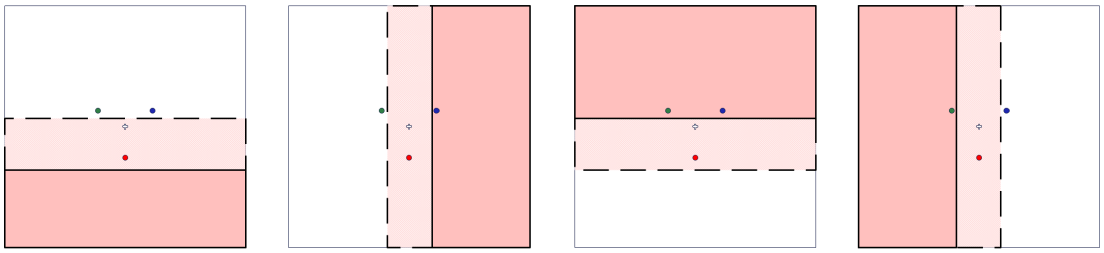

(a) The transition range for the red LED for vertical and horizontal movements relative to the red LED.

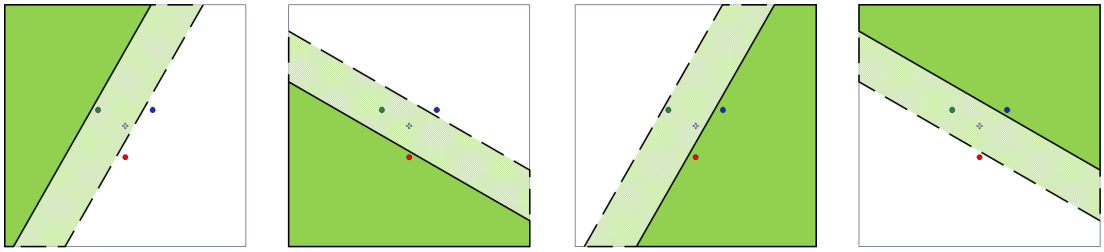

(b) The transition range for the green LED for vertical and horizontal movements relative to the green LED.

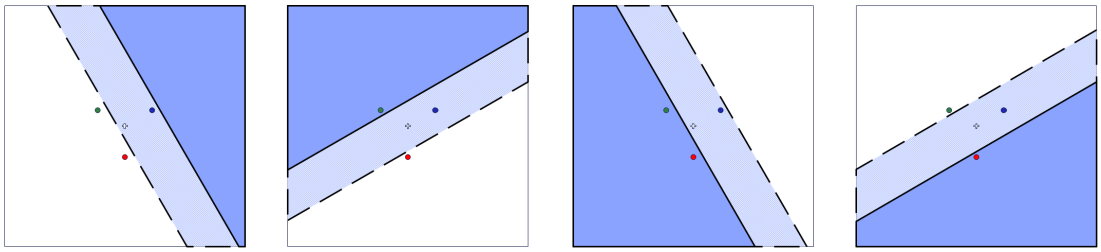

(c) The transition range for the blue LED for vertical and horizontal movements relative to the blue LED.

Figure 5: The transition ranges for all three LEDs.

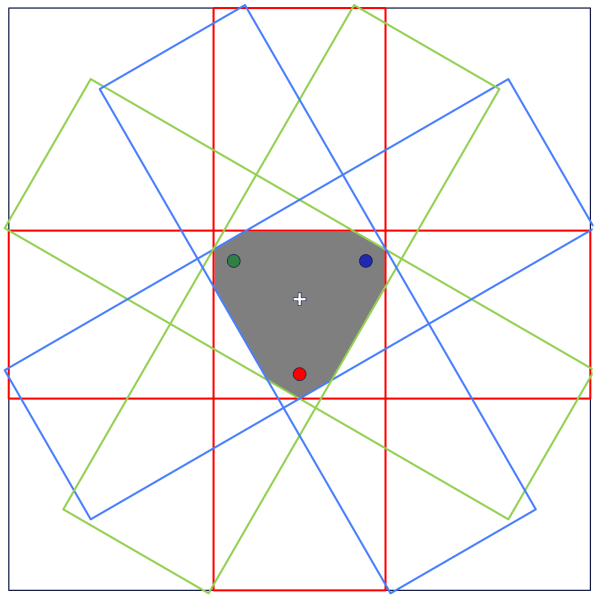

Figure 6: The area where the object edge can be measured when going through the grey part.

Contents

1 Introduction

In this chapter, an introduction is given about using multicolour optical fibres as a distributed vision sensor within a contactless handling system. The motivation for using optical fibres as a detection sensor is discussed first. This will be done by looking at the photovoltaic industry, like the semiconductor- and solar cell industry. In the state of the art, the contactless handling system is discussed together with using optical fibres as detection sensor and the working principle of the whole system with the use of multiple colours is elaborated. Next, the research objective of this thesis will be stated. This chapter will end with a thesis outline.

1.1. Motivation

The first thing that comes to mind when thinking of optical fibres is telecommunication, the electronic transmission of information or data over distances. This makes internet connection available. The fast-rising technology made it possible to reach distances of optical fibres that are going across oceans, as can be seen in Figure 1.1a. However, this is not the only application of optical fibres. Optical fibres are also used in other sectors of the industry. They are used in the medical sector as light guides, imaging tools and lasers in surgeries. For example, in Figure 1.1b an arterial blockage is removed with the help of an optical fibre. In the mechanical sector, optical fibres are used to observe or inspect areas that are impossible to reach [13]. There are also applications where the use of optical fibres is still under investigation. Research has been done in using optical fibres as a distributed vision sensor in edge detection of thin substrates in a contactless handling system [30]. In this thesis, a follow-up study will be done on this research.

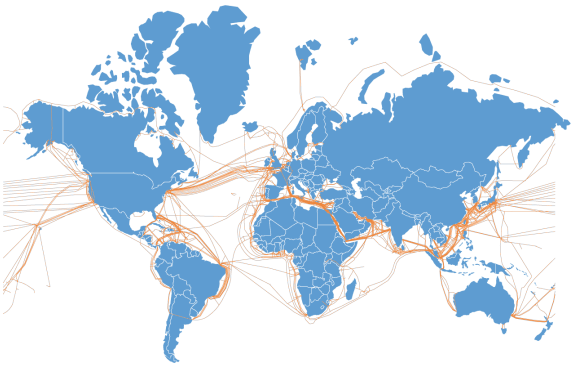

(a) Optical fibre infrastructure of the world [25].

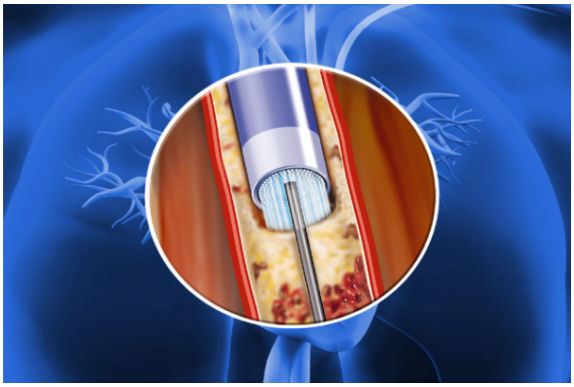

(b) Arterial blockage removal using an optical fiber [5].

Figure 1.1: Optical fibre applications.

Technological developments are rising exponentially in recent years. Not only innovations are invented, but also new technical solutions are found for problems that occur in the technology that already exists. This can be, simplifying the production process within a production or thinking of new energy sources that are used.

Technology has grown strongly and this will only grow more in the coming years. Technical developments can also bring problems. If something new is invented, it can influence the whole system where it is used in. Sometimes an entire machine has to be adapted if a certain working principle inside the machine has been changed. Nevertheless, if this working principle turns out to be a lot more efficient, it will yield more in the long term. The technology in the photovoltaic industry, for example, is improving. In the next subsections, some examples are given of the desires that the photovoltaic industry has to improve production. The problems that arise when working towards these desires are also discussed.

1.1.1. Semiconductor industry

The already existing technology is being used more over the years. Take the mobile phone for example. Worldwide, the number of mobile phone users in 2020 stood at 6.95 billion. Exactly one year later, this number has increased by 0.15 billion. As can be seen in Figure 1.2 the prediction is that this number will increase even more in the coming years [53].

	Number of smartphones	Number of mobile phones
2025*	7.33	7.49
2024*	7.13	7.41
2023*	6.92	7.33
2022*	6.64	7.26
2021	6.37	7.10
2020	6.05	6.95

Figure 1.2: Number of smartphone and mobile phone users worldwide, together with a forecast for the coming years (billions) [53].

This is not just the case for mobile phones. The number of users is also growing when you look at other electrical devices. This requires an increase in the production of computer chips. Computer chips are made on a wafer, a thin slice of semiconductor, and most of the wafers are made of silicon. This material has high conductivity, and it mainly occurs in the sand, so it is widely available on Earth [28]. An overview of the demand for silicon material in the different market sectors can be seen in Figure 1.3. The need for silicon material has only increased in recent years [38] [39]. The silicone material is already very expensive and what can be seen in the article from Bernreuter is that the price has increased even more in the year 2021 to 36.37USD/kg [21]. This increase is due to the COVID pandemic. Due to the pandemic, the demand for computer chips and therefore also for silicone material has increased. This creates a shortage, and it increases the price of the material. So the problems that occur are therefore not only higher costs, but also the inability to obtain the material, which means that production comes to a standstill. No production means that computer chips cannot be delivered to the suppliers, which results in a shortage of electrical devices.

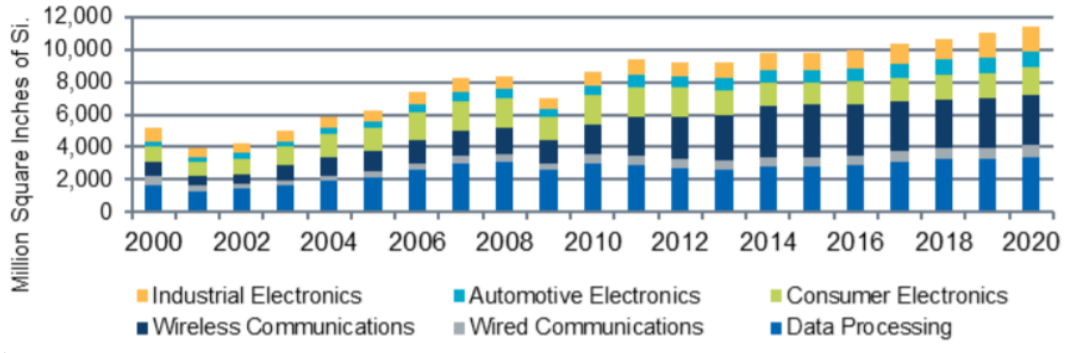

Figure 1.3: Silicon demand by market segment [39].

The machines that make computer chips are very big and there are a lot of operations that have to be performed with very high precision. According to ASML, one of the biggest suppliers to the semiconductor industry, the features on a computer chip can be as small as 10 nanometres [6]. With such small features damaging the wafer, which contains the computer chips, has to be prevented. Wafers are moving from one location to another very often. In today's industry, wafers are moved with a gripper. This gripper can have different

shapes. For example, one system moves a wafer by gripping the sides with two robot arms or another method is lifting the wafer from below [22]. The main similarity that all these grippers have is that they make contact with the object that they have to transport. One of the biggest damaging sources is the mechanical contact between the wafers and the handling tools [24]. The problems that can arise with such contact are tensions in the wafer or contamination of the wafer, which means there is a chance that the wafers will break. In addition, according to Brun and Melkote [22], the thickness of wafers plays a significant role in the magnitude of the distribution of handling stresses produced in the wafer. The influence of the wafer thickness on the breakage rate is shown in Figure 1.4a. The breakage rate will increase rapidly when the wafer thickness will decrease [48]. In Figure 1.4b, the prediction from the International Technology Roadmap for Photovoltaic (ITRPV) of wafer thickness over the years can be seen. In the first editions of the ITRPV, they predicted a decrease in wafer thickness in the coming years, but this prediction came quickly to an end. The industry saw the limitations of wafer thickness, because of the troubles that occur while handling thinner wafers. That is the reason that in the later editions of the ITRPV the prediction curve flattened. A solution has to be found to solve this limitation and let the industry make thinner wafers that reduce silicon usage and thus the production costs [15].

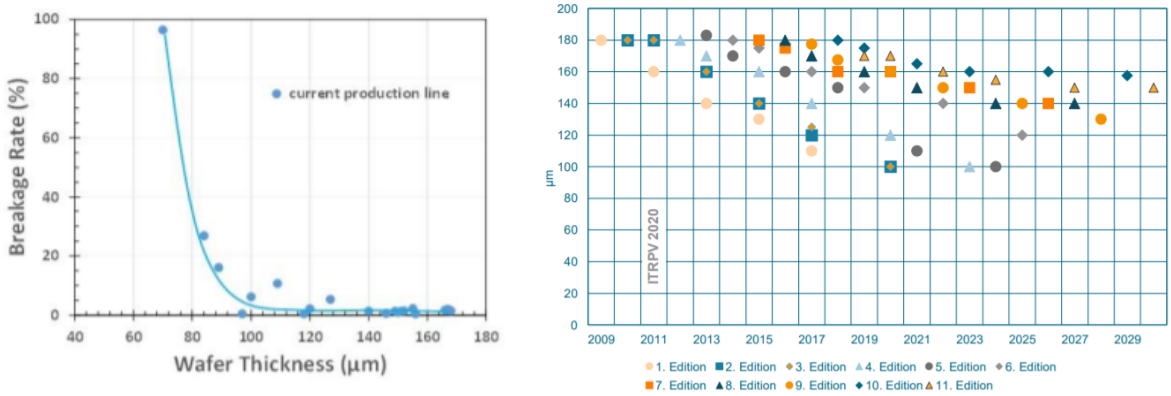

(a) Influence of wafer thickness on the breakage rate [48].

(b) The yearly prediction of ITRPV on wafer thickness [15].

Figure 1.4: Wafer thickness limitation.

1.1.2. Solar cell industry

In the Paris Agreement from December 2015, most of the world joined forces to do something about climate change. The agreement aims to hold the increase in the global average temperature to two, preferably one point five, degrees Celsius above pre-industrial levels. Greenhouse gases, such as carbon dioxide (CO2), methane (CH4) and nitrous oxide (N2O) trap heat in the atmosphere and warm the planet. The emission of these greenhouse gases has to be reduced to hold the increase of the global average temperature. These gases are released during the combustion of fossil fuels, such as coal, oil and natural gas, to produce electricity. An alternative has to be found to produce electricity. Solar energy is a renewable energy source that converts energy from the sun into electricity. In Figure 1.5a it can be seen that the share of solar energy consumption is still very low. This share has to be increased to achieve less emission of greenhouse gases. Solar energy is also the cleanest and most abundant renewable energy source available, so this is a perfect alternative for the production of electricity.

Solar cells are made from silicon wafers, so the problem of an increasing breakage rate when the thickness decrease also holds for solar cells. Around 90% of currently manufactured solar cells are based on crystalline silicon [8]. In the 2015 edition of the ITRPV, they stated that approximately 61% of the cell price comes from the cost of silicon material [10]. Next to that, it is said that solar cells can be made way thinner to come to the highest achievable efficiency. The thickness of the solar cells can decrease to around 70 micrometres [18]. In Figure 1.5b it can be seen that the maximal efficiency is reached when the solar cells have a thickness of 70 micrometres. The production of solar cells would then not only be cheaper because of the less material that is used, but the solar cells that will be produced will also have higher efficiency. This means that for the same amount of produced energy, fewer solar cells are necessary.

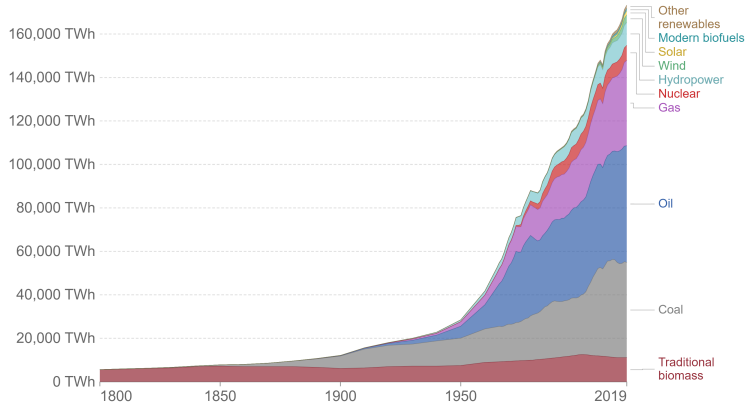

(a) Global primary energy consumption by source [49].

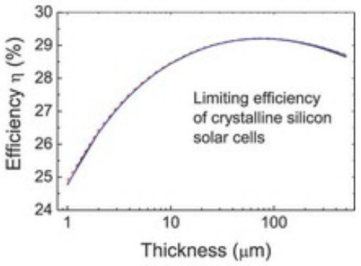

(b) The efficiency of a solar cell with respect to its thickness [18].

Figure 1.5: Energy consumption by source and higher efficiency that can be reached by using thinner solar cells.

1.2. State of the art

The removal of contact during the transport of wafers and solar cells will be the solution to remove friction on and stresses in these objects. But the non-contact system that will be applied is not enough by itself. A sensor is needed to know exactly where the object is positioned at any time. In that way, the system knows how it can move the object to the next location. This section will look at the basis of this research. The chosen transport system where thin materials, like wafers and solar cells, will be transported on, is explained first. Then, the use of optical fibres as a sensor in such a transport system will be substantiated. Optical fibres are not the only thing that is needed to let it work as a detection sensor. The requirements needed will be listed and explained.

1.2.1. Transport system

The high breakage rate that occurs with wafers and solar cells, described in section 1.1, cannot go unnoticed. The thin objects are still making contact with the handling tools during transport. If the wafers and solar cells are becoming thinner, they can handle less before breaking occurs. Cracks in wafers and solar cells do not only occur during transport. Cracks can also appear during the manufacturing process of these objects. In this research, the focus lies on what can be done about cracks that appear during transport and not during the manufacturing process. Studies have shown that various systems can eliminate contact with objects during transport. Vandaele et al. talks about different kinds of mechanisms that can be used to transport an object without making contact with it [55]. The main topics discussed are magnetic, electric, optical, aerodynamic and acoustic levitation. This research focuses on a system that uses air in the movement of an object.

Transport through air can be achieved by implementing air bearings in a table [50] [33]. These air bearings create a layer of air between the object and the table surface. This ensures that the object can float over the surface without contact. The air bearings can tilt so that the objects floating above them can be controlled. As can be seen in Figure 1.6 the air bearings are located under the object. This will be the best place for the air bearings because then the space above the object is available for other operating actions. The orientation and layout of such air system can look differently [26] [54] [50]. This research will look at the best way to track an object on an air system. The air system can be made in such a way that it meets the requirements that are needed for tracking. More about the orientation and layout of the air bearings can be found in section 3.3.

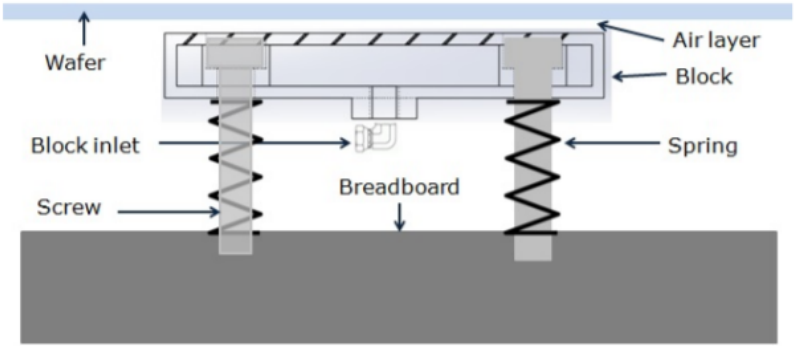

Figure 1.6: Contactless handling from below through air [26].

1.2.2. Detection sensor

Various sensors can be used for the detection of an object floating over an air-bearing table. In this research optical fibres have been chosen to use as a sensor because of their many advantages like small size, lightweight, low cost and resistance to electromagnetic interference [17]. Other sensors can be used. The literature has shown alternatives like sensors that use sound pulses or electrical signals [23] [19]. However, previous work showed that optical fibres have great possibilities and the fact that little research has been done on it makes it even a better choice [30].

Optical fibres are very thin cables where light can travel from one end to the other end. In that way, the light can be redirected to the exact location that is needed. The position of the object can be determined by placing receiving and transmitting fibres all over the air-bearing table. Light is sent into the transmitting fibres. Then, when an object floats above the table at a certain height, the light from the transmitting fibres will reflect against the object and falls into the receiving fibres. A camera can make an image from all the ends of the receiving fibres. In that way, the position of the object can be determined. The precision and accuracy of measuring the position are very important in the wafer and solar cell industry because of the small features on these objects. The placement of fibres will be beneath the object in the table. The space above the object will be available for other operating actions. The optical fibres and the air bearings are both positioned underneath the table. In Figure 1.7 a possibility is shown on where the optical fibres could be placed.

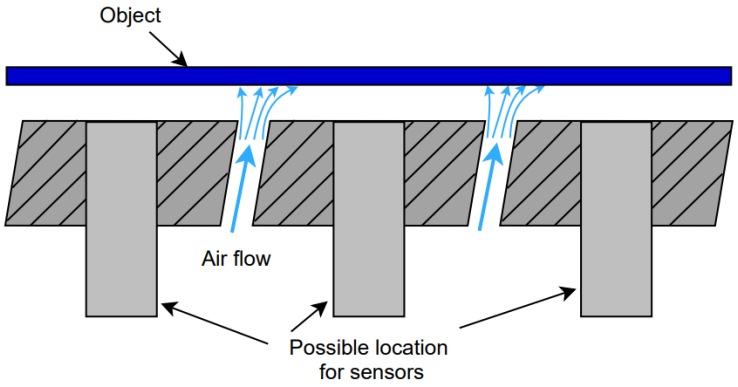

Figure 1.7: Possible locations for the fibres integrated into an air bearing system [30].

What Hecht says in his book, Optics: Light for a new age, is that most optical fibres with a plastic coating have a thickness of around 250 to 500 micrometres [32]. So a lot of fibres can be implemented in the surface of the table and because of that a lot of measurements can be done. In earlier research, more measurements would result in higher precision. In a previous master's thesis about this subject, linear array sensors were used to detect the height and position of the object [56]. Three Bachelor groups continued with this research by using optical fibres instead [27] [41] [52]. Figure 1.8 shows a top view of a possible setup of an air-bearing table with optical fibres integrated into it. The result of one Bachelor group was based on an on-off principle. If light

could be seen from the receiving fibres, the object is above the fibres (on) and if no light comes out of the receiving fibres, the object is not positioned above the fibres (off). Fritz has expanded this research further in his master thesis by placing a diffuser over the optical fibres [30]. The fibres will have more vision because the initial light point is now broadened and a wider light circle is formed. The middle of the light circle has the highest light intensity, and this slowly declines towards the edges. The result from Fritz can achieve higher precision compared to the Bachelor group. Figure 1.8a shows a top view of a table with optical fibres placed in it. The intensities received by the receiving fibres will be enlarged. Figure 2.4b shows the enlarged receiving fibres and the differences between using an on-off principle and using a diffuser on top of the fibres. The master thesis of Fritz has shown that the use of a light diffuser as a vision expander worked to achieve higher accuracy. That is the reason why in this research also a light diffuser will be used as a vision expander.

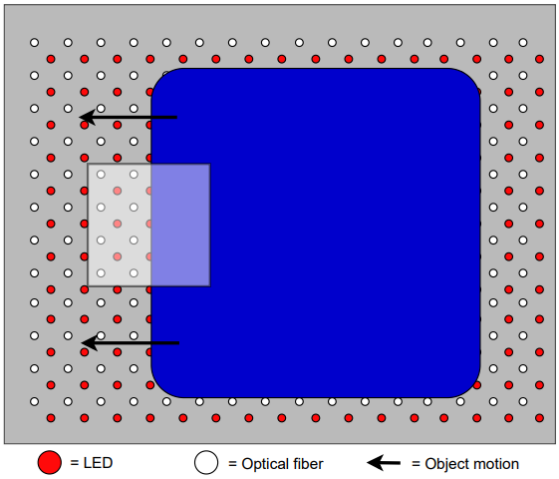

(a) Top view of the whole table with optical fibers.

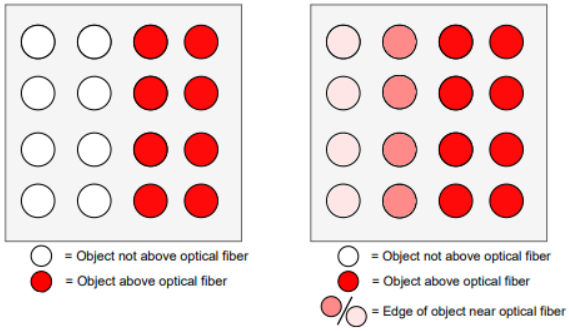

(b) On the left the on-off principle and on the right different received intensities.

Figure 1.8: Top view from a possible setup of the system with different outputs from the optical fibres [30].

1.2.3. Working principle

Optical fibres will be used as distributed vision sensors. An image will be made from underneath the object that floats above the air-bearing table. The fibres will transport the image to outside the system. Optical fibres itself is not enough to let it work as a sensor. More parts are necessary. In the previous subsection, it is mentioned that a light source is needed to send light into the transmitting fibres. This light source can be a simple LED. In Fritz his work, a light spot was received with decreasing intensity towards the edges, but in the middle of the light spot, a high light-intensity spot appeared. This high light-intensity peak created a white dot in the middle. In this research, a LED that can differ in light intensity is desired. The light intensity can be adjusted in such a way that this white high light-intensity spot will be eliminated. Also, a camera is needed to make an image of the ends of the receiving fibres. A camera can see if a receiving fibre received any light. If a receiving fibre emits light, an object is floating around that fibre. The information got from the image of the receiving fibres can be converted to the location of the object floating on the air-bearing table.

1.2.4. Multicolour optical fibres

Light will be sent into the transmitting fibres. Up to now, only the colour red was sent into the transmitting fibres. Another option is to use multiple colours for sensing the position and direction of the object. One way to accomplish that is by sending the three primary light colours red, green and blue separately into the transmitting fibres. The transmitting fibres are divided into three groups. Each group sends its light with a specific wavelength. The LEDs emit pure red, green or blue light.

The image made from the receiving fibres will make it clear where the object is floating and from which angle the object is coming. The assumption is that multiple things can be seen in the image, the individual colours red, green or blue or a combination of the three. Red and blue make magenta, red and green make yellow and blue and green makes cyan. A combination of all three colours makes white light. The different colours that

can be received can be seen in Figure 1.9a. Next to that, an intensity graph can be made from the image taken from the receiving fibres. In that way, the red, green and blue colours can be read out easily. An example of such a graph can be seen in Figure 1.9b. In Figure 1.9c two examples of orientations of an object can be seen. The receiving fibre emits magenta light when the object is above the red and blue fibres, as illustrated on the left. The receiving fibre emits cyan light when the object is above the red and green fibres, as illustrated on the right. The combination of colours can easily be read out by a software program like MATLAB.

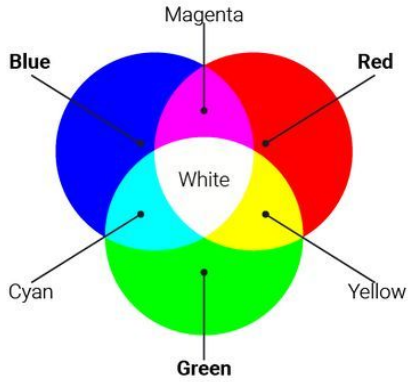

(a) The three primary light colours red, green and blue and the combination of those colours.

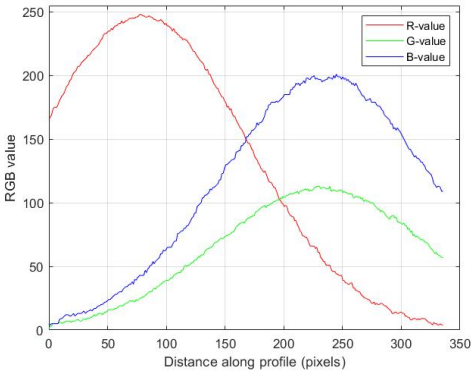

(b) Example of an RGB graph that can be received from a line drawn over a coloured picture.

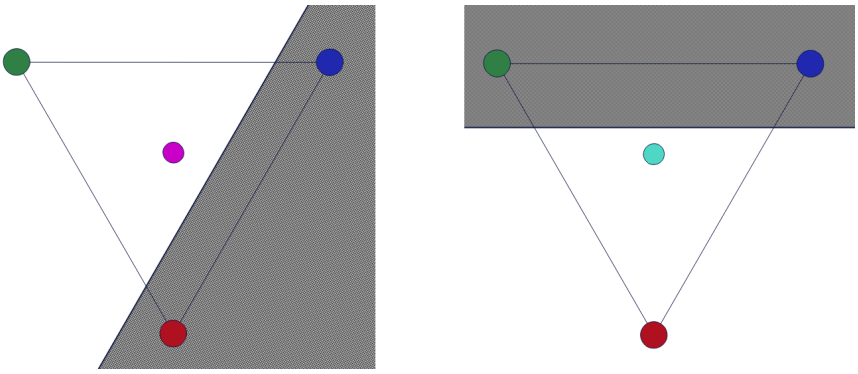

(c) Two examples of what the receiving fiber can emit with a certain object orientation indicated with the black part.

Figure 1.9: The use of the three primary colours red, green and blue.

1.3. Research objective

In previous research, the concept of one transmitting fibre and one receiving fibre was investigated. The view of a single optical fibre is optimized by using a volume diffuser. This thesis will continue by using multiple transmitting fibres and look if there is a positive advantage by using more fibres. The three different primary light colours red, green and blue will be used for the transmitting fibres as described in section 1.2. The presumption is that if the object floats above one transmitting fibre, then the corresponding receiving fibre will emit the colour the one transmitting fibre emits. If the object floats above two transmitting fibres, the corresponding receiving fibre will emit a combination of the two colours the transmitting fibres emit. If the object floats above all three transmitting fibres, the corresponding receiving fibre emits a combination of all three colours, which will be white light.

The research objective is stated as follows:

"Design and experimental validate an edge detection sensing surface with the use of optical fibres and the three primary light colours"

1.4. Thesis outline

The research is divided into multiple chapters. It will start in chapter 2 by giving an overview of the whole system. The parts of the system will be examined individually on their physics and working principles. In chapter 3 a theoretical analysis is executed. More attention will be given to the light spot that appears after being diffused by a volume diffuser. Also, the placement of the optical fibres in the air-bearing table is investigated. The image that is desired is simulated using MATLAB. Chapter 4 will explain the setup, that will be used in all experiments, in detail. It will start by looking at the experiments that want to be achieved. The design objectives for the setup are mentioned, after which all components of the setup are explained. A total of four experiments will be done. Chapter 5 shows the first experiment. The idea of this experiment is to scale the image received and use it for experiments two and three to reduce the amount of work that has to be done. The second experiment is explained in chapter 6. This chapter tests various types of volume diffusers. Eventually, a diffuser choice will be made, and this diffuser will be used for the last two experiments. In the third experiment, in chapter 7, an object comes into play. The influence of a moving object over the fibres will be investigated and see what influence it has on the RGB value. No reflection is included in this third experiment. The RGB value is measured at the receiving fibre location from the top. The fourth and last experiment is executed in chapter 8. This experiment will include reflection and uses a receiving fibre. The third and fourth experiments are exactly the opposite of each other, so those experiments can be laid next to each other to see if there are similarities. Chapter 9 will again look at the research question and will prove the concept by doing a small experiment and making a model of the system. Chapter 10 will give a discussion on all the results that came out of this research. A conclusion is given in chapter 11 and recommendations for future research are given in chapter 12.

2

System overview and literature research

In this chapter, more depth is given in the system overview. Going back to the global setup, three colours, distributed with fibres, are necessary. The transmitted light will go through a transparent diffusive layer, reflect against the object, through the same diffuse layer, collected in another fibre and transmitted to a camera. The physics of the parts used in the global setup will be investigated in the same order the light is travelling. Next to that, important choices for this research will be made. First, the working principle of the optical fibres will be explained in section 2.1. The two different types of fibres are laid down, and a choice will be made on which one will be used in this research. Then in section 2.2, a small insight will be given about the diffuser. There are two kinds of diffusers, both will be explained, and a choice will be made. Finally, in section 2.3 it is explained how an image, taken by a camera, can be converted into an object position.

2.1. Optical fibers

In this section, the optical fibres will be explained. How they work and what kind of different optical fibres there are. The idea to transport a piece of light with information over a long distance was already from the end of the 19th century. It became realistic in the 1960s when technology has evolved enough. From then, they started to install optical fibres all around the world [12].

2.1.1. Working principle optical fibres

Optical fibres can be seen as long cables where light can travel through. If the light will be shined at one end of the fibre, the light will travel to the other end by bouncing against the edge over and over again. Optical fibres consist of an inner core and a cladding. The diameter of each part depends on the type of fibre. This will be explained later in this section. The core of the optical fibre has a refractive index of n_1 and the cladding of the fibre has a refractive index of n_2. When a ray of light travels through the core with an angle of incidence of θ_1 against the cladding, the light has two possibilities it will refract with an angle of θ_2 or it will reflect with the same angle of the incident light beam θ_1 [4] [11]. In Equation 2.1 the relation can be seen between the variables. This equation is known as Snell's law.

$$n_1 \cdot \sin(\theta_1) = n_2 \cdot \sin(\theta_2) \tag{2.1}$$

In Figure 2.1 a light beam can be seen that refracts or reflects. This depends on the angle of incidence and the two refractive indices of the core and cladding. Total internal reflection is necessary for the optical fibres to work otherwise, light or information will be lost. Total internal reflection can only happen if the light is travelling in a medium with a higher refractive index than the refractive index from the material it travels to. If the angle of incidence is greater than a certain angle, the so-called critical angle (θ_c), the light will reflect completely [29]. In Equation 2.2 θ_1 is extracted from Equation 2.1.

$$\theta_1 = \sin^{-1}(\frac{n_2}{n_1} \cdot \sin\theta_2) \tag{2.2}$$

When total internal reflection happens, the light will stay within the fibre, no matter what shape the fibre has. If the core of the fibre is made from glass, the shape of the fibre is limited, but that will be discussed later

in this section. The cladding of optical fibres will not absorb any of the light, so it can travel long distances. Some of the light will be lost within the core because of the impurities of the material of the core. If total internal reflection is needed for optical fibres to work, it can be said that $\theta_2 = 90° \rightarrow \sin(\theta_2) = 1$. Equation 2.3 now calculates the minimum angle of the incident light beam θ_1, also called the critical angle.

$$\theta_c = \theta_1 = \sin^{-1}(\frac{n_2}{n_1}) \tag{2.3}$$

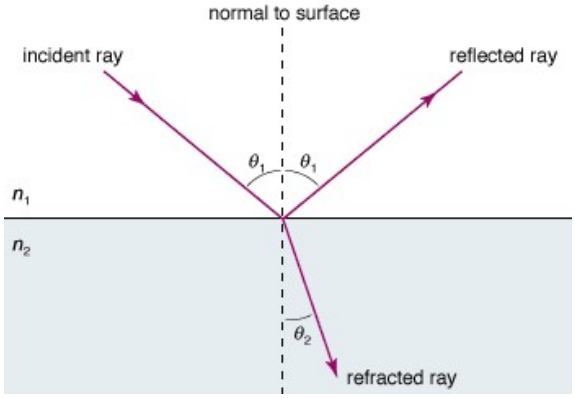

Figure 2.1: A light beam reacting when falling on a surface with a different refractive index [2].

Next to this, there is a numerical aperture (NA). This will tell what the largest angle of the incident light beam can be to let total internal reflection happen within the core of the fibre. In Equation 2.4 it is defined how the NA is calculated. The total acceptance angle of the incoming light beam is 2α. This is shown in Figure 2.2. Light rays outside the NA range cannot reflect within the fibre. The NA can be raised when making the relative refractive index of the core of the fibre (n_1) much higher than the cladding of the fibre (n_2). The downside of this is that the light will scatter more [1].

$$NA = \sin(\alpha) = \sqrt{n_1^2 - n_2^2} \tag{2.4}$$

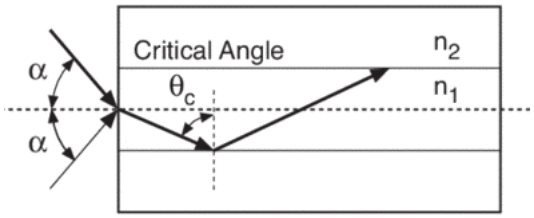

Figure 2.2: Cross-section of the acceptance angle of optical fibres [1].

2.1.2. Characterizations of Optical fibers

Before the world uses optical fibres for the transport of information, copper wires were used. Optical fibres are a huge innovation because the information can travel longer distances, the fibres have a higher resistance to electromagnetic interference and the fibres are light in weight. The use of optical fibres is way more profitable. A big change in telecommunication occurred in the last decades [40].

Optical fibres are made of really thin transparent material. There are plastic optical fibres (POF) and glass optical fibres (GOF). Both have their advantages and disadvantages. Below is an overview of both types of fibres.

Plastic Optical fibres (POF)
The core of plastic optical fibres is mostly made from polymethylmethacrylate (PMMA) or polycarbonate. The cladding is mostly made from silicon. There are two types of POF, small POF and large POF. The difference lies in the diameter of the core of the fibres, but they have the same performances and characteristics [9].

Glass Optical fibres (GOF)
Almost all cores from glass optical fibres are made from silica, which is pure glass. The cladding is made from plastic or less pure glass. Glass optical fibres sure have their advantages over plastic optical fibres, but has also its downsides. Below is an overview of both kinds of fibres and the important characteristics to distinguish them [9].

Material choice
In table 2.1 the most important characterizations, relevant to this research, are given for POF and GOF. It cannot be said that one material is better than the other. They have both advantages for different kinds of applications. Glass optical fibres can be used in very high or very low-temperature systems, for example in ovens or freezer equipment. Next to that, GOFs are a perfect choice if they have to cover long distances or if it is not desirable that the fibres wear much. If you need high flexibility or do not need to cover long distances, plastic optical fibres will be the best choice.

In the coming research, the fibres do not have to cover long distances, do not need to withstand high temperatures and flexibility is useful in the small amount of space that is available. So in this research, plastic optical fibres will be used.

	Plastic optical fibres (POF)	**Glass optical fibres (GOF)**
Numerical aperture (NA)	Small numerical aperture so less light can come in	Large numerical aperture allowing more light to come in
How does it react to temperature change	Cannot withstand high-temperature changes	Can withstand high-temperature changes
How material reacts to environment	Will easily degrade over time, it becomes yellow	Will not degrade in corrosive environments
Losses	Will relatively have more losses, especially when travelling long distances	Will not have big losses, also for long distances
Diameter size	Can have larger core diameters, around 1 mm	A limited diameter size, typically a maximum of 0.15 mm
Fragility/flexibility	Very flexible, can bend without breaking	Very fragile, low flexibility
Costs	Lower material costs	Higher material costs
Outside noise	Can handle the vibrations or other unsteady environments from the outside world better	It is harder to handle the unsteady environments

Table 2.1: Characterizations of POF and GOF relevant for this research [31] [47] [58].

Multimode optical fibres
Apart from the fact that fibres can be made from different materials, there is also an option to have a single-mode fibre or a multimode fibre. A single-mode fibre is a fibre that allows only one direction area of light rays within the fibre core. An example of a single-mode source is a laser. A multimode fibre is a fibre that allows multiple area directions of light rays within the fibre core. An example of a multimode source is the sun. This research will use multimode fibres because a LED is used as a light source and a LED emits multiple light rays [42]. The average total diameter of a multimode fibre is 125 micrometres. The core size of multimode fibres is typically around 50 or 62.5 micrometres [16]. Multimode fibres are perfect for low bandwidth and high attenuation. Multimode fibres can only be used in short distances, with a maximum of 300 to 550 meters. Fortunately, this research comes not even near this distance.

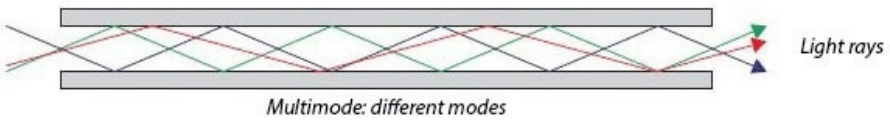

Figure 2.3: Light rays travelling in multimode optical fibres [3].

2.2. Light diffusers

The light that comes out of the optical fibres is limited to a specific diameter. That means that it is also limited to a specific vision. In this research, it is necessary to extend the vision of each fibre to get a higher precision of the position of the object. Fritz has done research about this issue in his master's thesis [30]. The vision was extended by laying a diffuser over the fibres, as illustrated in Figure 2.4a. A light diffuser scatters the incoming light into a so-called soft light. Fritz used volumetric diffusers in his research. The light gets scattered within the volume of the transparent medium, as can be seen in Figure 2.4b. Both, transmitting and receiving fibres, are covered with a diffuser so the diffusing effect is doubled. That is because the light first gets diffused when leaving the transmitting fibre, and it gets diffused again after the light reflects from the object back into the receiving fibre. After a lot of testing, Fritz concluded to use the most diffuse diffuser, namely the PRIMO® XT N381. The light spot size with the diffuser was compared with the light spot size without the diffuser, and a significant increase was achieved. The settings from the camera are important as well to minimize the blooming effect.

The working principle of putting a diffuser over optical fibres has been proven to be very robust. It has only been tested with a receiving fibre and transmitting fibre. It is unknown if this concept also works when more optical fibres will be used. It will be investigated in this research. Also, the different possibilities for the diffusers will be investigated one more time to check if the PRIMO® XT N381 is the best option.

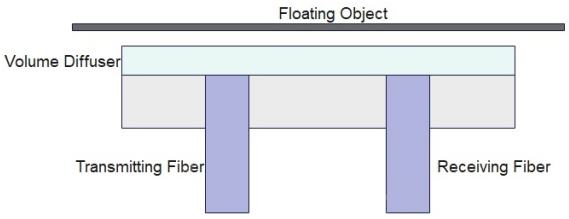

(a) Schematic overview on how the vision of the fibers can be broadened by laying a diffuser over the fibers.

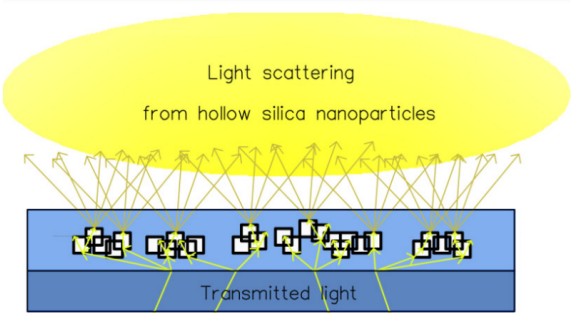

(b) Illustration on how the light gets diffused in a volume diffuser.[51]

Figure 2.4: Diffuser illustration.

2.3. Image readout

Earlier it has been said that the light sent into the transmitting fibres will be diffused causing a wider viewing angle. The light rays that the receiving fibres will catch need to be converted into an image where the object position can be taken from. Every receiving fibre has a different intensity and colour or RGB value. A camera is used that can read the different intensities and catch the RGB values from all the receiving fibres. The image needs to be clear enough to take results out of it.

2.3.1. Camera

An image sensor is needed in the camera to catch the light signals that come out of the receiving fibres. A charge-coupled device (CCD) or complementary metal-oxide-semiconductor (CMOS) can be used for this. All image sensors are made from photodetectors or pixels. The sensor will convert the incoming light into electrons. It makes a total image of all the pixels of information the sensor got [45] [43]. CCD and CMOS

sensors are very similar but have some differences. A CCD sensor is an analogue device and a CMOS sensor is digital. The CMOS sensor is the cheaper and faster version of the CCD sensor. So the CMOS sensor will be used more in the coming years [14]. For this research, it does not matter which one will be used. The image made by both sensors consists of pixels. Each pixel has an RGB value. The pixels inside the receiving fibre decide the brightness. How brighter the pixels are, how closer the object is positioned above the receiving fibre. The closer the object is located to the receiving fibre, the more light reflects against the object into the receiving fibre. A big advantage of using an image sensor is that it can achieve high precision, which is needed in this research [43].

In previous work, it was investigated how to couple the CCD/CMOS camera sensor to the receiving fiber bundle. Two options were given. The first option is to use a camera with a lens. The second option is to use a fibre optic taper. Because of the high costs of a fibre optic taper, a camera with a lens was used. This will also be used in this research. A disadvantage of using a camera with a lens is that the camera needs to be placed at a certain distance from the object because otherwise, it cannot see all the fibres. The distance will be longer when more receiving fibres will be used because the total surface is larger. This is something to keep in mind when using a camera with a lens as a vision sensor.

2.3.2. Image translation

The images received by the camera need to be translated into an object's location. The images include all the receiving fibres. These fibres are laid down in the same order as in the table. The Bachelor group and the Master thesis worked with the light that comes out of the receiving fibres to calculate the object's position. The Bachelor group looked at the on-off principle. When the object is above that fibre it will emit light, and otherwise, it will not. A received image from the bachelor group can be seen in Figure 2.5. The Master thesis looked at how bright every receiving fibre is to get more information about the location of the object. If the receiving fibre emits more light, the edge of the object is closer to that receiving fibre. A bright spot means that the fibre is fully covered. While a dark spot means that the fibre is not covered at all.

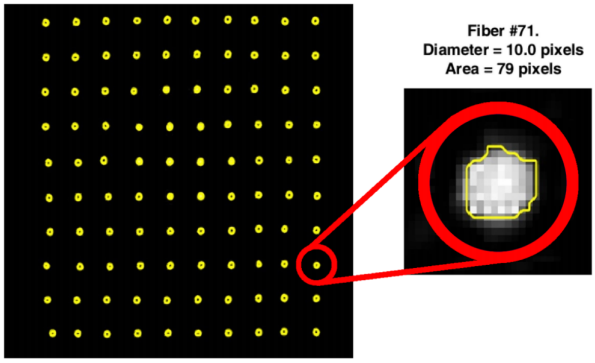

Figure 2.5: Received image of the end project from the Bachelor group [27].

In this research, an extra component will be added. There will be looked at if the use of multiple colours has a positive advantage in measuring the direction or angle movement of the object. This can be measured by looking at the transition of colour from the receiving fibres

2.4. Conclusion

In this chapter, an in-depth view is given of optical fibres. The physics is explained and the characterizations of the different optical fibres are mentioned. In this research, plastic optical fibres will be used because of their ease of handling. The limited view of optical fibres is a downside. The viewing angle will be increased by laying a volume diffuser over the fibres. The exact volume diffuser will be discussed later in chapter 5. The light that the receiving fibres receive has to be converted into an image. This will be done with a camera that is directly connected to a computer where the settings can be adjusted. The expected result is an image of fibres with different colours, which tells where the object is located and under which angle the object is moving.

3

Theoretical analysis

In this chapter, a theoretical analysis will be done about the light intensity profile that can be achieved on the object and how that will be reflected. There are different methods to model the propagation of light. There are geometrical optics that describes the light as rays travelling in straight lines from the light source. In wave optics, the light travels as a wave. The propagation is described by Maxwell's equations. At last, there is quantum optics which describes light as a wave as well but looks at the photons, individual quanta of light, that interact with atoms and molecules. Because all the objects in this research are far greater than the wavelengths that will be used and to simplify the model, geometrical optics is chosen.

In previous work, an analysis is done about the trajectory of the light rays when leaving the transmitting fibre and reflecting into the receiving fibre. This is done without a diffuser layer on top of both transmitting and receiving fibre. In this chapter, there will be looked at the consequences when a volume diffuser is used and what result this has on the light intensity. First, the distribution of the light intensity will be investigated. How the light is spread on the object if it is positioned above the fibres. After that there will be looked at the fibre placement and which one will be used in this research. With the light intensity distribution and the fibre placement known, a MATLAB simulation can be done. This simulation will show one set of fibres or what can be seen as one 'building block' from the whole system. A bottom view of the light intensity distribution on the object is simulated. This simulation shows how the different colours will react when they overlap each other.

3.1. Light spot intensity

The light that leaves the optical fibre will be diffused by the volume diffuser that lies on top of it. The light rays that travel through the volume diffuser will spread towards the object at a certain scattering angle. A circular-shaped light spot will appear on the object. What will be expected is that the centre point of the light spot has the highest light intensity and how further you go to the outside of the circle how lower the light intensity will be. At the centre point, the scattering angle will be close to zero and the scattering angle will become higher when going to the outside of the circle. When light rays will scatter through a surface diffuser, the light intensity is proportional to the beginning intensity multiplied by the cosine of the scattering angle. Of course, a volume diffuser will have a different result, but a kind of similar course is expected.

The light rays, that will shape the circular light spot, will reflect against the object at the same angle as the incoming angle. Before entering the receiving fibre, the light rays will be diffused another time by the volume diffuser that also covers the receiving fibres. The light intensity that the receiving fibre will receive has to be known for estimating the viewing range the fibres can cover. The system will be simplified by looking at a 2D intensity profile when intersecting a fibre exactly in the middle. It is really difficult to find a formula that gives the light intensity after being diffused by a volume diffuser. That is because there are a lot of unknowns that are hard to put a value to, for example, the properties of the particles inside the volume diffuser like size, shape and orientation that causes the light scattering. With these unknowns, it is hard to come up with a specific number for the light intensity at every point on the object. What can be measured is the shape the

intensity profile approximately will have. A lot of literature papers have tested similar setups experimentally. Some results can be seen in the graphs in Figure 3.1. Figure 3.1a and Figure 3.1b shows a graph of the incident angle versus the scattering angle. In this case, the scattering angle is the total angle at which the light rays can be diffused when the light hits the surface with a certain incident angle. The incident angle is the angle between the incoming light ray and the normal axis of the fibre, as illustrated in the graphs. A smaller incident angle results in a higher scattering angle [34] [37]. The middle of the light circle will have the highest intensity spot because it will receive the most light rays, and this intensity decreases when going to the edges of the light circle. This corresponds with the assumption earlier made. In Figure 3.1c the scattering angle versus the related intensity is illustrated. The scattering has a different meaning in this graph. This angle is now the angle between the outgoing light ray and the normal to the fibre. This graph tells that a low scattering angle results in a high-intensity peak [36]. This results as well with the assumption earlier made. What can be seen is that every graph shows an intensity profile that is shaped like a Gaussian or normal distribution. More literature confirms this as well [35] [44]. This assumption will be the basis of the theoretical analysis. In chapter 5 this will be experimentally tested and look if this assumption is true.

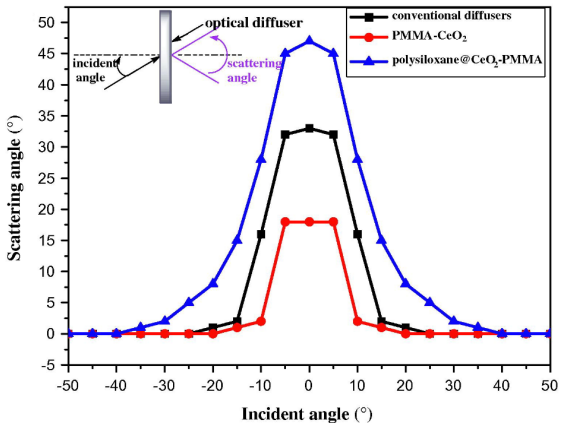

(a) Incident angle versus scattering angle for different diffusers [34].

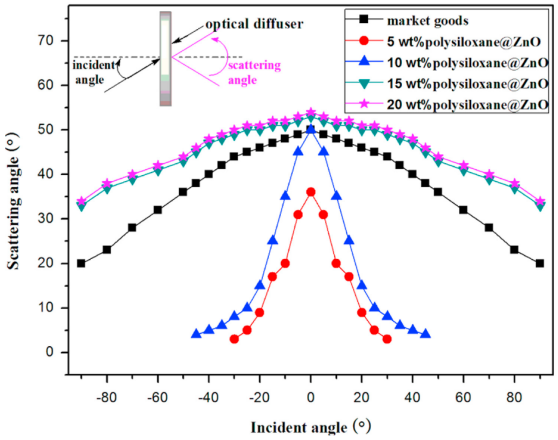

(b) Incident angle versus scattering angle for different diffusers [37].

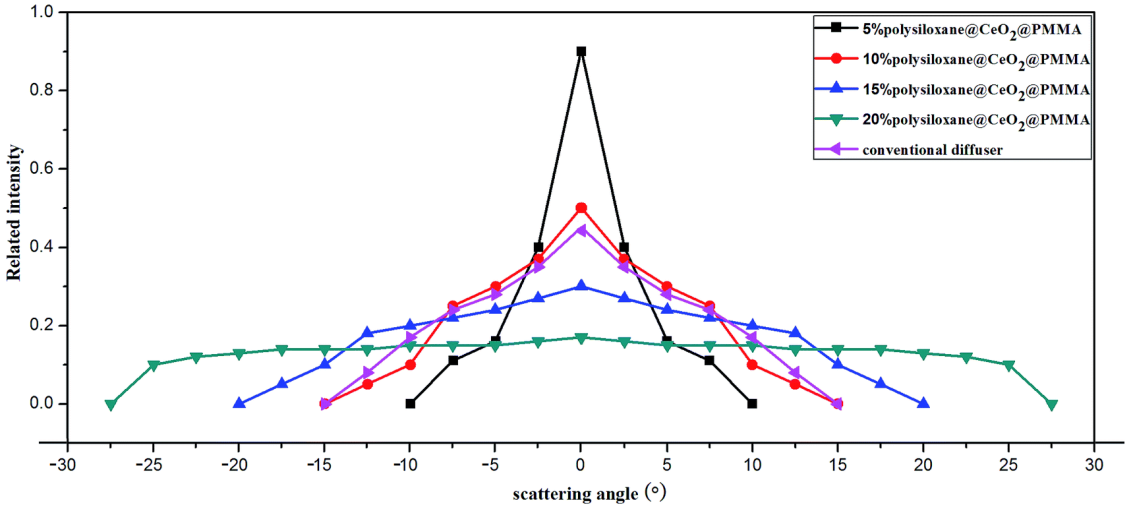

(c) Scattering angle versus related intensity for different diffusers [36].

Figure 3.1: Examples from the literature that shows a clear Gaussian distribution for various diffusers used.

3.2. Gaussian Distribution

In section 3.1 it was explained that for the light intensity distribution a Gaussian form can be assumed. Later, in chapter 5 this assumption will be evaluated and checked. In this section, the Gaussian distribution will be explained more in detail. A Gaussian distribution or also called a normal distribution has a bell-shaped curve with an asymptotic behaviour when going to the left and right. The curve is shaped with the variables a, b and c as can be seen in Equation 3.1.

$$f(x) = a\exp(-\frac{(x-b)^2}{2c^2}) \tag{3.1}$$

The parameter a is defined as the height of the curve's peak, b is the position of the centre of the peak and c controls the width of the curve. Sometimes Equation 3.1 can be rewritten into another form with expected value $\mu = b$ and variance $\sigma^2 = c^2$. This results in the probability density function, as can be seen in Equation 3.2. In Figure 3.2a it is illustrated what will happen with the curve if the expected value μ or the variance σ^2 changes. Figure 3.2b illustrates how the probability density is spread along the curve per extra standard deviation, σ, higher and lower than the expected value μ.

$$g(x) = \frac{1}{\sigma\sqrt{2\pi}}\exp(-\frac{1}{2}\frac{(x-\mu)^2}{\sigma^2}) \tag{3.2}$$

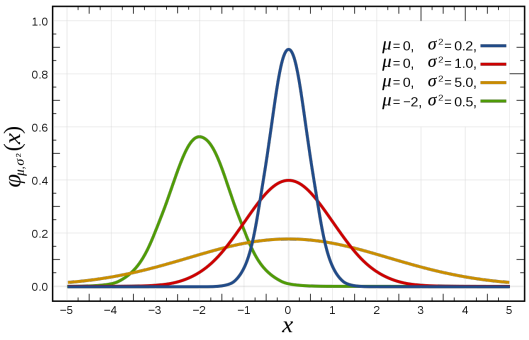

(a) Influence on the Gaussian curves with different expected values and variances.

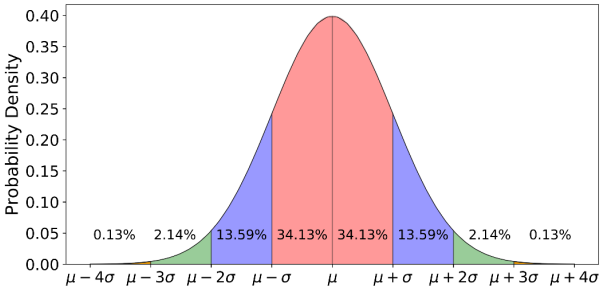

(b) The influence of the standard deviation on the probability density illustrated in percentages.

Figure 3.2: Illustrations on how the Gaussian curve is built up.

The light intensity coming out of the transmitting fibre will have a bell-shaped curve. When Figure 2.4a is enlarged, the light intensity distribution can look like Figure 3.3b. The total width of the bell-shaped curve is not known yet. This depends on the diffuser type that will be used in this research. The different diffuser types are investigated in chapter 5 and the most optimal one for this research will be chosen. When the width of the intensity circle is known, a calculation can be made on the distances between the fibres in the air-bearing table.

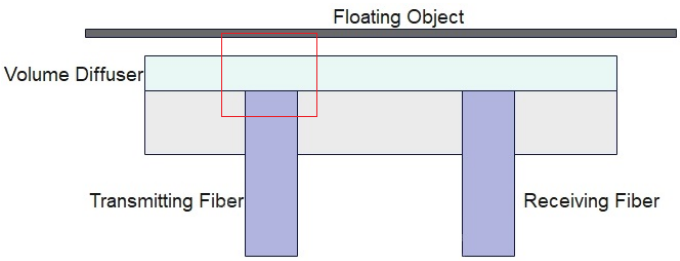

(a) Schematic overview of fibers with a volume diffuser on top.

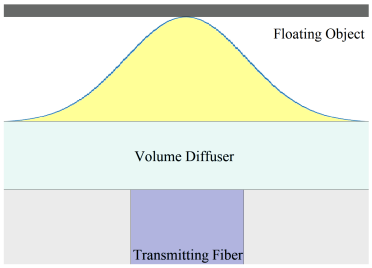

(b) Light intensity distribution if Gaussian form is assumed

Figure 3.3: Light intensity distribution if Gaussian form is assumed

3.3. Fibre placement

The optical fibres will be placed inside the air-bearing table. This table cannot hold an infinite amount of fibres. The table has a particular setup. When this setup is known, there are only a limited number of places where the fibres can be placed. A topside view from the air-bearing table is needed. There are a lot of different possibilities, but for this research one setup will be used. The chosen setup will be well substantiated.

An important thing for the air bearing layout to have is symmetry. When there is symmetry in the system, only a part of the system is needed for the calculations and simulations. If this smaller part of the system is working, the entire system will work as well. The smaller part can be seen as a 'building block' of the whole system. More building blocks can be added if a larger system is required. It is useful to look at smaller parts because large systems get complicated fast. The only thing that has to keep in mind is that when more building blocks are connected, interference can occur. This interference can have a positive or negative effect on the measurements. The easiest way to achieve symmetry is by using air-bearing shapes that fit together well and does not leave holes between them. Multiple shapes can also be used for an air-bearing setup, but that will make the system more difficult. There are only three shapes that meet the requirement, namely squares, triangles and hexagons. Next to the shapes of the air bearings, the fibre placement in the setup is also important to achieve symmetry in the system. The possible locations to place the fibres are at the edges of the chosen air-bearing shape. Another requirement is that every receiving fibre has to be surrounded by all the different colours used. So when using the three colours RGB, every receiving fibre has to be surrounded by each of them.

In section 1.2 the use of multicolour LEDs is explained. The three primary colours red, green and blue (RGB) will be used because of the easiness of handling. In Figure 3.4 three possible setups are illustrated, one for each shape. What can be seen is that the square setup needs one extra colour to achieve symmetry. A combination of the two primary colours is needed for the fourth colour. Figure 3.4a illustrates yellow as the fourth colour, a combination of the colours red and green. Every receiving fibre has to be surrounded with four colours instead of three. Also, when this setup will be used the yellow light, coming out of the transmitting fibre, has to be separated into red and green colour values. The receiving fibre can not only receive the red colour from the red LED, but also from the yellow LED. It is difficult to know from which fibre the red light will come. So to make it easy, the square setup will not be chosen. So the triangle and hexagon setup can only be used to achieve symmetry and using only three light colours. In Figure 3.4b and Figure 3.4c both setups are illustrated. Some research has been done about the surface of the air-bearing table and the possible locations to place the fibres. Vuong has demonstrated a so-called Flowerbed air-bearing table [57]. This is shown in Figure 3.5a. The surface consists of hexagonal segments that can be tilted as shown in Figure 3.5b. Because this shape shows great potential, this hexagon-shaped air-bearing table will be used in this research.

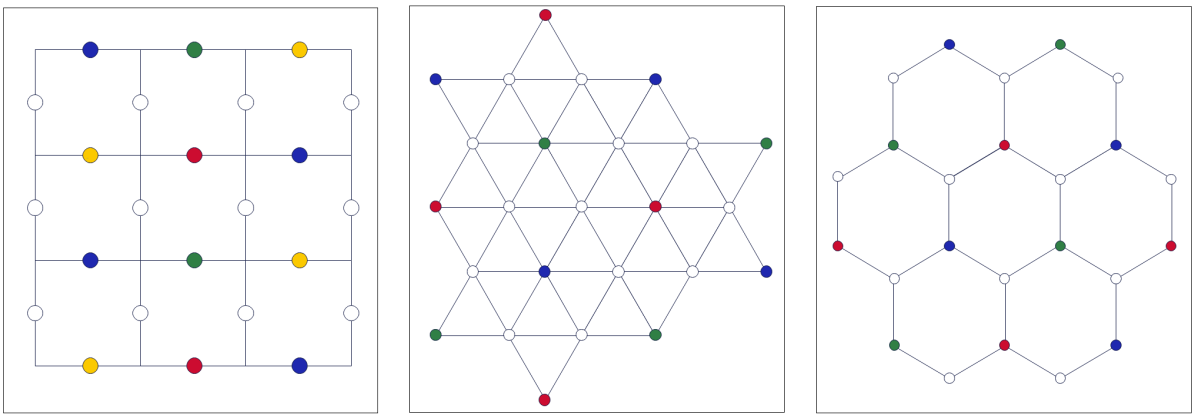

(a) Square-shaped air bearings. (b) Triangle-shaped air bearings. (c) Hexagon-shaped air bearings.

Figure 3.4: Three possible setups for different shapes of air bearings.

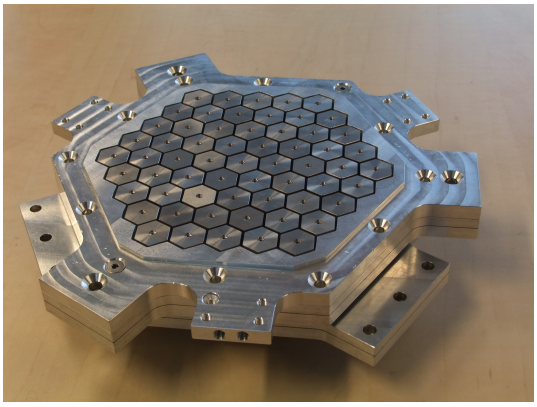

(a) Flowerbed air-bearing table [7].

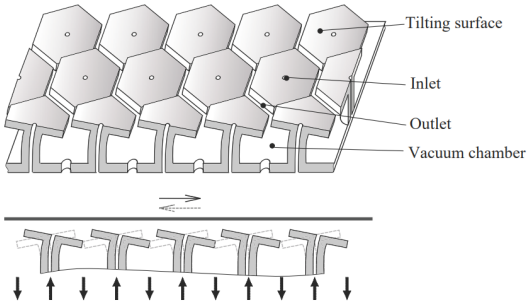

(b) Schematic illustration of the Flowerbed working principle [46].

Figure 3.5: Representation of the Flowerbed.

3.4. MATLAB simulation

In this section, a MATLAB simulation will be done to give a clear image of what a downside view will look like from one building block of the hexagon air-bearing table. One building block from a hexagon-shaped air-bearing table is chosen to be one receiving fibre surrounded by the three colours red, green and blue, each separated 60 degrees from the other. The distance between the fibres can not be known yet because this depends on the diffuser type that will be used. The diffuser type will be chosen in chapter 5. For now, it does not matter how far the fibres are separated from each other. An illustration will be made from the approximate image.

An image is needed from the three-colour circles, each decreasing in intensity towards the edges. The intensity gradient is shaped like a Gaussian distribution, as told in section 3.3. First, the three circles will be made individually. This will be done by making a lot of circles, with each circle a small increase in the radius of its inner neighbour. Each circle that gets a small increase in radius gets a small decrease in light intensity, or a decrease in RGB value. The RBG value is calculated using Equation 3.1. A simple distribution is enough, so the height of the curve can be set to one, the position of the centre can be set to zero and the width of the curve is not known, so a value can be chosen, $a = 1$; $b = 0$; $c = 0.35$.

This results in the following RGB values for each circle:

Red Circle:
$[R,G,B] = [\exp(-\frac{(r/r_{end})^2}{2\cdot(0.35)^2}\ 0\ 0]$

Green circle:
$[R,G,B] = [0\ \exp(-\frac{(r/r_{end})^2}{2\cdot(0.35)^2}\ 0]$

Blue Circle:
$[R,G,B] = [0\ 0\ \exp(-\frac{(r/r_{end})^2}{2\cdot(0.35)^2}]$

Where each radius-increasing circle is defined by r and the last largest circle is defined with r_{end}. The images that are received can be seen in Figures 3.6a, 3.6b and 3.6c. The position of the circles does not matter, only the orientation is important and the circles have to overlap each other if the images are combined. In Figures 3.6d, 3.6e and 3.6f the RGB graph from the corresponding colour circle is shown. What can be seen is that the graphs have the wanted Gaussian form, like in Figure 3.2. The light seen in the figures is two times diffused. One time by leaving the transmitting fibre, and the second time when reflecting from the object back into the receiving fibre. A total image of all three intensity circles can be made. When the images in Figures 3.6a, 3.6b and 3.6c are combined, there will be some overlapping parts. The overlapping parts will result in a combined colour. Figure 3.7 shows the combined image of the three circles.

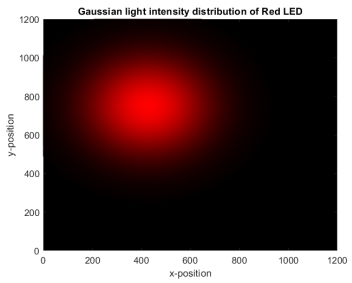

(a) Gaussian light distribution of Red dot.

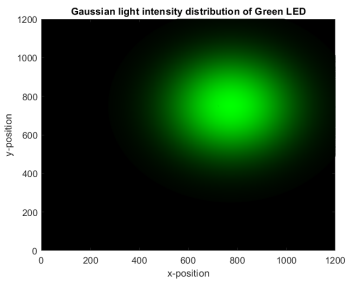

(b) Gaussian light distribution of Green dot.

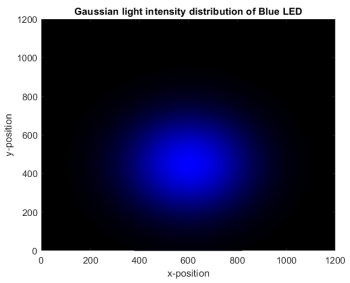

(c) Gaussian light distribution of Blue dot.

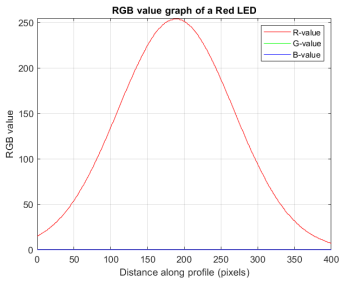

(d) RGB value graph of a Red LED.

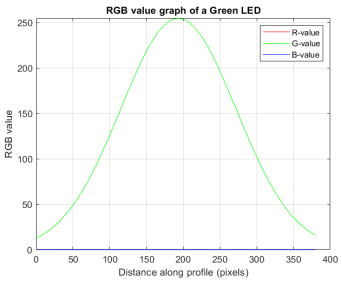

(e) RGB value graph of a Green LED.

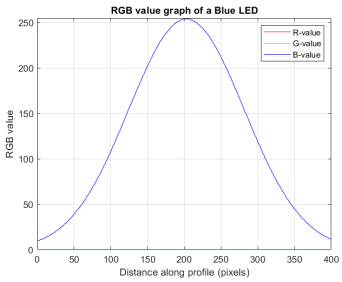

(f) RGB value graph of a Blue LED.

Figure 3.6: Gaussian light distribution of each light colour with the RGB value graph.

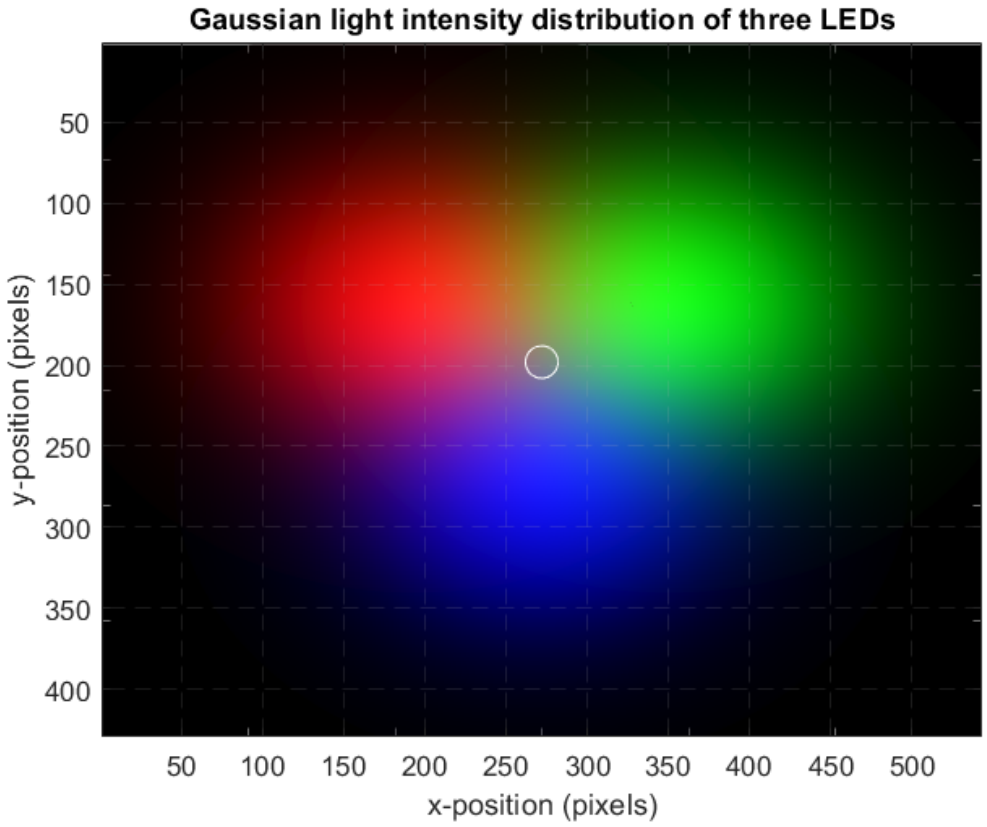

Figure 3.7: The three-colour circles combined in one image, with an imaginary receiving fibre in the middle illustrated as a white open circle.

Let's say there is an imaginary receiving fibre located exactly in the middle of the three circles. This is illustrated with the white open circle in Figure 3.7. The light that is seen in that circle will be received by the receiving fibre. Ideally, all individual values of the RGB value from the centre point are the same. Because this example is a perfect Gaussian distribution, the RGB values are indeed the same.

$$[R \quad G \quad B] \quad = \quad [131 \quad 131 \quad 131]$$

The presumption is that if the object is floating over all three-colour fibres, this RGB value will be the result coming out of the receiving fibre. The value coming out of the receiving fibre will change when, for example, only the colours red and green are covered because the blue light will not get reflected. This simulation investigates light that gets reflected twice. Once coming out of the transmitting fibre and the second time by reflecting from the object into the receiving fibre. To simplify the simulation, two imaginary diffuser layers are stacked on top of each other. This will also be done in the experiments in chapter 5, chapter 6 and chapter 7. The experiments done in chapter 8 will have the final setup where the light will get reflected. If the object in this simulation floats above the red and green LED but not above the blue LED, the light from the red and green light will be diffused twice, but the blue light will be diffused once. The receiving fibre will notice a decrease in the blue value. The image received can look like Figure 3.8. The RGB value of the white dot is in this case:

$$[R \quad G \quad B] \quad = \quad [131 \quad 131 \quad 18]$$

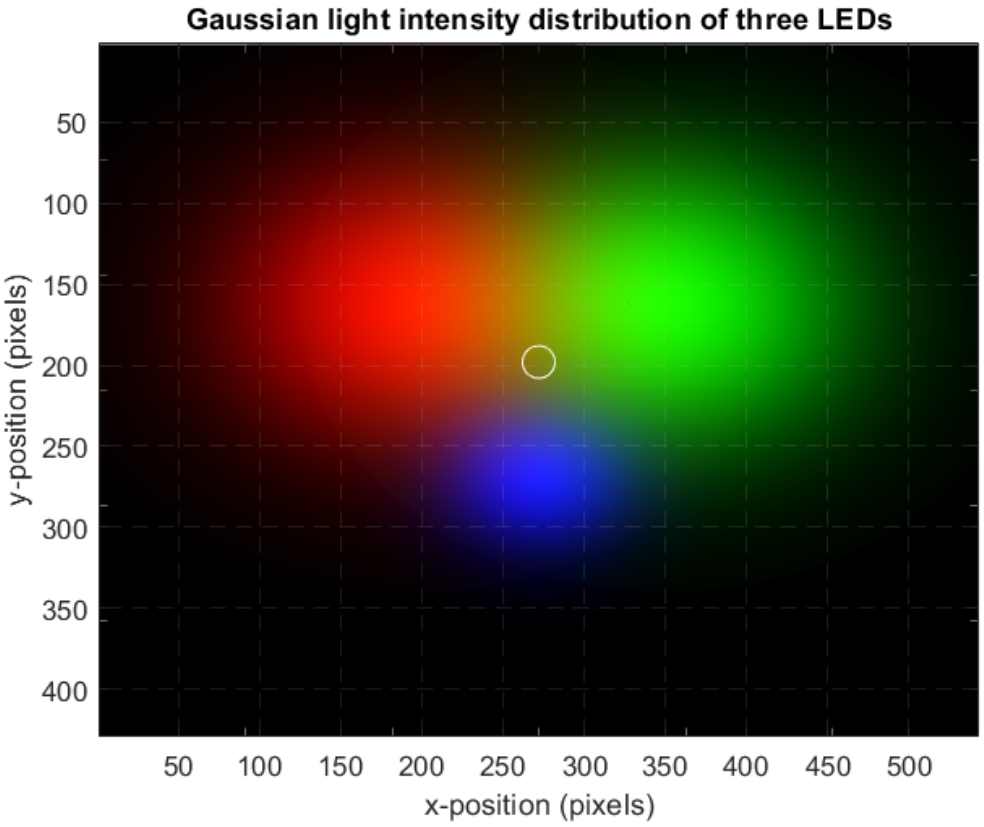

Figure 3.8: An image that can be achieved when the object is floating above the red and green transmitting fibres.

3.5. Conclusion

In this chapter, a theoretical analysis is done about the light intensity distribution from a fibre emitting light after being diffused by a volume diffuser. Various literature papers have experimentally shown that a Gaussian distribution shape for the light intensity profile can be approximated. The shape of the light intensity is known, but the width of this distribution is still unknown. That is because this depends on the diffuser type that will be used. The diffuser type will be tested and chosen in chapter 5. The fibre placement is investigated. The air bearings being used can have various shapes. Eventually, the hexagon-shaped air bearings are used because these shapes connect well without leaving holes in between and there has been done research on it, so it shows great potential. The hexagon-shaped air bearings exclude possible locations for the receiving and transmitting fibres. The corners of the hexagons will be used for the placement of the fibres. Receiving and transmitting fibres will be placed alternately. In this case, the transmitting fibres are 60 degrees separated from each other. A MATLAB simulation of one receiving fibre surrounded by three transmitting fibres is done. From now on, this is the building block where this research will continue with to do experiments on. Each transmitting fibre will have a decreasing Gaussian light intensity spot. The RGB value is calculated exactly in the middle of the light spots. At this place, an imaginary receiving fibre is located. Ideally, each value in the RGB value is the same. The value of a colour can and should decrease when that light colour is blocked by the floating object.

4

Experimental design description

In this chapter, the setup used for all experiments in this research is explained in detail. First, there will be looked at all the different experiments that will be done later in this research. In that way, there can be looked at what objectives the design should meet to let all the experiments succeed. When it is known which experiments have to be achieved and what the design objectives are, the setup can be worked out. All requirements are mentioned and a total 3D design is made.

4.1. Experiments to be achieved

A total of four experiments will be carried out. In these experiments, various things will be investigated. Below is an overview of all four experiments and a brief description of the goal of each experiment.

1. In the first experiment, there will be looked at the scale of the setup. First, the specifications for the camera are tested, like the focussing. When this is done, a scale can be made from the distance in the image compared to the distance in real life. This experiment aims to gain more insight into the scale with which future experiments will be carried out. This will make further experiments easier.

2. In the second experiment, the diffuser type will be investigated. Multiple volume diffusers are chosen and compared on light transmission, diffusivity and layer thickness. The first experiment can be used to get a better insight into measuring the diffusivity of each volume diffuser because the scale is known now. The goal of this experiment is to choose the best volume diffuser to use in future experiments. Previous research tested only three types of diffusers. In this research, more diffusers will be tested and seen if the diffuser chosen in previous research was the right choice.

3. The third experiment is the penultimate step before the final experiment is performed. The concept of combining the three primary light colours is tested and seen what kind of result the image gives when covering one or two fibres with a non-transparent, non-reflective thin material. Reflection will not yet be used in this experiment. The final concept will be imitated by placing two diffuser layers on top of each other and placing the thin material between these two layers.

4. In the fourth and last experiment, the final concept will be tested. Reflection will now be used. This will be done by putting a reflective material above one diffusing layer. In addition to the three transmitting fibres, each of which emits a primary light colour, there is also one receiving fibre positioned exactly in the centre of the three transmitting fibres. The goal of this experiment is to see if the final concept works and what the final measurement range will be of the object moving over the fibres. Also, the third and fourth experiments will be exactly the opposite of each other. Pieces of material will be cut that fit exactly in the available range in the measurement plane. Those pieces of material are cut at a certain angle. One piece will be used in the third experiment and the other piece will be used in the fourth experiment. In that way, the results can be compared with each other. The assumption is that the results will almost be the same.

4.2. Design objectives

The experiments that will be carried out are mentioned in section 4.1. Before making a design, it is necessary to come up with the design objectives. The goal is to execute all experiments with a single setup. This way, the setup does not have to change every time a new experiment has to be performed. The design objectives are mentioned below.

⇒ *Environment sealed from other light sources*
The light coming from the transmitting fibre is the only light source allowed. All other light sources must be eliminated to avoid interference. The biggest disturbance will be ambient light. A completely enclosed environment is required.

⇒ *Light intensity controllable RGB LED strip*
Previous research has used a single-colour LED strip. This LED strip was directly connected to the power supply. This results in an uncontrollable LED strip. The LED had two positions, on and off. This causes some blooming problems. Three colours are used in this study. Each transmitting fibre is connected to an RGB LED strip, each transmitting its own colour. A controller is needed to set the light colour and dim the light intensity to see if blooming can be prevented.

⇒ *Camera that is easy to use*
A camera connected to a computer is very convenient for obtaining images. The camera can transfer the images directly to the computer. The ease of use of the camera is completed when the camera settings can also be adjusted on the computer.

⇒ *A low-cost setup*
The whole idea behind this research is that costs can be reduced. This research is unnecessary if the setup is too expensive. A setup is required that is not too expensive and can solve all problems.

⇒ *Fibre holder block for transmitting and receiving fibres*
In the experiments, a fibre holder block is needed for three transmitting fibres and one receiving fibre. The fibres must be fixed as no movement is allowed. The distances between the fibres must be known in advance so that the scale can be determined. Next to that, the fibres need to come straight out of the fibre holder block because otherwise, the camera will not see a perfectly round light source but an ellipse form. The calculations will be harder then.

4.3. Design and requirements

A setup is needed on which the experiments can be performed. First, it is explained what the setup will roughly look like. Then each part of the setup is explained. Finally, a 3D design is made in which everything comes together. It is important to have a compact design where adjustments can be made easily.

The design is built around the optical fibres because that is where the results should come from. The optical fibres are placed in a 3D-printed object. To perform all experiments, it should be possible to place three transmitting fibres and one receiving fibre in the object. A camera is placed at a certain height above one side of the 3D-printed object with the upward-pointing fibre ends in it. The space between the camera and the fibres is closed off from other light sources with another 3D-printed object. The light source that will be sent into the optical fibres will come from a controllable RGB LED strip. The colour and light intensity is adjustable. An electrical circuit is required for this to work. The circuit must be easily detached for adjustment if necessary.

4.3.1. Optical fiber choice

In chapter 2, it is explained that plastic optical fibres (POF) will be used in this research. The same fibres will be used from Fritz's work. The fibres have a core made from polymethylmethacrylate (PMMA), a fluoropolymer cladding and a coating made from polyethylene (PE). In Figure 4.1a the construction of a plastic optical fibre can be seen. The chosen fibre has a core with a diameter of 980 μm and a cladding thickness of 10 μm. This adds up to a diameter of 1000 μm. The coating has a thickness of 600 μm. The total diameter of the optical fibre is 2200 $\mu m = 2.2\ mm$.

The cutting of the fibres will be done with a sharp razor blade. The end of the fibre will be ground with

very fine sandpaper. Research has shown that this is a valid way to cut the plastic optical fibres [30]. To check if there are no damages, a camera will look at the fibre like in Figure 4.1b.

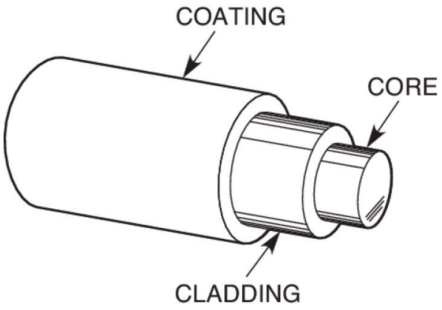

(a) Structure of a plastic optical fiber [20].

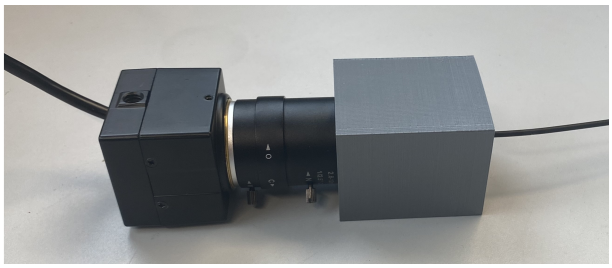

(b) A camera that checks the optical fibers for damages.

Figure 4.1: Plastic optical fiber validation.

4.3.2. Camera

The same camera will be used in this research as in the previous research from the bachelor's project and the master's thesis. The choice they made was an ELP-USBFHD01M-BFV. The camera is a webcam that can capture videos at 60 frames per second in 720p HD and 30 frames per second in 1080p full HD. The varifocal lens of the camera is adjustable between 2.8 mm and 12 mm. This allows a short distance between the camera and the measurement plane, resulting in a compact design. The camera is directly connected to a computer. MATLAB can easily be used to automatically capture and analyse pictures and adjust the settings of the camera. Another camera is used to check that the optical fibres on damages. The camera used for this is an ELP-USB8MP02G-SFV. This camera also has an adjustable varifocal lens between 2.8 mm to 12 mm.

4.3.3. RGB LED strip controller

A red-coloured LED was used as the light source in previous research. The LED was pointing to one end of the optical fibre. The different diffuser layers were placed on the measurement plane to carry out the experiments. The LED could be seen as a switch. It could be turned on or off. The light intensity could not be controlled, resulting in a lot of blooming and white spots of high light intensity in the centre of the light circle formed on the diffuser layers. What was told in chapter 1 is that the use of multiple colours will be investigated. The three primary colours red, green and blue will be used, so three transmitting fibres are required, each connected to its own LED. The desire for this research is to find a way to control the light intensity coming out of each LED, and in that way also the light intensity coming out of the fibres. Fritz used a red LED strip that was directly connected to a 12V power supply. Three RGB LED strips will be used in this research. Each RGB LED strip is connected to a different transmitting fibre. An electrical circuit is required between all LED strips and the power supply. Potentiometers can be used to control electrical devices. It has a sliding or rotating contact that forms an adjustable voltage divider. The voltage that goes through the LED strip and thus the light intensity that comes from the LEDs are adjustable. The electric circuit that will be used can be seen in Figure 4.2.

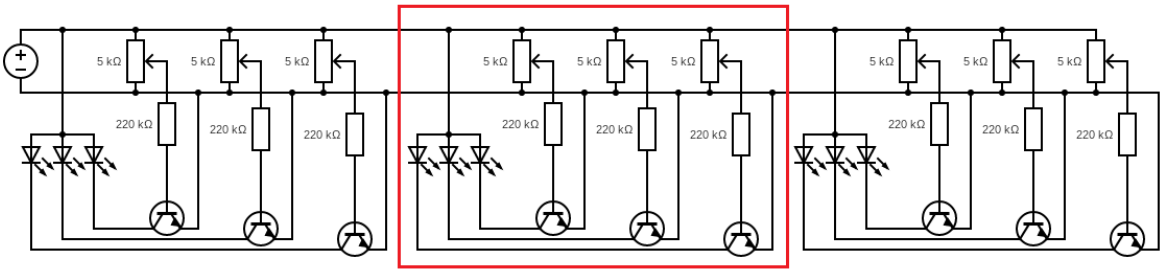

Figure 4.2: Total electric circuit used to control each colour from each RGB LED strip. One individual RGB LED strip is shown in the red box.

4.3.4. 3D-print design

A 3D-print design is needed where all previously mentioned components can be placed in. The setup needs to be sealed from other light sources like ambient light. In Figure 4.3, a SolidWorks model can be seen that illustrates the final design. It is a hollow box with three lids on top of it. The two blue lids are connected to an electrical circuit that is located inside the hollow box. To control the light intensities of the optical fibres, three potentiometers per optical fibre are located on top of the box. The part that fixes the optical fibres, the so-called fibre holder, is located on top of the yellow-coloured middle lid. The fibre holder has four holes on the top side and four holes on the bottom side. Three holes are meant for the three transmitting fibres and the fourth hole is for one receiving fibre. Only one setup will be made. For that reason, not all holes will be used in all experiments. The holes at the bottom side of the fibre holder are directly connected to the LED strips. The holes at the bottom side are always located at the same position, but the distances between the holes at the top side can be adjusted by printing a new block. In that way, the middle lid does not have to be printed again if the distance between the holes is adjusted. The optical fibres will bend in the fibre holder because the holes are not aligned. The images made with the camera can easily be scaled if the distance between the fibres is known in real life. The edges of the fibre holder are slightly higher to accommodate the diffuser layers and thin material placed on top. At last, a cap will be placed over the fibre holder with a camera on top of it. This is not illustrated in the figure.

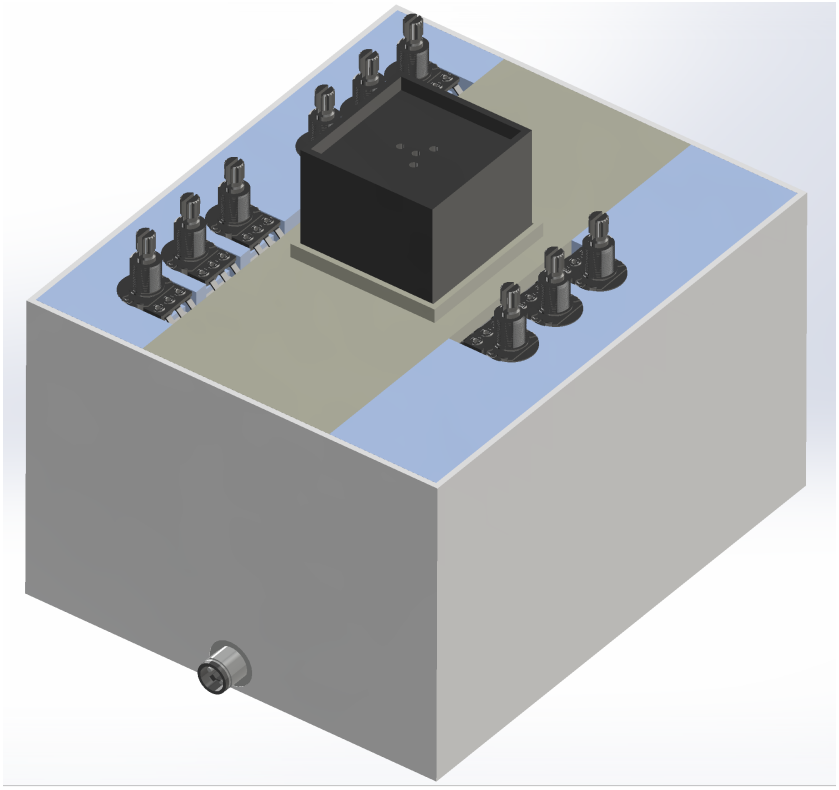

Figure 4.3: Solidworks 3D-model of the whole setup without the cap that keeps out external light and without the camera.

4.3.5. Result

The final result of the whole setup can be seen in Figure 4.4. Figure 4.4a shows the setup with the cap, which eliminates external light sources, and the camera on top. In Figure 4.4b the setup can be seen without the cap and camera, like in the 3D model in Figure 4.3. The bottom side of the setup where the integrated electrical circuit is located van be seen in Figure 4.4c.

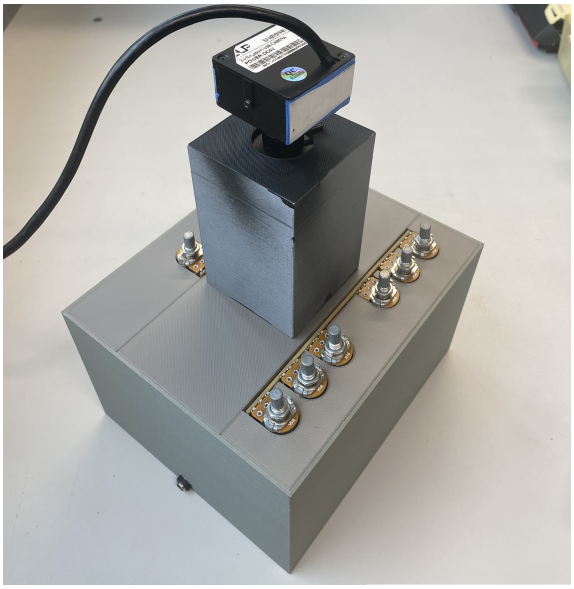

(a) Top view of the setup with cap and camera.

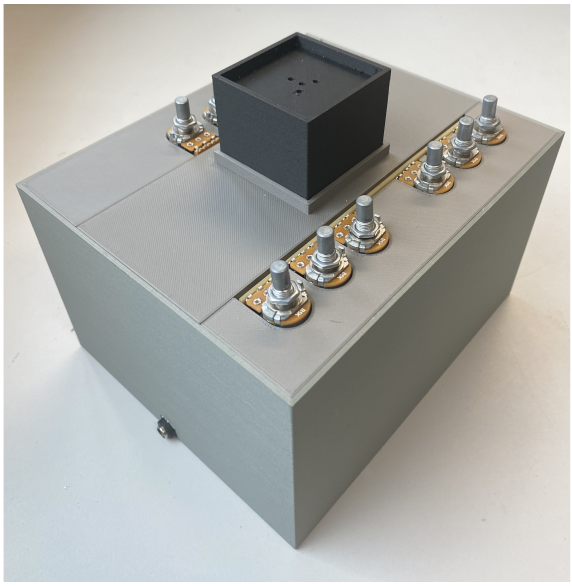

(b) Top view of the setup without cap and camera.

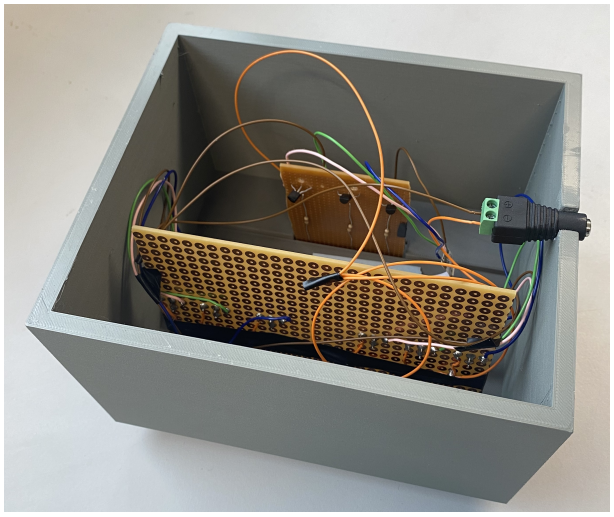

(c) Bottom view of the setup..

Figure 4.4: Total setup to execute all experiments.

4.4. Conclusion

This chapter provided insight into the complete design to perform experiments on. First, all four experiments that will be done are listed and the purpose of the experiments is explained. The goal of the first experiment is to get more insight into the scale of the setup. The distances in the image and in real life can be compared. The diffuser type that will be used is explained in experiment two. The third experiment will test the concept of combining the three primary light colours and what the result will be in the images when looking from the top down at the measurement plane. The last experiment will also test the use of three colours, but in this case, there will be looked at what the influence will be if reflection is used. In the second section of this chapter, all the design objectives are mentioned to know what the design must meet. The third section is all about the design itself and the requirements. The optical fibre that will be used is explained as well as the camera, the RGB LED strip and the 3D-print design. Now that the entire design has been thoroughly worked out, the experiments in the following chapters can be carried out.

5

Experiment 1: Scaling the system

The whole setup is explained, so the first experiment can be performed. This experiment aims to scale the system from real millimetre distances to pixels in the images captured by the camera. In the experiments that will be executed, a lot of images will be captured. The centre of each optical fibre will be calculated once to prevent that for each image the centres of the fibres have to be calculated individually. A MATLAB code will find automatically the centres of the transmitting fibres and compute the position of the receiving fibre. Next to that, this chapter finds the most optimal camera position. In later experiments, the known scale and camera position will be used for choosing a diffuser type in chapter 6 and to translate a received RGB value in object displacements or object positions in chapter 7 and chapter 8. The assumption for this experiment is that it can work very well if the scale is calculated in the right way so that a small offset does not influence the scale much.

5.1. Experiment layout

The design explained in chapter 4 will be used. In this experiment, only the three holes in the fibre holder where the transmitting fibres will be placed are used. No diffuser layers are laid over the fibres yet. The light intensity of each fibre is set to a very low value via the potentiometers. Then the camera will focus the image. What is expected and also desired is that saturation is prevented. The camera will be set to a fixed position away from the fibre block that will be used for making all the pictures in later experiments. The camera will make a picture from the three transmitting fibres, each emitting its own colour. MATLAB can compute the centre positions of the transmitting fibres. From those centre positions, the position of the receiving fibre can be calculated, because that is positioned exactly in the middle between the transmitting fibres. Multiple pictures will be taken to make the offset as small as possible. The coordinates can be used for further experiments. In section 5.2 two ways will be explained on how the scale can be computed. The design preparations are mentioned in section 5.3 This scale that will be calculated in section 5.4 will be used for later experiments.

5.2. Possibilities measuring the scale

The picture created in this first experiment consists of only three circles of light, red, green and blue, each circle represents one transmitting fibre. The scale of the picture can be calculated in several ways. Two ways are explained and investigated.

1. The diameter of each fibre is known in real life. When the three circles of light are imaged, MATLAB can count the number of rows and columns that make up each circle. In this way, a scale can be made to express one pixel in a certain distance in millimetres and to convert one millimetre into a number of pixels. There may be an offset, so this can be done for all three circles of light to try to make this offset as small as possible. The mean can be calculated to get a more accurate value.

2. Another method is to use the distance between the transmitting fibres, which is also known in advance. The distance is set in SolidWorks and the fibre holder is printed with a 3D printer. There may be a small offset when printing, but the diameter of the holes is very small compared to the distance between the

fibres, so an offset will not have much of an impact. Again, the distances between all three transmitting fibres can be averaged to get a more accurate value.

Both methods seem to work, but one has the advantage. It has been said that the diameter of the holes where the fibres are placed is very small. The total number of pixels in the rows and columns that make up the circle of light will be small. A small offset will affect the scale enormously. An offset may develop when saturation occurs. The desire is to eliminate saturation, but because the diameter is so small, just a little bit of saturation gives a big scale difference. In the second method, the distances between the fibres are way larger compared to the diameter of the fibre. An offset does not affect the scaling enormously. Therefore, the second method will be used.

5.3. Design preparations

Before starting the experiment, some preparations need to be made. The setup has already been explained in chapter 4, but the requirements need some insight. The optical fibres must be checked for damage before using them. Some programming is also required. The centre pixel coordinates of the light circles created by the optical fibres have to be measured in a way. MATLAB can automatically find the centre positions of these light circles. These positions are necessary to measure the distances between the fibres and come up with a scale for the design. Finally, some mathematical preparations relevant to this experiment will be examined.

5.3.1. Optical fibres

Three transmitting optical fibres will be used in this experiment. The fibres must be placed in the fibre holder, therefore they must be cut to specific sizes. Chapter 4.3 explains how the fibres are handled. The fibres are cut with a razor blade and finished with fine sandpaper. The setup shown in figure 4.1b will be used to see if there are any cracks in the fibre core. The result can be seen in Figure 5.1. All three fibre cores show no cracks and are perfectly usable.

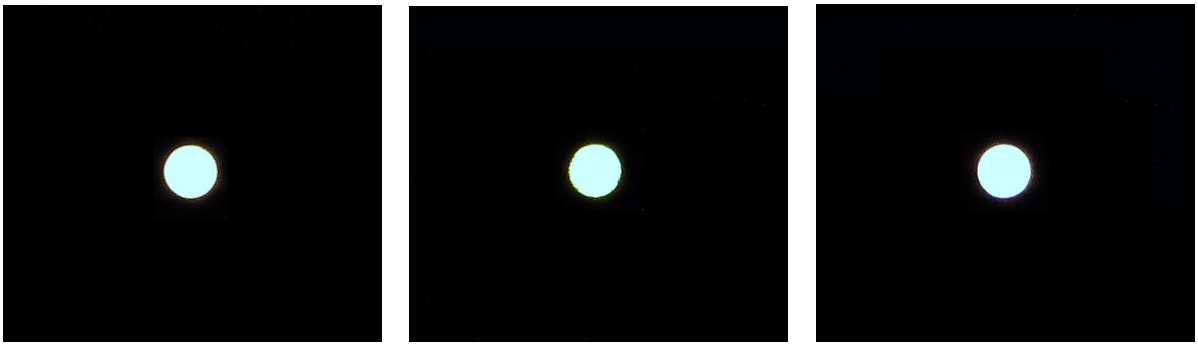

(a) First optical fiber. (b) Second optical fiber. (c) Third optical fiber.

Figure 5.1: Checking for cracks in the to-be-used three transmitting fibres.

5.3.2. MATLAB programming

The position of each optical fibre has to be found. A MATLAB code can be created that finds these positions automatically. The code can be found in appendix B. In this section, the code is broken down into small parts, after which each part is briefly explained.

An image consists of pixels. Each pixel consists of a colour code. The colour code can be in grey code or RGB code. Grey code only has one 2D matrix. Each pixel has a value between 0 and 255. This value indicates how black or white a pixel is. Zero means a completely black pixel and 255 means a completely white pixel. Everything in between has a grey scale. RGB code is a 3D matrix where each pixel has a code for each colour. There are, in an RGB code image, a total of three 2D colour matrices for red, green and blue. When an image is loaded into MATLAB, the code looks at every colour matrix individually. The code first looks at the red colour of the image. All low values are filtered out to remove distortions in the image. The result is a matrix with zeros and high numbers in the places where the red circle of light is located. The code finds the rows and columns that contain these high numbers. The mean is taken from the rows and columns to find the pixel

coordinates of the centre of the red light circle. This should also be done for the green and blue matrices. The result is three coordinates of the centre of each transmitting fibre. The distances between the centres can be calculated and compared. The three distances should be the same but may have a slight deviation in the order of a few pixels. The distance between the points has a relatively large number of pixels, so an offset of a few pixels will not affect the measurements much. The position of the receiving fibre can be calculated using the fact that all fibres are the same distance from each other. So an equilateral triangle is formed if the centre points are connected. How the centre can be calculated is explained in the next subsection.

5.3.3. Introducing coordinate system

In this section, some mathematical preparations will be made to find the desired results of this first experiment. A coordinate system will be introduced that is used for all experiments executed in this research. In section 3.3, it is explained that a hexagonal air-bearing table will be used. The optical fibres are ideally placed on the edges of the hexagons. The choice was made to place the fibres on the corners. There are a few things to keep in mind when placing the fibres. Each receiving fibre must be surrounded by all three differently coloured transmitting fibres, and the distances between the fibres must be the same. In that way, symmetry in the system can be achieved. The placement of the fibres looks like Figure 3.4c. One building block is examined. One building block contains one receiving fibre surrounded by three transmitting fibres, red, green and blue. When the three transmitting fibres are connected, a triangle appears. The nice thing about this triangle is that it is equilateral. This makes each corner also equal, namely 60 degrees. A schematic illustration can be seen in Figure 5.2. The position where the receiving fibre is located is the origin of the coordinate system, point (0, 0). The distance between the transmitting fibres is set to variable m. The intersection of the three lines that are perpendicular drawn from the centre of the sides of the triangle to the opposite transmitting fibre is the centre of the triangle, where the receiving fibre will be positioned. The length of one line segment is set to variable n. The relation between m and n is shown in Equation 5.1.

$$n = \sqrt{m^2 - (\frac{1}{2}m)^2} = \sqrt{\frac{3}{4}m^2} = \frac{\sqrt{3}m}{2} \Rightarrow m = \frac{2n}{\sqrt{3}} \tag{5.1}$$

The coordinates of the transmitting fibres can be written in n and m.
R(0, $-\frac{2}{3}n$), G($-\frac{1}{2}m$, $\frac{1}{3}n$), B($\frac{1}{2}m$, $\frac{1}{3}n$).

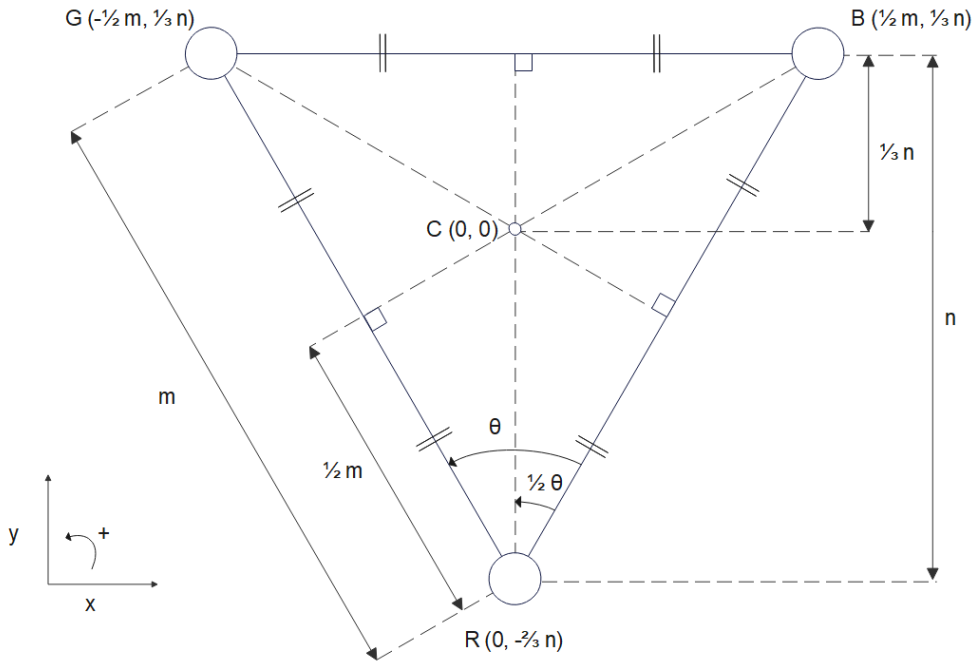

Figure 5.2: Schematic overview of the three transmitting fibres and the receiving fibre in the middle.

5.4. Results

The results of the first experiment will be shown and discussed in this section. Before experimenting, the distance m, which indicates the distance between two transmitting fibres, must be set to a certain value. This is possible in the SolidWorks model of the fibre holder block. The distance between the transmitting fibres is set to a certain value. The importance of this value will be noticeable in later experiments. The distance m is set to 10 millimetres. All preparations have been made so that the camera is ready to take an image of the measuring plane. Multiple pictures will be made with the same variables to make up for possible offsets. The picture created can be seen in Figure 5.3a. Figure 5.3b shows the MATLAB result of the picture. Lines are drawn between the centre pixel coordinates of the three light circles. Also, Four circles are drawn, three circles around the centre pixel coordinates of the three transmitting fibres and one to illustrate the centre of the appeared triangle to get a similar picture as in Figure 5.2. The distances between the fibres should be checked first to see if they are the same. If they are not about the same, something went wrong in the MATLAB code or when specifying the distances in the SolidWorks model. One more check is performed to ensure that the correct method is used. The midpoints of the lines between the transmitting fibres are calculated and lines are drawn perpendicular to their opposite transmitting fibre. The three lines intersect each other at point C. It can be assumed the right method has been used. The distances between the fibres are shown in Table 5.1.

	Length between fibers (pixels)	**Scale 1 millimetre (pixels)**	**Scale 1 pixel (millimetres)**
Red → Green	304.266	30.4266	0.0329
Red → Blue	306.297	30.6297	0.0326
Green → Blue	310.000	31.0000	0.0323

Table 5.1: Distances between the centres of the transmitting fibres with the corresponding scale.

The average can be taken from the distances in Table 5.1 to get an average scale. The scale below will be used in future experiments. The inaccuracy range is also shown. This accuracy is about 2% which is acceptable.

$$\begin{aligned} 1 \quad millimeter &\approx 30.686 \quad pixels \\ Inaccuracy \quad range &\approx 0.5734 \quad pixels \end{aligned}$$

$$\begin{aligned} 1 \quad pixel &\approx 0.0326 \quad millimetres \\ Inaccuracy \quad range &\approx 0.0007 \quad millimetres \end{aligned}$$

The resolution of the picture is 1080x1920p. The pixel coordinate system will only be used in the calculations in later experiments. The centre pixel coordinates of the receiving fibre and the transmitting fibres are listed in Table 5.2. It also stated how many rows and columns the three transmitting fibres consist of.

	Centre coordinates (pixels)	**Dimensions fibre (pixels)**
Red fibre	[688, 965]	28x28
Green fibre	[425, 812]	29x28
Blue fibre	[425, 1122]	29x29
Receiving fibre	[513, 966]	N/A

Table 5.2: Distances between the centres of the transmitting fibres with the corresponding scale.

The second method from section 5.2 can check whether the measured scale is somewhat correct. Table 5.2 gives an average dimension for the three transmitting fibres of 28.67x28.34 pixels. In real life, the fibres have a diameter of one millimetre. The scale will be 1 millimetre = 28.5 pixels, or 1 pixel = 0.0351 millimetres. This is close to the previously calculated scale. The difference lies in the small diameter of the fibres. A small offset results in a large change in scale

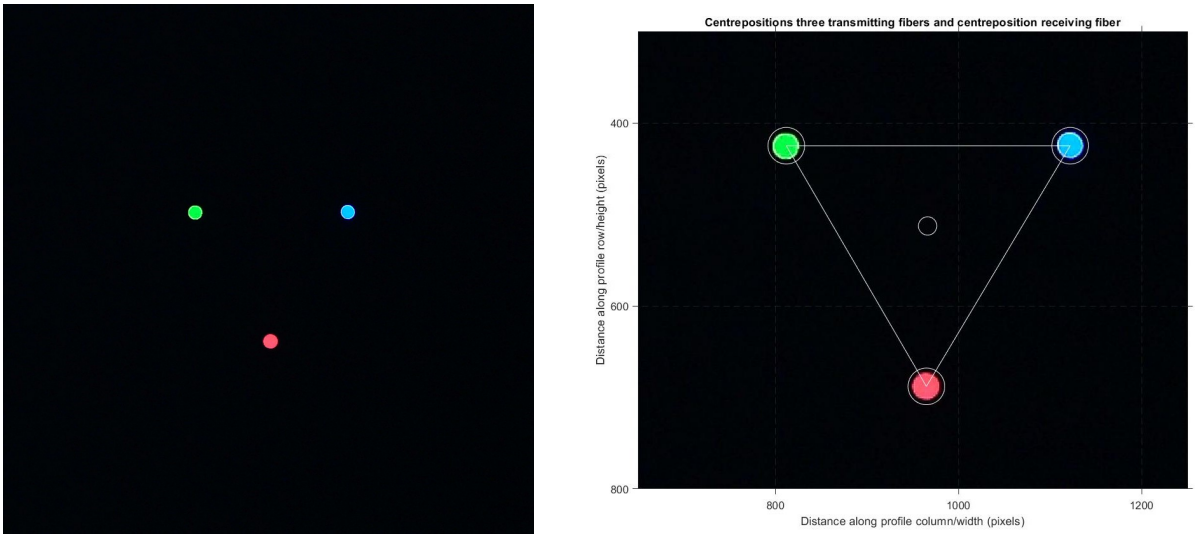

(a) Picture of the measurement plane without diffusers.

(b) MATLAB result picture.

Figure 5.3: The picture that was taken with the camera with the MATLAB result.

5.5. Conclusion

The goal of this first experiment is to get a good understanding of the pictures taken with the camera and to get the scale from that. This is done by first explaining how the experiment will be carried out. After that, two ways have been found to calculate the scale of the picture taken by the camera. The first way is by calculating the dimensions of the circle of light that appeared. This can be converted to a scale when compared to the diameter of a fibre in real life. The second method is by comparing the distance between two transmitting fibres to the distance it has in real life. The second option was chosen because the distance between the transmitting fibres is greater than the fibre diameter. An inaccuracy in measuring the distance in the picture does not lead to a big inaccuracy of the scale. After this method was chosen, the design preparations were made. The optical fibres were checked for cracks, the MATLAB code, which automatically finds the scale of an image, is explained, and some mathematical preparations have been made. The mathematical preparations explained the relationship between the distances in the equilateral triangle that appears when the transmitting fibres are connected. The coordinate system from 5.2 will be used for the experiments executed in later experiments. The pixel coordinate system, with the centre pixel coordinates, will only be used in the calculations executed in MATLAB in later experiments. In the last section, the results are discussed. The method that calculates the scale of a picture is explained by making multiple pictures with the same variables. The average of the pictures will be taken to compute the scale for the picture. Finally, the centre pixel coordinates of the fibres are calculated. These coordinates are necessary for later experiments.

6

Experiment 2: Diffuser realization

In this chapter, the second experiment is performed. The experiment aims to find the most optimal volume diffuser to use for future experiments. Different diffusers will be experimentally tested. The results can give a clear idea of which diffuser is best. It is also possible that the results do not differ from each other. Then it does not matter which diffuser is going to be used. Finally, one volume diffuser is chosen. This chapter starts with a more detailed explanation of the experiment, such as what design preparations are needed and what kind of results are desired. It also explains how to compare the diffusers. The second part describes the properties of the diffuser and how it affects the light that passes through it. The volume diffusers used are listed next. The results will be mentioned and the diffusers with the most potential will be shown. These diffusers will be further investigated. Finally, it will be concluded which diffuser will be chosen and which will be used in further experiments. The presumption is that the diffuser will be chosen with the highest diffusivity and that shows the least amount of blooming in the middle. The high diffusivity can be used for higher measure accessibility, and the blooming has to be prevented because of the thought that object positions or movements can otherwise not be distinguished.

6.1. Experiment layout

This experiment aims to find the best diffuser to use in this research. To do this, several diffusers are experimentally tested. The design explained in chapter 4 will be used again. Three transmitting fibres are placed in the fibre holder block, each fibre transmitting its own colour. The camera will look at the measurement plane from the top. The final concept will be imitated. If the object is moving over the air bearings and covers one building block completely, so covering all three transmitting fibres, light from each of the three surrounding transmitting fibres will reach the corresponding receiving fibre in the centre. The light coming from the transmitting fibres will pass through two diffuser layers. The light comes out of the transmitting fibre through the diffuser layer and reflects against the object. The light will again go through the diffuser layer into the receiving fibre. This concept is imitated by putting two identical diffuser layers on top of each other onto the measurement plane and looking down at it with the camera. The light intensity from each LED is set to one specific value that is used for testing all diffuser types. In that way, the images can be compared to each other. The pixel coordinates of the centre positions are calculated in chapter 5. A small area around the centre coordinates is taken and the average of the RGB value is calculated. A light intensity graph is made across a line that goes through one light circle. This will be done for all pictures to see how the light intensity decreases when moving further away to the outside.

The diffusers with the most potential will be chosen for more evaluation. Now three light-intensity graphs will be made going through all light circles. The light intensity of each individual LED will be adjusted in such a way that all light intensity graphs show the same course. This will be done by looking at the slopes of each light intensity graph. It can be assumed that the light distribution from each LED has the same course if the slopes are about the same. The reason why the light intensity graphs need to be the same is that probably the measurements will be easier. Possible displacements of the object can be seen in Figure 6.1. Ideally, the change in R-value along the red line must have the same gradient as for the change in G-value along the

green line and for the change in B-value along the blue line. If the course of the light intensity graphs is not the same, each colour must be calibrated for the specific gradient it has in its light intensity, which makes the measurements more difficult. The experiment will show if this is possible with the setup and requirements that have been chosen earlier.

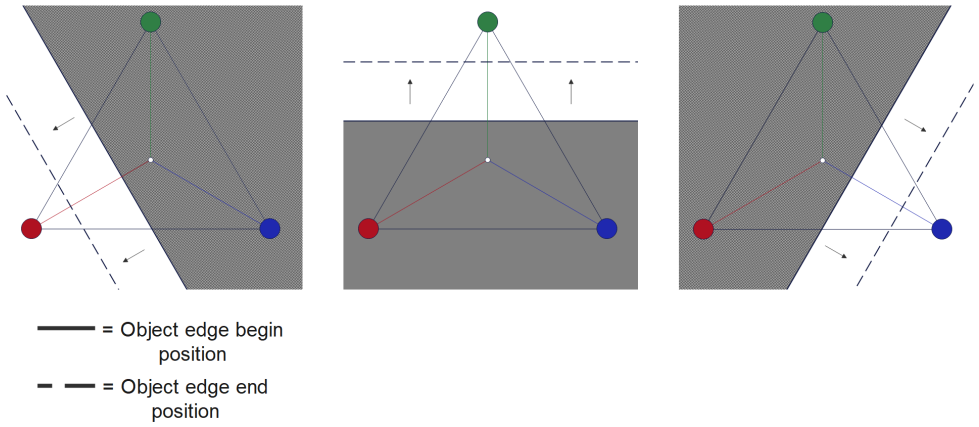

Figure 6.1: Schematic representation where the change in the red, green and blue value in the RGB code should be the same when travelling the same distance to the red, green and blue transmitting fibre respectively.

6.2. Diffusers being tested

The volume diffuser choice is crucial in this research as it depends on the diffuser how the light is diffused and this will influence the final results. To choose the best volume diffuser, a group of volume diffusers is tested. First, the three most important properties of a volume diffuser are explained. The list of diffusers that will be tested is mentioned next, and finally, the method is explained on how to compare the diffusers.

6.2.1. Diffuser properties

The working principle of a volume diffuser has been explained in section 2.2. There are a lot of different volume diffusers that can be chosen. Each diffuser has its own applications. What is good to know is which properties are important in this research. The three most important diffuser properties are listed below.

⇒ *Light transmission*
A high transmission means that more light will pass through the volume diffuser. So less light is needed. It is measured as a percentage of light that remains, out of the total light being sent into the diffuser. The transmission is not really important, but a somewhat high transmission is needed for acceptable efficiency. The transmission and diffusivity cannot both be high. The experiments have to show which combination of diffusivity and transmission fits best in this research.

⇒ *Light diffusivity*
The size of the light spot is important. High light diffusivity means that the light will spread with a wider angle, which causes an increased light spot size. Light diffusivity is measured in a percentage. A higher value means a wider spreading angle. The increased light spot size causes a wider viewing range of each transmitting fibre. In that way, the distance between the transmitting and receiving fibres can be larger. The most ideal expectation is that the receiving fibre is located around the middle of the gradient of the light intensity circle. At this point, the derivative of the intensity curve will be the largest. A small movement of the object would probably result in a highly noticeable change in RGB value.

⇒ *Layer thickness*
The volume diffusers will be placed over the optical fibres. The amount of light that will pass through the diffuser depends also on the thickness of the diffuser. A thicker layer means less light passes through, and a thinner layer means that more light passes through. The reason for that is that there are some light intensity losses because light also reflects backwards inside the volume diffuser. How thicker the diffuser layer is, how more light is reflected backwards. There is not an unlimited amount of space, so

the thickness of the diffusers cannot be too big. Also, a diffuser that is too thick is difficult to cut into the desired dimensions. It is important to keep in mind that how thicker the diffuser layer will be, how more light will reflect backwards. So more light can be achieved in the receiving fibre only through back-scattering. This can affect the measurements in a bad way. The amount of light that gets reflected backwards must be derived from the experiments.

6.2.2. Diffusers being tested

A choice has to be made about which diffusers will be tested. Table 6.1 shows the six diffusers that will be experimentally tested. The diffusers are chosen in such a way that there are different combinations between the light transmission, light diffusivity and layer thickness explained in the previous subsection. In this way, the ideal combination of the three diffuser properties can be found.

Diffuser type	**Light transmission (%)**	**Diffusivity (%)**	**Layer thickness (mm)**
PRIMO N381 PMMA XT	71	56	2
PRIMO XT N385	33	89	2
Makrolon DX NR 139 cool	63	87	1.5
Makrolon DX NR 139 cool	55	79	3
Pyraled YT275 PMMA	77	67	1.8
Setacryl M2002 opal	41	91	3

Table 6.1: The six diffusers that are tested with their most important properties.

6.2.3. Comparing method

To choose between the volume diffusers, a comparison method is needed. It is helpful to get a clear view of how the light travels from the transmitting fibre to the receiving fibre. It is important to keep in mind that the light within the diffuser can scatter in all directions. Figure 6.2 shows a side view of two possible paths that light rays can make when travelling. These two light paths are not the only ones, but they illustrate an example. The bold red line represents a possible light spot on the floating object. The figure clearly shows that the light that will be received by the receiving fibre can come from any point of the light spot on the floating object due to the scattering effect within the volume diffuser. This scattering effect, which is caused by the small particles inside the volume diffuser, is explained in section 2.2. The whole light spot created by each volume diffuser must be examined when comparing the pictures. A second thing that is important to look at when the diffusers will be compared is how wide the light spot is. If the bold red line in Figure 6.2 is too small, there is a possibility that the object will not receive any of the light rays. The edge of the object is floating between the fibres, just outside the light spot size. This can lead to inaccurate measurements. The last thing to look at is whether a light spot created by a transmitting fibre is so wide that it affects other receiving fibres that are not adjacent. The system may still operate when light from the transmitting fibres reaches receiving fibres that are not just adjacent. A requirement that has been chosen in this research is that the light from the transmitting fibres only reaches the adjacent receiving fibres and no others. Below is an overview of how the diffusers should be compared.

1. The light spot created on the floating object should be evenly distributed. Blooming is not desired in the light-intensity graph. If the red LED is investigated, the middle of the light spot should not have a lot of blue and green in it. Also, horizontal lines in the light intensity graph are not desired. A horizontal line in the light intensity graph means that the light spot has the same intensity along a certain distance. This mostly happens when there is blooming in the middle of the light spot. This can sabotage the measurements because a small displacement of the object can result in no difference in RGB value in the centre.

2. The light spot size should be as wide as possible, but not too wide. The light from a single transmitting fibre must reach all adjacent receiving fibres to get any result. When looking from the other side, one receiving fibre must always receive light from all the transmitting fibres adjacent to it if the floating object covers the receiving fibre. There is only one limitation, the light coming from a transmitting fibre can only reach the adjacent receiving fibres.

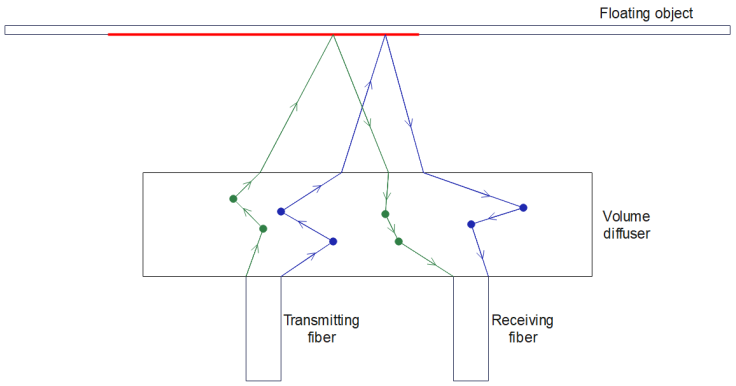

Figure 6.2: Schematic representation of how the light can travel from the transmitting fibre to the receiving fibre.

6.3. Results

This section tests the diffusers from table 6.1. The only difference in the whole experiment is that a different diffuser type will be used. All other variables are the same. The light intensity is set to one value, which is used to test all diffusers. The camera is always the same distance away from the measurement plane with the same focus. This results in the same coordinates for the centre point in each picture. In chapter 5 the same distance between the camera and the measurement plane is used, so the centre pixel coordinates of the LEDs and the position of the receiving fibre can be used for measuring the RGB values and making the light intensity graphs. Offsets are solved by taking a 40x40 pixel matrix around the centre coordinate. The mean value of the matrix of the RGB code is calculated. The RGB values in each picture are compared to see which diffuser can diffuse the light the most. Next to that, the middle of all light circles is investigated to see if blooming occurs. After the six diffusers are tested, the ones with the most potential will be investigated more.

6.3.1. All diffusers

The pictures taken by the camera for the different diffuser layers can be seen in Figure 6.3. In Figure 6.4, the light intensity graphs can be seen for each picture. The light intensity is measured on the line that runs from the x-coordinate of the green LED, through the middle of the red LED, to the x-coordinate of the blue LED. The line is illustrated in Figure 6.5a. The red intensity peak will be in the middle of the graph, where the red light source is located. The green and blue value is shown as well to illustrate blooming. Blooming happens when the red line becomes horizontal at its maximum of 255 and also high values of green and blue can be observed in the middle of the graph. What can be concluded from the light intensity graphs is that the graphs can be approximated by a Gaussian form, which has been predicted in chapter 3. In Table 6.2 extra information is given from the pictures in Figure 6.3. The mean of the RGB value of the matrix around the centre position is given. The blooming is shown by mentioning the number of pixels where the red intensity is 255. At last, the slope is calculated from the curvature. The slope is calculated in a change in R-value per pixel displacement. A high slope means a fast-decreasing intensity. A slow decreasing intensity is desired because that gives a wider light circle.

6.3.2. Potential diffusers

The pictures and corresponding light intensity graphs will be investigated to find one or multiple diffusers to examine more. What can be seen in the pictures is that Figures 6.3a, 6.3c, 6.3d and 6.3e shows big white spots in the middle of the light circles. This corresponds with the light intensity graphs in Figures 6.4a, 6.4c, 6.4d and 6.4e where the overexposure is high and the green and blue values in the middle are relatively high. The white spots can be eliminated by adjusting the light intensity. The problem is that the RGB value will also decrease when the light intensity is taken down. What can be concluded from Table 6.2 is that the RGB value

of the receiving fibre location in each picture is about equal. If the light intensity will be taken down for the PRIMO N381, Pyraled YT275 and the two Makrolon diffusers the RGB value will be worse than the PRIMO XT N385 and Setacryl M2002 opal. Also, Figures 6.3b and 6.3f, which illustrate the light intensity graphs from the PRIMO XT N385 and Setacryl M2002 opal, show that the red value has not reached its maximum yet. The light intensity can be set even higher. This also results in a higher RGB value at the receiving fibre location. The PRIMO XT N385 and Setacryl M2002 opal diffusers will be examined more to see their full potential.

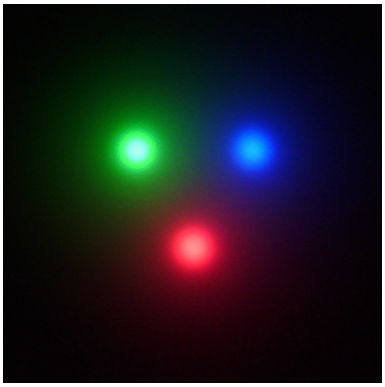

(a) PRIMO N381 PMMA XT

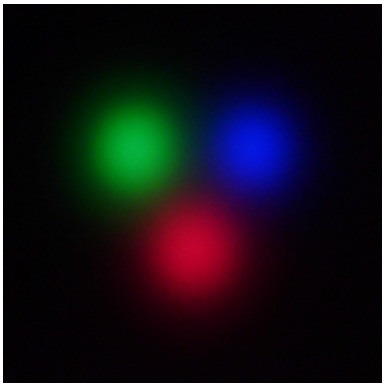

(b) PRIMO XT N385

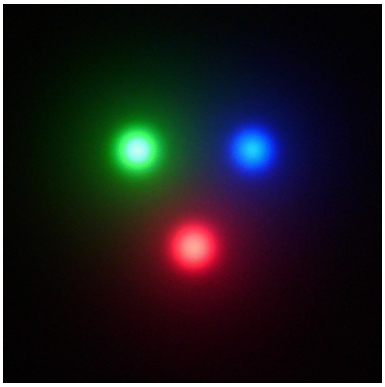

(c) Makrolon DX NR 139 cool 1.5mm

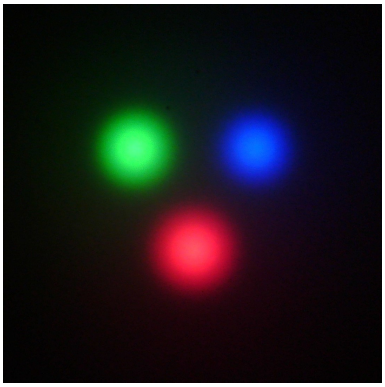

(d) Makrolon DX NR 139 cool 3mm

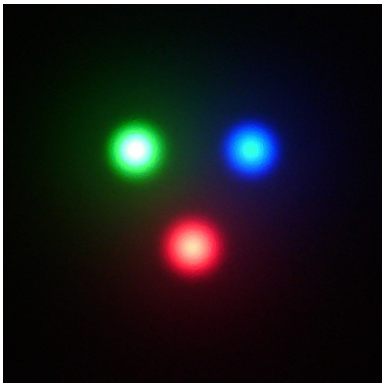

(e) Pyraled YT275 PMMA

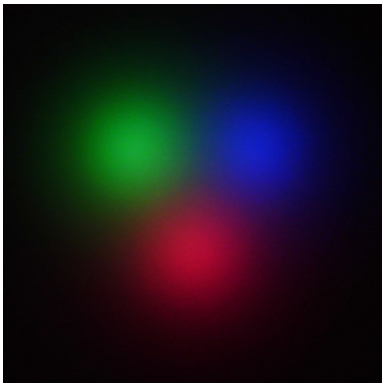

(f) Setacryl M2002 opal

Figure 6.3: All six pictures made by the camera with different diffuser layers.

Diffuser type	**RGB value receiving fiber (0-255)**			**Blooming (pixels)**	**Slope (R-value/pixel)**
PRIMO N381 PMMA XT	61	60	66	112	~ 2.86
PRIMO XT N385	45	27	43	0	~ 0.66
Makrolon DX NR 139 cool 1.5 mm	58	49	54	114	~ 3.17
Makrolon DX NR 139 cool 3 mm	39	28	32	122	~ 2.37
Pyraled YT275 PMMA	47	41	45	131	~ 4.68
Setacryl M2002 opal	62	53	70	0	~ 0.46

Table 6.2: The six diffusers that are tested with their RGB value.

The PRIMO XT N385 and Setacryl M2002 opal diffusers will be examined by adjusting the light intensity in

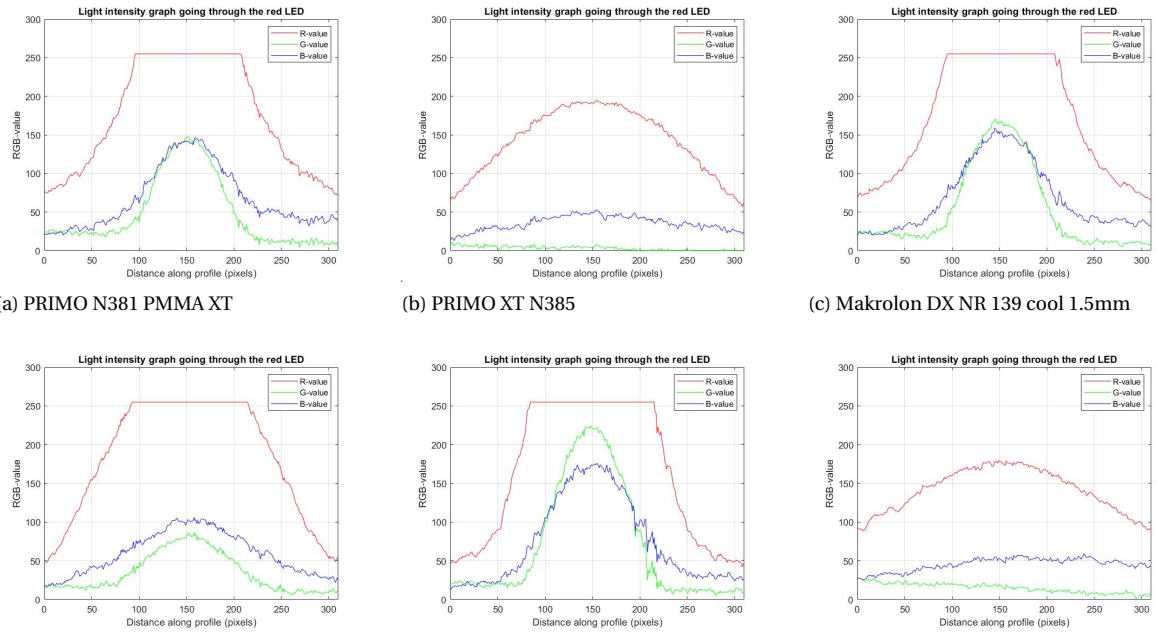

(a) PRIMO N381 PMMA XT

(b) PRIMO XT N385

(c) Makrolon DX NR 139 cool 1.5mm

(d) Makrolon DX NR 139 cool 3mm

(e) Pyraled YT275 PMMA

(f) Setacryl M2002 opal

Figure 6.4: Light intensity graph of a measurement line going through the centre of the red LED of each picture.

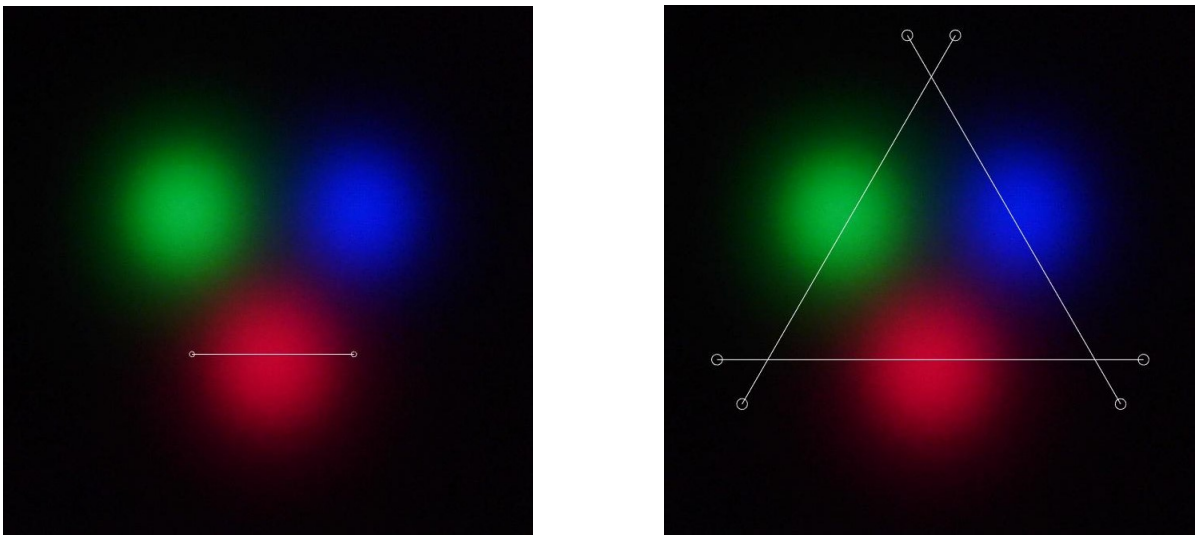

(a) The measurement line along which the light intensity graph is made for all six diffusers.

(b) The measurement lines along which the three light intensity graphs are made for the diffusers that are more examined.

Figure 6.5: Measurement lines along which the light intensity graphs are made with the PRIMON381 diffuser used as an example picture.

such a way that the middle of each LED has a maximum light intensity of 255 without horizontal lines. Three light-intensity graphs of all three light circles will be made. Figure 6.5b shows the three lines along which the three light intensity graphs are made. Also, a similar table like Table 6.2 will be made.

Figure 6.6 shows the results of the PRIMO XT N385 and Figure 6.7 shows the results from Setacryl M2002 opal. What can be seen in all light intensity graphs is that there are some of the other colours present as well. This is because the middle of the LEDs is not pure red, green or blue. There is always some noise in the middle of the LEDs. What is important to see is that, for example, Figures 6.6b and 6.7b show an almost zero

blue value on the left side of the graph and an almost zero green value on the right side of the graph. This corresponds if the line is examined in Figure 6.5b. The beginning of the line is far away from the blue LED, so no blue light intensity is expected, and at the end of the measurement line is far away from the green LED, so no green light intensity is expected at that side. This can also be seen in the other light intensity graphs. To choose between the diffusers, a table is made. Table 6.3 shows a bigger RGB value in the centre position for the Setacryl diffuser with no blooming and a relatively small slope. The Setacryl diffuser does not spread the light so far that it reaches a receiving fibre that is not adjacent to itself because what can be seen in the light intensity graphs is that the intensity is already almost zero at the left and right sides. The measurement line in Figure 6.5b only reaches adjacent receiving fibres when multiple building blocks are connected.

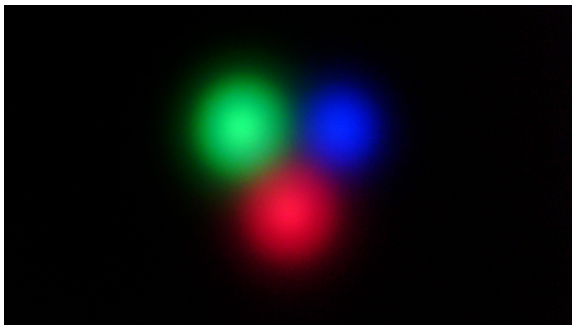

(a) PRIMO XT N385

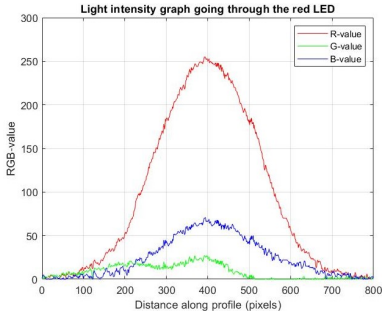

(b) Intensity graph through the red LED.

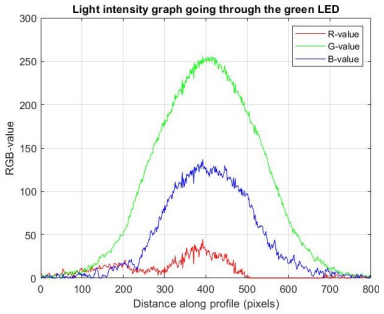

(c) Intensity graph through the green LED.

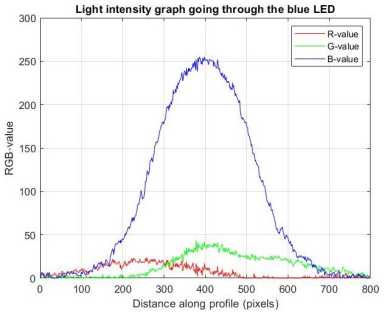

(d) Intensity graph through the blue LED.

Figure 6.6: Results of the PRIMO XT N385 diffuser.

Diffuser type	**RGB value receiving fiber (0-255)**			**Slope of the curves (value/pixel)**		
	R	G	B	R	G	B
PRIMO XT N385	79	64	67	~ 0.82	~ 0.81	~ 0.83
Setacryl M2002	111	143	147	~ 0.68	~ 0.61	~ 0.63

Table 6.3: The two diffusers that are more examined with their RGB value and slope of the curves.

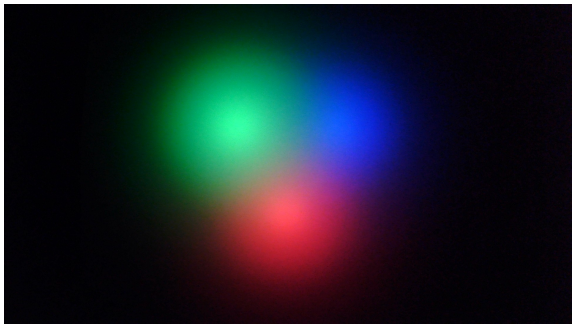

(a) Setacryl M2002 opal

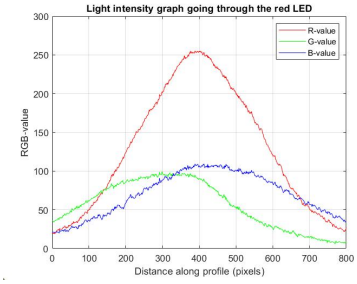

(b) Intensity graph through the red LED.

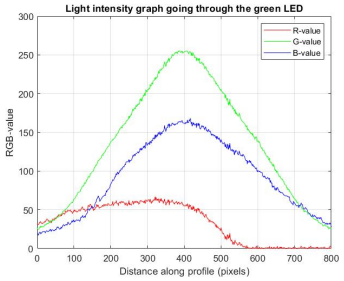

(c) Intensity graph through the green LED.

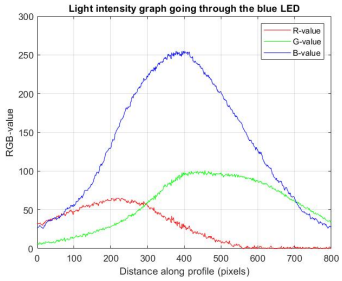

(d) Intensity graph through the blue LED.

Figure 6.7: Results of the Setacryl M2002 opal diffuser.

6.4. Conclusion

This chapter aimed to make a diffuser choice using an experiment. The diffuser that will be chosen will be used in future experiments. The setup, on which the experiment is executed, has been explained earlier in chapter 4. Two diffuser layers were put on the fibre holder block where three transmitting fibres are placed in. The two diffuser layers imitated the final setup when the floating object covers all three transmitting fibres that are part of one building block. Reflection has been left out in this experiment. The light intensity is set to a certain value and the camera is set to a certain distance away from the measurement plane. The centre pixel coordinates, calculated in chapter 5, were used. Six diffusers were chosen to compare with each other with different combinations of light transmission, light diffusivity and layer thickness to find the best combination. The pictures made from each diffuser were compared by looking at the light intensity graphs from a line going through the red LED. The graphs must not show high blooming peaks that are illustrated by horizontal lines at a maximum value of 255. These horizontal lines were seen in four out of six diffusers. The horizontal lines can be eliminated by reducing the light intensity, but a second comparing point is to make the RGB value at the receiving fibre location as big as possible. With the chosen light intensity, the RGB values were around the same for each picture, so reducing the light intensity would result in a lower RGB value in the centre. For that reason, the four diffusers were not chosen to examine more. The PRIMO XT N385 and the Setacryl M2002 opal were examined more to see their full potential. This is done by adjusting the light intensity of each LED in such a way that all light intensity graphs will hit their maximum and then reduces again. The light intensity graphs were made of the lines going through all three LEDs to compare them with each other. What can be concluded from the results is that the LEDs have the same light distribution because the slope of each LED is about the same. The Setacryl M2002 opal has a greater light spreading that resulted in a higher RGB value at the centre location. Also, the Setacryl diffuser will not reach other receiving fibres that are not adjacent to it when multiple building blocks are connected. For that reason, the Setacryl diffuser is chosen for future experiments. The assumption that was made is indeed true. The diffuser with the highest diffusivity is chosen with no blooming. The biggest downside that came out of this experiment is that it is really difficult to emit pure red, green or blue light from a LED. The light intensity graphs of, for example, the red LED showed high values for green and blue as well, which was not desired. The light intensity graphs of the three transmitting fibres showed the same course, but because of the other two undesired colours in the graphs, the wanted change in RGB value along each line from Figure 6.1 will probably not be the same. If this is the case, will be concluded from the next experiments.

7

Experiment 3: Influence object displacement on RGB value; without light reflection

This chapter describes the third experiment, which is the penultimate step before testing the final concept of this research. This experiment will continue where the experiment in chapter 6 ended. No receiving fibre is used in this experiment, so reflection will not be used either. It explores the concept of combining the three primary light colours and looks at the change in RGB value at the centre when a non-transparent non-reflective thin material is placed between the two diffuser layers that partially cover the light emitted. A receiving fibre should be placed in the centre of the transmitting fibres. This will be done in chapter 8 where the last experiment is executed. The experiment in this chapter only looks at the RGB code at the position of the receiving fibre when the light is partially covered. The camera is still looking at the measuring plane from above. This chapter will begin with a detailed explanation of how the experiment will be executed. It is explained how the design from chapter 4 will be used and what requirements are additionally needed, such as the material used to place between the diffuser layers. Next, the first part of the experiment is executed where the material is cut at different angles. For each angle, multiple pieces of material will be cut with a small displacement. In that way, the difference in RGB value can be measured with a known displacement. The second part of the experiment focuses more on straight object movements. A lot of material pieces will be cut with a small difference in length to get more information about the total movement and not only a small part of the movement. At the end of the chapter, a conclusion is given.

7.1. Experiment Layout

The third experiment will be explained in detail in this section. The setup from chapter 4 is used with some extra components. Next to that, the coordinate system introduced in chapter 5 will come back in this experiment. The value m is set to 10 millimetres, so the coordinates can be calculated as done in Figure 7.1. The final concept is imitated by again placing two diffuser layers on top of each other on the fibre holder block. Reflection is not taken into account, so a camera is looking down at the measurement plane. The floating object is imitated by placing a non-transparent, non-reflective, thin material between the two diffuser layers. The area that is not covered by the material imitates the floating object from the final concept. The reason behind that is that in this experiment reflection is left out and because of that the sight is exactly the other way around. The non-transparent, non-reflective, thin material can be anything, but it must not transmit light, it must not reflect light and the material is very thin otherwise there will be a gap between the diffusers. All of this can affect the measured RGB value in the centre position. In the final concept, the object floats above the table, so there is a gap, but the gap is so small that it is negligible. For that reason, the piece of material can be placed flat between the diffuser layers. In Figure 7.2 a top view is given of the fibre holder block together with the distances. The pieces of material, that will be placed between the diffuser layers, have to be cut in such a way that it fits in the 44 by 44 millimetres area square. The idea of this intermediate experiment is to better understand the influence of a certain movement of the object, which partially obscures the light, on

the change in RGB value and to see if this is comparable with the final concept.

When the final concept of an air-bearing table with a floating wafer or solar cell is examined, it turns out that the object can travel at any angle. Therefore, this experiment will test three displacements at multiple angles first. The second part of this experiment is to investigate this more for the straight object displacements. Graphs will be made for multiple displacements at 0 and 90 degrees. This research will examine objects with straight lines and without curvatures. In chapter 8 the final concept, which includes reflection, is executed. This will be done through an experiment that also examines three displacements at multiple angles and a more detailed investigation of the angles 0 and 90 degrees. The only difference between the experiment in this chapter and the experiment in the next chapter is that the experiment in this chapter contains no reflection and the experiment in chapter 8 does contain reflection. This can be used in some way. If the same material can be used, squares can be cut that fit exactly on top of the fibre holder block. Then the squares are cut into two pieces. One part can be used in this experiment and the other part can be used in the experiment that will be performed in chapter 8. This makes it easy to make comparisons because the working principle of the experiments is the opposite of each other. The problem is that the material has to be non-reflective for the experiment performed in this chapter, and it has to be reflective for the experiment performed in the next chapter. To solve this problem, the pieces of the squares used in this experiment are sprayed black with metal spray paint. The spray paint is matt to prevent reflections. The used material to place between the diffuser layers is 50 micrometres thick brass foil paper.

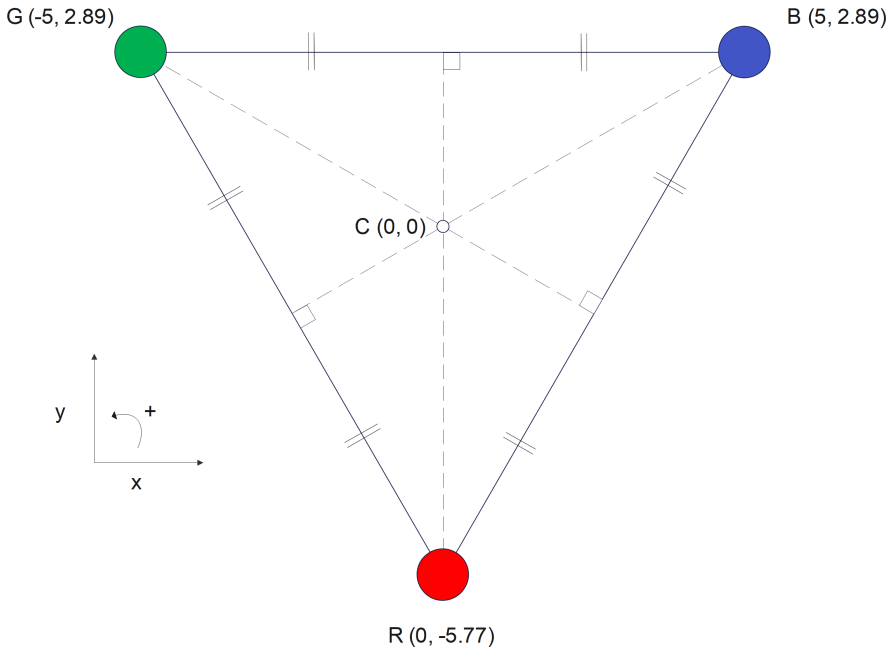

Figure 7.1: The used coordinate system of the research, with the calculated coordinates for the distance between the transmitting fibres set to m = 10 millimetres.

7.2. Multiple angle object displacements

The final goal is to translate an RGB code from the receiving fibre into a position or displacement of the floating object. The experiment will test this by calculating the other way around. There will be observed what will happen to the RGB code if the object moves over a known distance. This section investigates all possible object movement angles. The object movement angles are from 0 to 360 degrees. There is symmetry in the system. The movements between 0 and 180 degrees and between 180 and 360 degrees are the same but then coming from the other way around. The angles between 0 and 90 degrees can be compared to the angles from 90 to 180 degrees. The only difference lies in which transmitting fibre will be covered first, but the order of covering does not matter. For that reason, the angles between 0 and 90 degrees will be investigated.

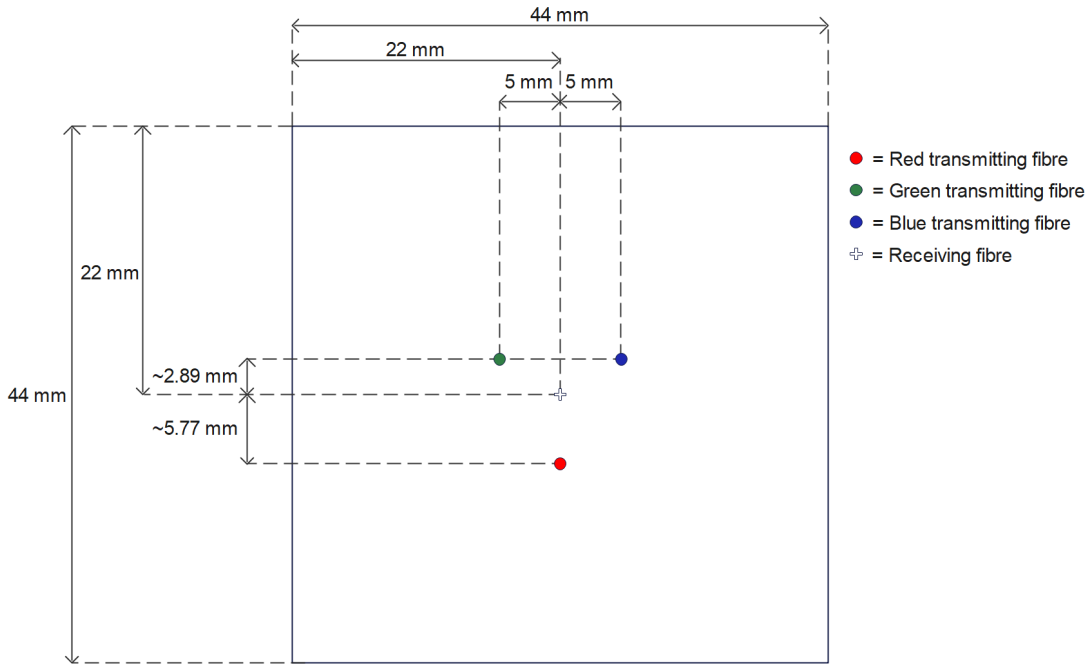

Figure 7.2: Top view of the fibre holder block. Two diffuser layers with a piece of brass foil paper between them are placed within the square.

7.2.1. Cutting of the squares

The angles 0, 30, 45, 60 and 90 degrees are chosen to examine. The cutting of the squares needs to be done in such a way that the piece, that will go between the diffuser layers, does not block the position where the imaginary receiving fibre is positioned because otherwise nothing can be measured. In Figure 7.3, the cutting of the squares can be seen. The pieces that are indicated with the number one are used in this experiment. The pieces that are indicated with the number two are used in the experiment in the next chapter. All rows have three different squares. Every next square has a displacement of the cutting line of about two millimetres. In that way, the RGB code difference can be calculated if an object moves over a distance of two millimetres. The first row of squares will test the angles of 0 and 90 degrees because the cut-off pieces can also be held vertically. The same holds for the squares in the second row, which will test the angles of 30 and 60 degrees. There is a possibility there is an offset in the cutting of the squares. The exact lengths will be measured after cutting to get precise results. Every material piece has a 90 degrees angle, that corner will be held in the bottom left corner of the square seen in Figure 7.2. The chosen angle will be the angle between the bottom horizontal line of the square and the cutting line through the square.

7.2.2. Results

The angles 0, 30, 45, 60 and 90 degrees are investigated. Three pieces of material for each angle will be tested, with each next piece of material a change of around two millimetres. There will be some offsets in the pictures taken. To get precise RGB values, four pictures will be taken for each piece of material put between the diffuser layers. The mean of the RGB values of the four pictures will be taken to get an average RGB picture. An example of the offset that can appear with the same piece of material used is shown in Figure 7.4.

Three example pictures with a piece of material placed between the diffuser layers can be seen in Figure 7.5. A piece of material with an angle of 30 degrees between the two diffuser layers can be seen in Figure 7.5a, a material with an angle of 60 degrees can be seen in Figure 7.5b and a material with an angle of 90 degrees can be seen in Figure 7.5c. The material that is placed between the diffuser layers is indicated with the yellow lines. The measured RGB values together with the difference of RGB value and the absolute difference in millimetres in comparison with the previous material piece of the same angle can be seen in Table 7.1. The difference between the pieces of material was intended to be two millimetres, but what can be seen in the

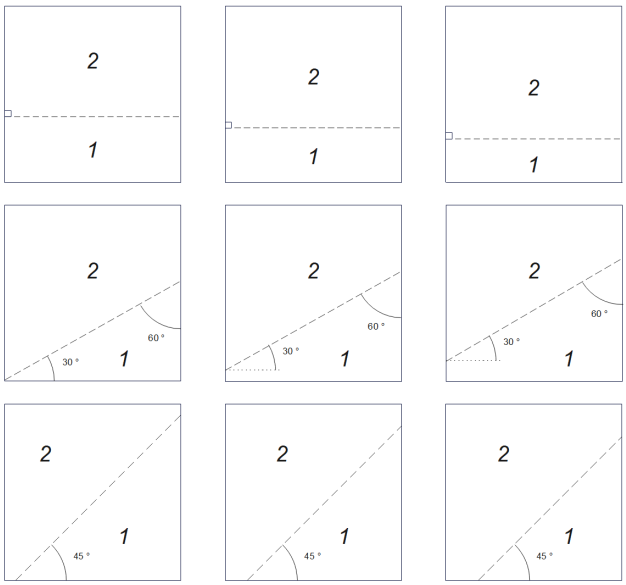

Figure 7.3: Illustration on how the squares, that will be placed between the diffuser layers, are cut. The pieces indicated with the number one will be used in this experiment, and the pieces indicated with the numbers two are used in the experiment in the next chapter.

table is that the difference is not exactly two millimetres. This is due to the inaccuracy in cutting the squares in the exact wanted shapes. Also, what can be seen is that the differences in RGB values for all angles between the first and second samples are not the same as for the difference between the second and third samples. This is because the RGB values do not run linear but have a Gaussian gradient as proven in chapter 6.

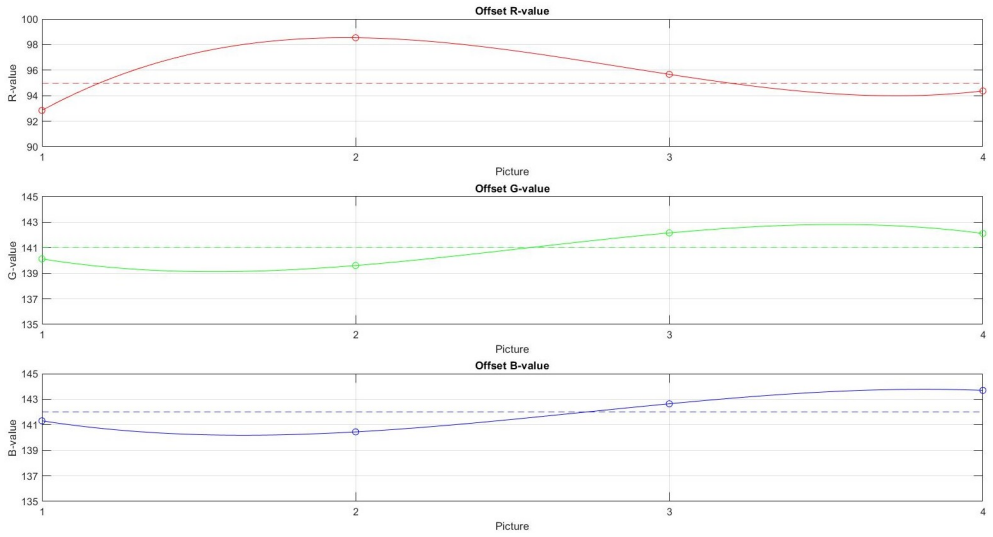

Figure 7.4: Example of the first badge of pictures taken from the 0-degree measurement. The RGB values of the receiving fibre position of all four pictures are shown.

7.3. Perpendicular object displacements

It is easy to think that the floating wafer or solar cell on top of the air-bearing table can travel in all directions at all possible angles. This does not necessarily have to be true. The system can also be programmed to only allow perpendicular object movements. The only movements possible are then left, right, up and down or 0, 90, 180 and 270 degrees. This section will investigate those movements in more depth. Symmetry will be used again in this section.

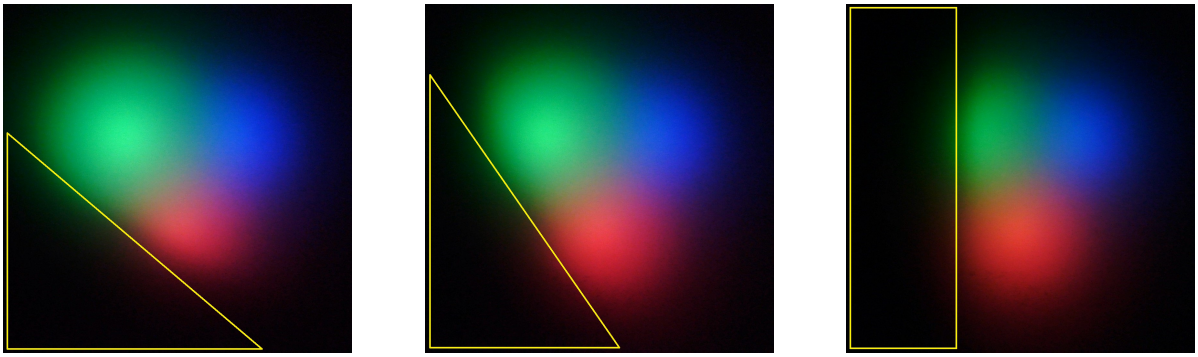

(a) 30 degrees (b) 60 degrees (c) 90 degrees

Figure 7.5: Example pictures of the pieces of material, with different angles, that are placed between the two diffuser layers.

Angle (degrees)	**RGB value receiving fiber (0-255)**			**RGB value difference (0-255)**			**Absolute displacement in comparison with previous piece (mm)**
	R	G	B	R	G	B	
0	95	141	142		N/A		N/A
	78	140	141	17	1	1	~ 1.9
	30	134	134	48	6	7	~ 2.1
30	110	141	142		N/A		N/A
	101	141	137	9	0	5	~ 2.30
	71	136	126	30	5	11	~ 1.56
45	108	141	139		N/A		N/A
	96	135	130	12	6	9	~ 2.55
	62	128	116	34	7	14	~ 0.9
60	111	141	137		N/A		N/A
	108	136	130	3	5	7	~ 2.30
	96	128	112	12	8	18	~ 1.56
90	110	137	122		N/A		N/A
	93	120	90	17	17	32	~ 1.9
	65	83	50	28	37	40	~ 2.1

Table 7.1: The object movement angles with the corresponding RGB value of the receiving fibre location.

7.3.1. Cutting of the squares

The three displacements for each angle investigated in section 7.2 are not enough. The measurements done are some examples of possible object movements and do not include everything. In this section, a more detailed measurement will be executed. It is easier now because fewer angles are included. The angles 0 and 90 degrees are chosen to examine. They were also investigated in the previous section, but now more measurements will be done. A total of 11 measurements will be done. Starting at no material between the diffusers and every next measurement, two millimetres will be added. The measurements will continue till the piece of material has a length of 20 millimetres because at 22 millimetres the receiving fibre location will be covered, as can be seen in Figure 7.2, and nothing can be measured. The coordinate system from Figure 7.1 will be used. The edge will go from the $y = -22$ line till the $y = -2$ line for the 0-degree object orientation movement, as can be seen in Figure 7.6a. For the 90-degree object orientation movement, the object edge travels from the $x = -22$ line till the $x = -2$ line, as can be seen in Figure 7.6b. The pieces will be cut very precisely, but there is a possibility there is an offset. Again, the exact lengths of the pieces of material will be measured. So it is possible that every next displacement will not be two millimetres exactly.

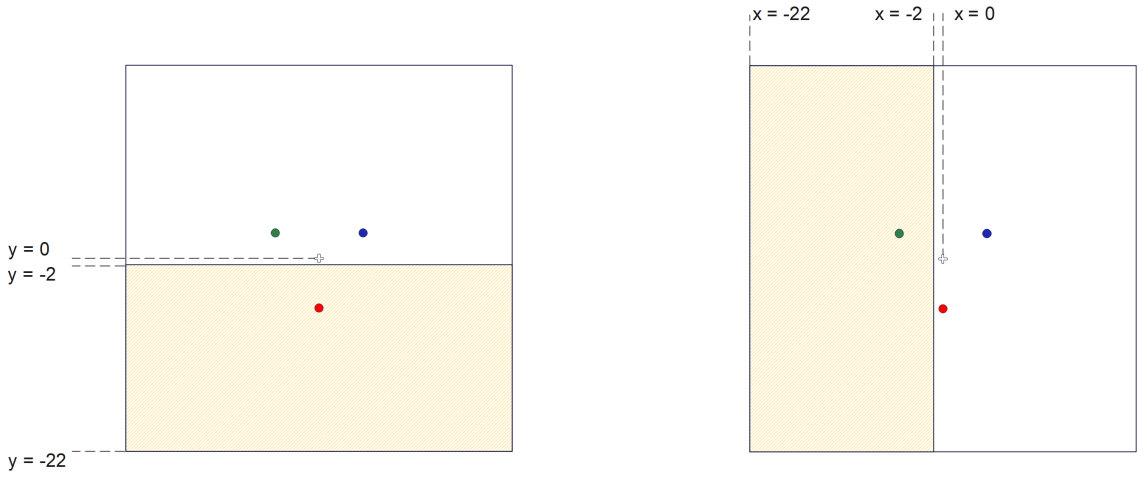

(a) The measurement area for the movement of the 0-degree object orientation.

(b) The measurement area for the movement of the 90-degree object orientation.

Figure 7.6: The area where the object is located during the measurements for vertical and horizontal object movements.

7.3.2. Results

The exact results of the measurements can be seen in Appendix A in Table A.1. Again, the RGB values together with the difference of RGB value and the absolute difference in millimetres in comparison with the previous material piece are noted. In Figure 7.7 and Figure 7.8 the graphs can be seen of the course of the RGB values. What is obvious is that the RGB values do not change in the beginning. It stays the same for a while. A change in RGB value is noticeable in the last measurements. A change in RGB value for the movement of the 0-degree object orientation starts at the $y = -8$ line, which can be seen in Figure 7.7. A change in RGB value for the movement of the 90-degree object orientation starts at the $x = -10$ line, which can be seen in Figure 7.8. If the LEDs gave pure light, it is expected that this course also holds when moving with the same object orientation over the green and blue LEDs. However, the LEDs do not give one pure light colour, so what happens when the object is sliding in from the green or blue LED is not known for sure.

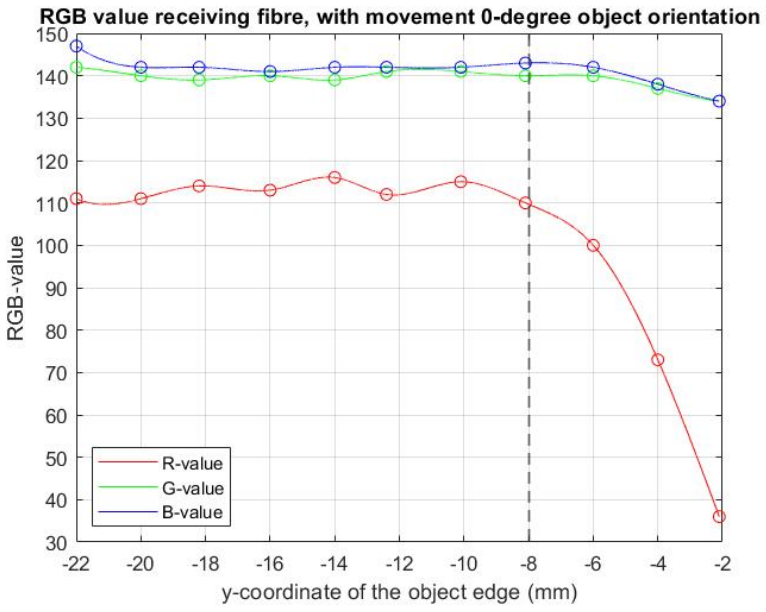

Figure 7.7: Course of RGB value for a movement of 0-degree object orientation.

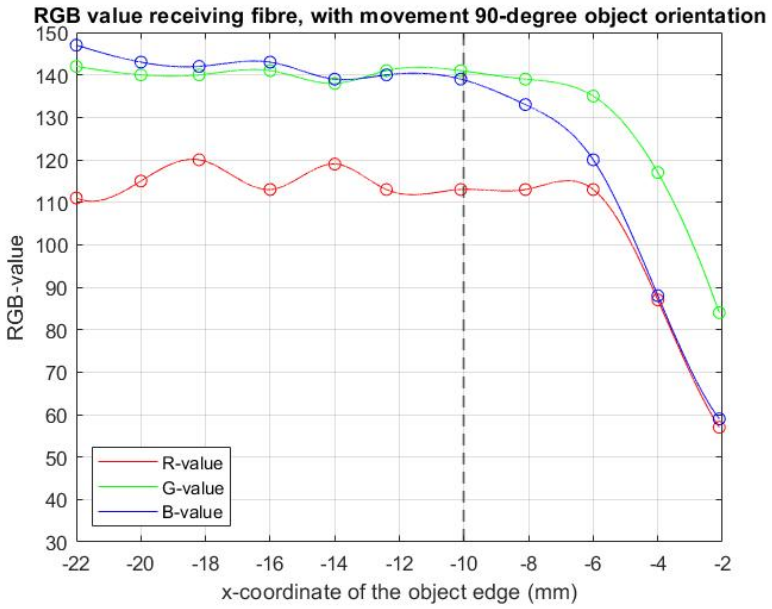

Figure 7.8: Course of RGB value for a movement of 90-degree object orientation.

7.4. Conclusion

This chapter began with investigating object movements, in this case, 50 micrometres of brass foil paper, with multiple angles. Each angle that was investigated had three pieces of material, with each next material a displacement of around two millimetres. The displacements were around the receiving fibre but not covering the receiving fibre because otherwise nothing could be measured. A change in RGB value was noticeable, but way too few measurements per angle were executed to come up with precise results. For that reason, perpendicular object movements were investigated more in detail. A total of 11 measurements were done with each next material a displacement of two millimetres till the material reached 20 millimetres. What can be concluded from the results is that a negligible RGB difference was observed in the beginning. The RGB value stayed the same for a long time until the material between the diffuser layers reached the line $y = -8$ for the vertical movements and the line $x = -10$ for horizontal movements. From that length till the last piece of material, the RGB value dropped rapidly. So, apparently, the edge of an object only can be measured when it lies between this range. The expectation was that this range would be wider, but if this range also holds in the last experiment, it will be enough. That is because when multiple building blocks will be connected, the measurement ranges that appear are enough to come up with an object's edge position and displacement. In the next chapter, there will be looked at if this conclusion also holds for the end concept where reflection is included.

8

Experiment 4: Influence object displacement on RGB value; with light reflection

The final concept of this research is tested in this chapter through the fourth and final experiment. This experiment involves the concept of light reflection. Light reflection occurs when the object, moving across the air-bearing table, is moving over a specific transmitting fibre. When the light comes out of the transmitting fibre and passes through the volume diffuser and hits the object, it will reflect because the object has a reflective surface. This concept is imitated in this last experiment. This chapter starts with an experiment layout. The execution of the experiment is explained, and it is shown how the results will be reported. Then the experiment is performed and the measurements are discussed. More measurements will be executed than in chapter 7 because all lengths of the material can be included. The measurement range of the system is calculated. The chapter ends with a conclusion about what the results say about the whole system. The presumption is that the perpendicular movements will give an RGB graph that has a jump in it. So it stays at a certain value and when it comes to the measurement range the RGB value will increase till it leaves the measurement range. After leaving the measurement range, the RGB value will again remain the same for the last part.

8.1. Experiment layout

This last experiment also uses the setup from chapter 4. The setup will again make use of the holes in the fibre holder block. In addition, unlike in previous experiments, the hole in the centre of the fibre holder block is also used. The receiving fibre is placed in this centre hole. In previous experiments, the measurements were done at the position where the receiving fibre should be placed. Now the receiving fibre is placed in that position. The experiment will look at the RGB value this receiving fibre will receive. To do that, another camera position is needed. The camera has to look at the end of the receiving fibre. The setup from Figure 4.1b, where the fibres were checked for damages, is used. The other end of the receiving fibre is put in the centre of the fibre holder block. The camera can be placed inside the housing of the whole setup. In Figure 4.4c it can be seen that there is enough space for the camera. The cap, which eliminates external light sources, is also used. The camera with the cap can be seen in Figure 4.4a. The cap avoids offsets in the measurements that are due to external light sources, like ambient light. If no cap is used, the external light rays would also fall into the receiving fibre, and that is not desired. The camera that is located in the cap will not be used in this experiment because reflection is now taken into account. However, the camera is placed in the hole to fill the gap to also eliminate external light sources from that side of the system.

One diffuser layer is placed on top of the fibre holder block. The distances of the available space can be seen in Figure 7.2. On top of the diffuser layer, a material piece will be placed that is cut in a specific size. In chapter 7, thin brass foil paper was used. Squares of 44 by 44 millimetres were cut that fit exactly inside the fibre holder block edges. Then the squares were cut like in Figure 7.3. Chapter 7 used the numbers one after

spraying it with metal black paint because reflection was not included in the experiment executed in that chapter. In the experiment in this chapter, the numbers two are used. The pieces of material are not sprayed black because reflection is needed. This will be again the first part of the experiment. The second part of the experiment will again give a more detailed insight into straight object movements. The obtained image by the camera will be a circle of light. The RGB value is calculated with the help of MATLAB. The RGB values from an area inside the circle of light are taken. The average of the measured RGB values will be the final RGB value of the corresponding image.

8.2. Multiple angle object displacements

This section investigates the working principle of the measurements using the receiving fibre in the centre of the fibre holder block. The pieces of thin brass foil that are cut in specific sizes indicated with the numbers two in Figure 7.3 are used to imitate a floating object. There will be looked at if the same results will appear. This assumption was made because two pieces that are cut from one 44 by 44 millimetres thin brass foil square are the opposite of each other. In the previous experiment in chapter 7, the receiving fibre location was investigated without using reflection and thus a receiving fibre. A camera looked down at the surface of the fibre holder block. In this experiment, reflection is included so if the other piece of the square is used, the idea is that the same RGB value is measured.

8.2.1. Results

In Table 8.1 the results can be seen. The first thing that is immediately obvious is that the RGB values are not the same as in Table 7.1. An investigation of the receiving fibre has to be done to see how this is possible.

Angle (degrees)	**RGB value receiving fibre (0-255)**			**RGB value difference (0-255)**			**Absolute displacement in comparison with previous piece (mm)**
	R	G	B	R	G	B	
0	132	128	121		N/A		N/A
	126	120	114	6	8	7	~ 1.9
	123	115	111	3	5	3	~ 2.1
30	123	117	109		N/A		N/A
	123	120	114	0	+3	+5	~ 2.30
	123	116	110	0	4	4	~ 1.56
45	126	123	116		N/A		N/A
	122	117	112	4	6	4	~ 2.55
	122	115	110	0	2	2	~ 0.9
60	129	123	114		N/A		N/A
	128	125	119	1	+2	+5	~ 2.30
	125	118	113	3	7	6	~ 1.56
90	128	123	117		N/A		N/A
	121	113	109	7	10	8	~ 1.9
	116	105	102	5	8	7	~ 2.1

Table 8.1: The object movement angles with the corresponding RGB value of the receiving fibre.

8.2.2. Investigation receiving fibre

The assumption that the results from the third experiment in chapter 7 and the results in this chapter are the same is not true. Now is the question of how this is possible. The receiving fibre is investigated more in detail. An image of the end of the receiving fibre will be checked when no object is on top of the diffuser layer. An almost black image is expected because almost no light should be received by the receiving fibre. Only a little bit of light is expected from the light that will be reflected downwards when travelling through the diffuser layer. This was explained in section 2.2 and illustrated in Figure 2.4b. Figure 8.1a shows the received image from the receiving fibre without material on top of the diffuser. In the graph in Figure 8.1b the RGB values can be seen. The mean RGB value is as follows:

$$[R \quad G \quad B] \quad = \quad [104 \quad 92 \quad 91]$$

The light reflected backwards inside the diffuser layer is so much that the RGB value is high even when no object is on top of the diffuser. The assumption that the third experiment can be compared with this experiment does not hold. This does not mean that nothing can be measured. In the next section, a more detailed measurement will be done with perpendicular object movements.

(a) Image taken by the camera.

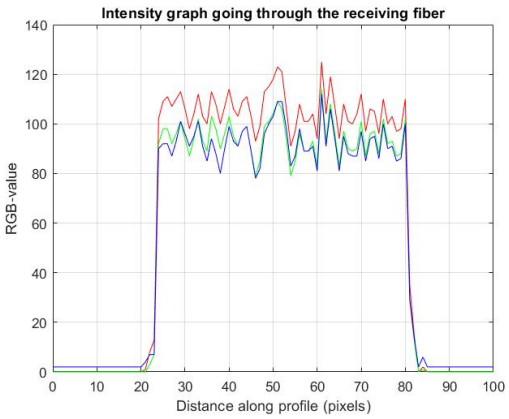

(b) RGB graph going through the middle of the circle of light

Figure 8.1: Image of the end of the receiving fibre without a piece of material on top of the diffuser layer, together with RGB graph going through the middle of the circle of light.

8.2.3. Investigation other diffuser

The fact that a lot of light is reflected in the diffuser layer into the receiving fibre needs to be reinvestigated. Maybe the diffuser choice was not the best after all. This subsection investigates what the receiving fibre would see when no object is above the fibres, but now using the PRIMO N381 diffuser. This one is chosen to compare because this diffuser has a higher transmission and a lower diffusivity. The assumption is that it should eliminate the backwards scattering a bit. Figure 8.2 shows the end of the receiving fibre when the PRIMO diffuser is used. Still, a lot of light is noticeable in the image seen in Figure 8.2a. This is substantiated by the RGB graph in Figure 8.2b. The mean RGB value is as follows:

$$[R \quad G \quad B] \quad = \quad [82 \quad 70 \quad 68]$$

So the RGB value is less than the RGB value from the Setacryl diffuser. The only thing that happened is that the diffusivity is also less, so the RGB values in the receiving fibre when an object is moving over the surface will be also less than the found RGB values from the Setacryl diffuser. So in the end, the total change from one plateau to the other will about be the same. For that reason, the Setacryl diffuser will still be used in further experiments.

8.3. Perpendicular object displacements

This section will investigate straight object movements more in detail. In the previous experiment, in chapter 7, it was noticed that nothing happened with the RGB value until the piece of material was covering the transmitting fibre it was travelling to. So for the movement of the zero degrees angle, the RGB value changed when the material was just before the red transmitting fibre. For the 90-degree object orientation movement, the RGB value changed when the piece of material was just before the green transmitting fibre. The pieces of material were cut to a total length of 20 millimetres. Otherwise, the material would cover the receiving fibre location and nothing could be measured. In this experiment, this does not matter because reflection is included. All lengths, to a total of 44 millimetres, will be included. The same coordinate system as used in chapter 7 will be used. In Table A.2 in appendix A the exact results can be seen for a 0-degree object orientation movement. Every next piece of material has a change of around two millimetres. A total of 23 measurements were executed and again for every measurement four pictures were taken to eliminate any offsets. A graph of the results can be seen in Figure 8.4. The same has been done for the 90-degree object orientation movement. The results can be seen in Table A.3 in appendix A and the corresponding graph can be

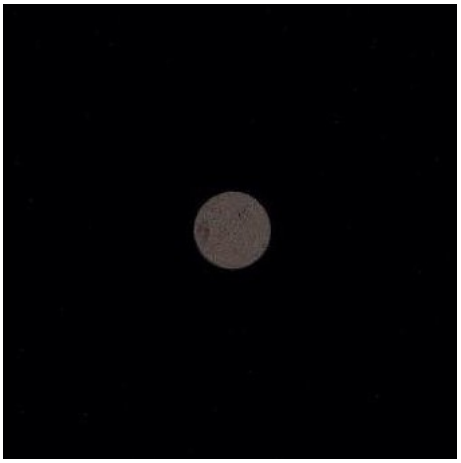

(a) Image taken by the camera with the PRIMO diffuser used.

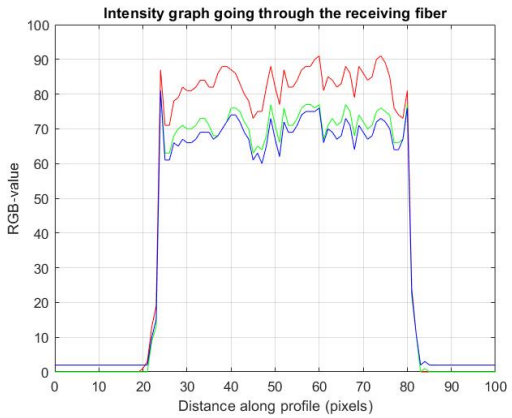

(b) RGB graph going through the middle of the circle of light

Figure 8.2: Image of the end of the receiving fibre without a piece of material on top of the diffuser layer, together with RGB graph going through the middle of the circle of light.

seen in Figure 8.5. Both graphs show an almost constant RGB value till it reaches a certain point where it rises fast. The range where RGB value can be measured is schematically represented in Figure 8.3a for the movement of the 0-degree object orientation and Figure 8.3b for the movement of the 90-degree object orientation.

More measurements were executed in the ranges where the RGB value difference was noticeable. The range of the 0-degree object orientation lies between the axis $y = -2$ and $y = 4$, and the range of the 90-degree object orientation lies between the axis $x = -8$ and $x = 2$. Every next measurement was executed with a difference of around two millimetres. To get a better insight into the range where the RGB value increases, the extra measurements in that range had a difference of around one millimetre. In both graphs, a not smooth gradient is observed. This can be because, for example, the red transmitting fibre not only emits red light but also green and blue light. The amount of green light that is emitted by the red transmitting fibre does not have to be the same as the green light emitted by the blue transmitting fibre and because of that, a not smooth gradient is noticeable in the graphs.

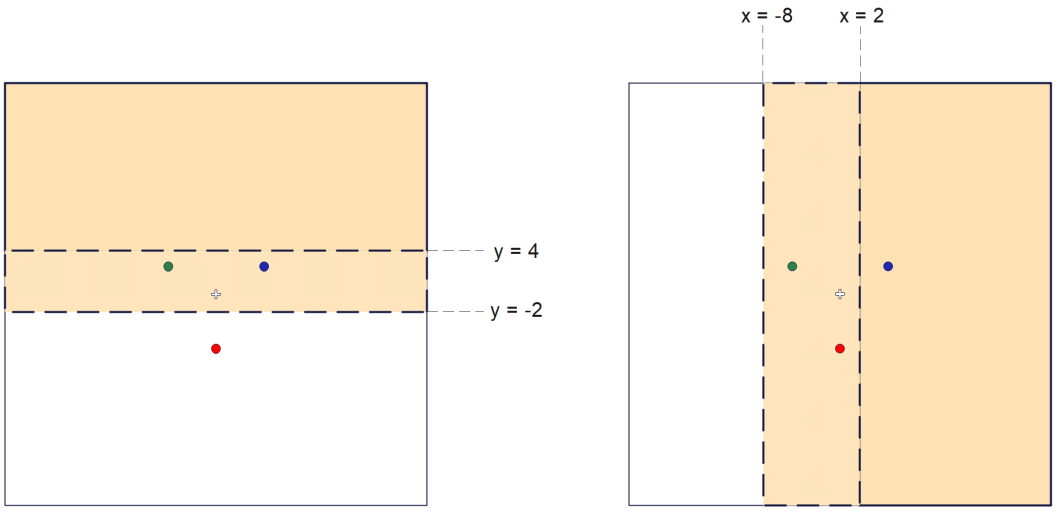

(a) 0-degree range.

(b) 90-degree range.

Figure 8.3: The range where RGB value difference can be measured of the 0 and 90 degrees movements.

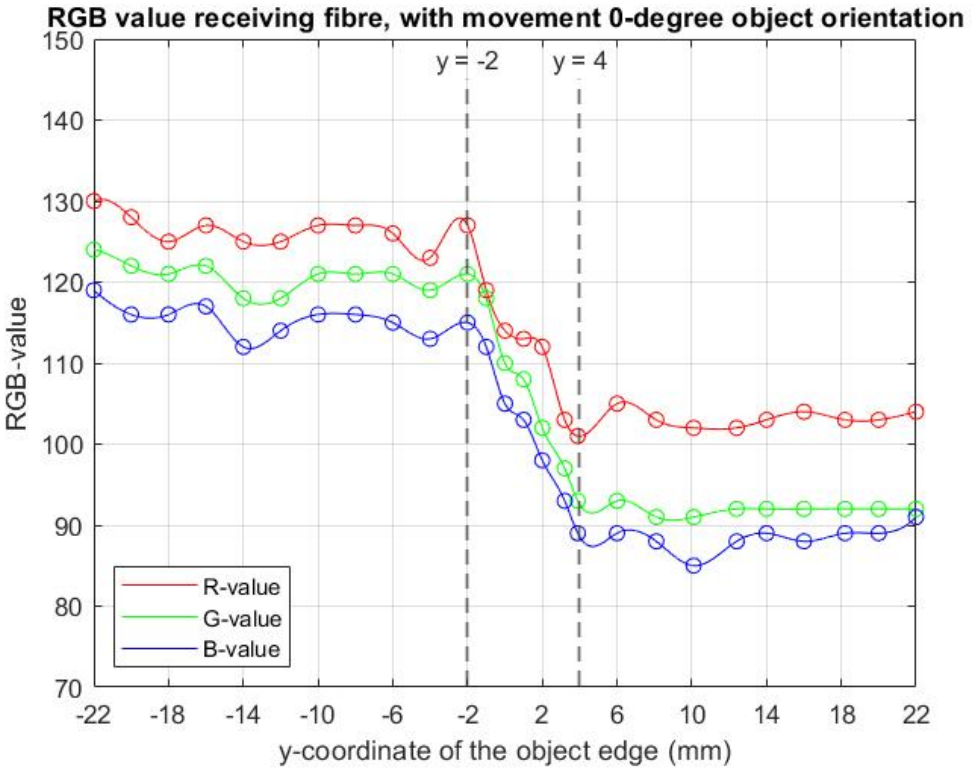

Figure 8.4: Graph of the RGB value course when a piece of material is travelling over the diffuser layer with a 0-degree angle.

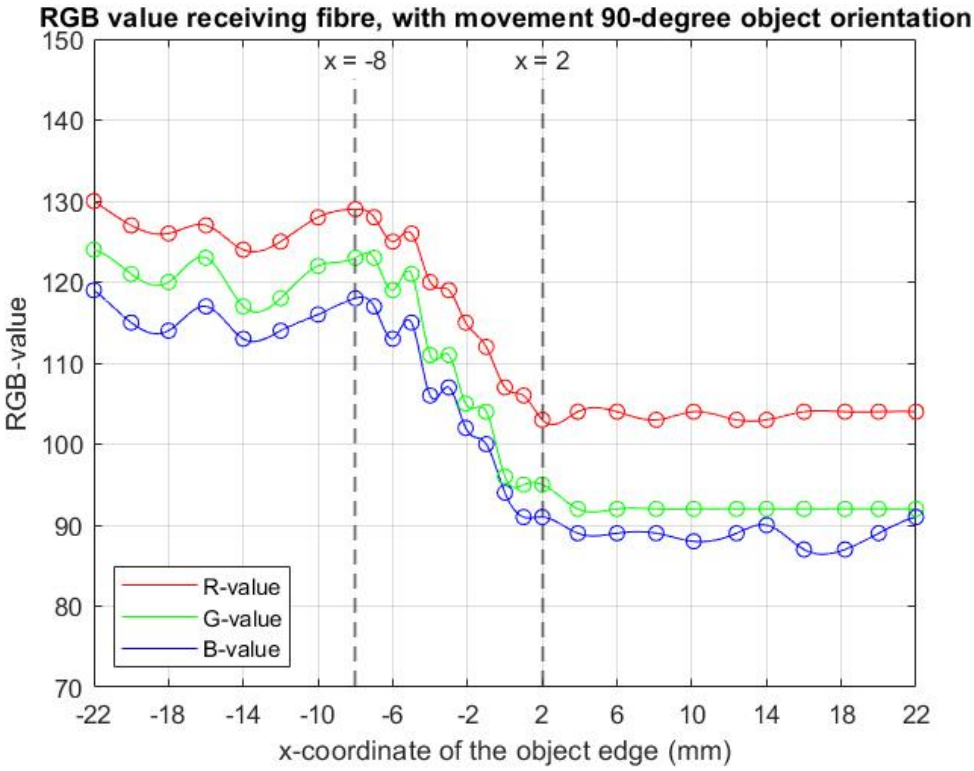

Figure 8.5: Graph of the RGB value course when a piece of material is travelling over the diffuser layer with a 90-degree angle.

8.4. Conclusion

This chapter investigated the final concept of this research, where an object is floating over an air-bearing table with fibres in it. This is done by looking at one building block of the whole system that includes three transmitting fibres, each 10 millimetres away from the other, and one receiving fibre in the centre of the transmitting fibres. A 50-micron brass foil paper is used to imitate the floating object. This foil paper was placed on one diffuser layer that was chosen in chapter 6. Multiple-angle movements were investigated first. The other parts of the cut squares from the third experiment in chapter 7 were used. The assumption was that the RGB values from the third experiment and this experiment will be the same because the experiments are the opposite of each other. This assumption turned out not to be true at all. The cause turned out to be that the receiving fibre captured light even when no material is placed on top of the diffuser layer. The measurements were disrupted because of this backscattering, but still, something could be measured. Perpendicular object movements were investigated more in detail. It turned out that for the movement of a 0-degree object orientation, only an RGB value difference was measurable between the lines $y = -2$ and $y = 4$. In this range, more measurements were executed to get more precise values. The range for the movement of 90-degree object orientation turned out to be between the lines $x = -8$ and $x = 2$. The graphs showed not a smooth curve, which can be due to the unavoidable presence of, for example, the colours green and blue in the red transmitting fibre. But in the end, for both object movements, an observed RGB value change can be translated into a certain displacement of the object. The assumption that earlier has been made is indeed true for the 0-degree object movement and 90-degree object movement. The RGB value stays at a certain value till it reaches the measurement range. In this range, the RGB value rises to a certain value. If the object's edge is out of the measurement range, the value will be constant again. A problem that occurred in this experiment is that different object orientations are hard to distinguish when only looking at the RGB value received by the receiving fibre. This was because there were disruptions of other light colours in the LEDs. In the next chapter, a model will be made and discussed that illustrates what happens if the LEDs do emit only one light colour.

9

Influence individual LED on RGB value; with light reflection

Chapter 7 and chapter 8 did not give the results that were expected. This was because the LEDs emit, next to the wanted colour, also the two other light colours. In this chapter, there will be looked at the influence of a single LED and its transition range. The two other light sources will be sealed off. Light reflection will again be included because this illustrates the end concept the best. If the calculated transition range also holds for the other two light sources, some modelling can be done to see if it is possible to know the position of the object with every possible angle. The expectation is that this will be possible because it is known that a change in a specific colour in the RGB value has to come to the corresponding LED that sent that colour. A change in, for example, R-value has to come from the red LED. In the other chapters this was different because a change in, for example, R-value could come from all three LEDs. This chapter will begin with a layout of the experiment that has to be done in advance. The results of the experiment will be discussed next. Then the modelling begins, where in the end the total range will be given where the object edge position can be measured. A conclusion of the chapter is given at the end.

9.1. Influence individual LED

This section explains the layout that will be used in the experiment necessary for modelling the position of the object edge, which will be done later in this chapter. The results of the experiment are mentioned as well with the use of light intensity graphs versus the object edge position. This section is discussed briefly because a lot of the measurements were executed in the same way as in chapter 8.

9.1.1. Experiment layout

The setup from chapter 4 is used again. The plane where the measurements are executed has been shown earlier in Figure 7.2 in chapter 7. The execution of the measurements is the same as done in chapter 8. The only difference is that two light sources have to be eliminated in a way. The red LED is chosen for the execution of the experiment, so the green and blue light sources have to be eliminated. This is done by placing a piece of thin non-transparent material directly on top of the fibre holder block, so before travelling through the diffuser layer. Reflection is included, so a camera is looking through the receiving fibre. Two graphs will be made to illustrate where the transition range lies for two different object orientation movements. One is made when travelling with a 0-degree object orientation from the top to bottom, and the other is made when travelling with a 90-degree object orientation from the right to the left. The two transition areas that are calculated indicate the positions of the object edge where something can be measured. Of course, there will be some green and blue distortions in the measurements because that is the reason why this chapter is necessary. These green and blue values are set to zero.

9.1.2. Results

The results of the movement of a 0-degree object orientation can be seen in Figure 9.1. The corresponding measurements can be found in appendix A in Table A.4. The transition range lies between the lines $y = -7$

and $y = 2$. The results of the movement of a 90-degree object orientation can be seen in Figure 9.2. The corresponding measurements can also be found in appendix A in Table A.4. The transition range lies between the lines $x = -4$ and $x = 4$. This experiment investigated only the movements from top to bottom and right to left, but when travelling the other way the transition area will be the same but mirrored. All transition areas for object movements from bottom to top, right to left, top to bottom and left to right are shown in Figure 9.3. The fact that there is a difference in the transition area in comparison with the results in chapter 8 is due to that the LEDs did not give pure red, green or blue light. The disturbances gave transition areas that were not realistic to the final concept. The transition area calculated in this chapter is way more realistic because if, for example, the 90-degree object orientation is better looked at, the red transmitting fibre and receiving fibre are exactly aligned and positioned on the $x = 0$ line. So the transition area must have the same distance to the left and right of that line. The graph shows that this is true.

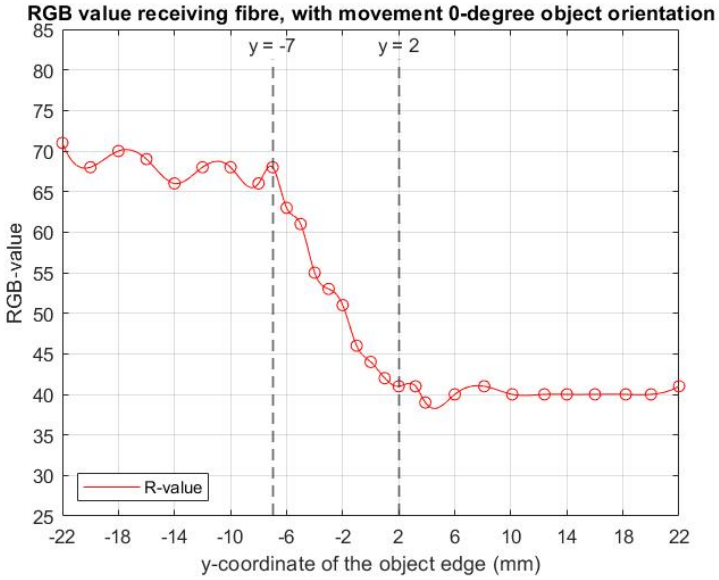

Figure 9.1: The course of the R-value of a movement of a 0-degree object orientation when travelling from the top to the bottom.

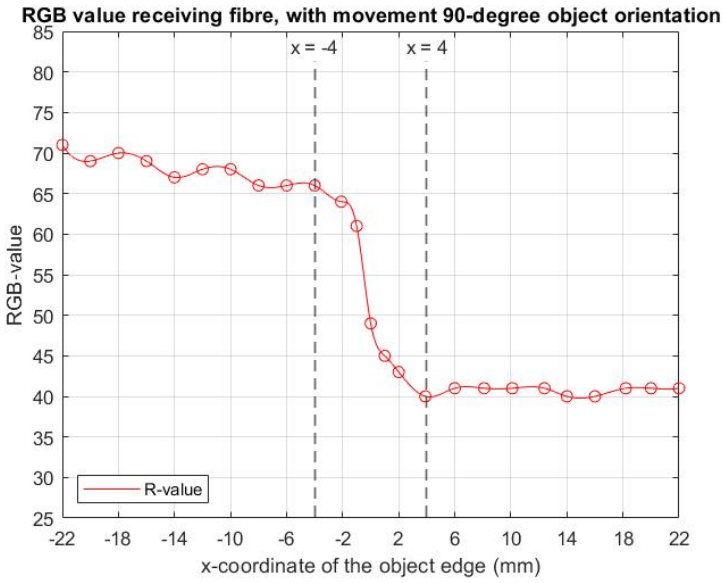

Figure 9.2: The course of the R-value of a movement of a 90-degree object orientation when travelling from the right to the left.

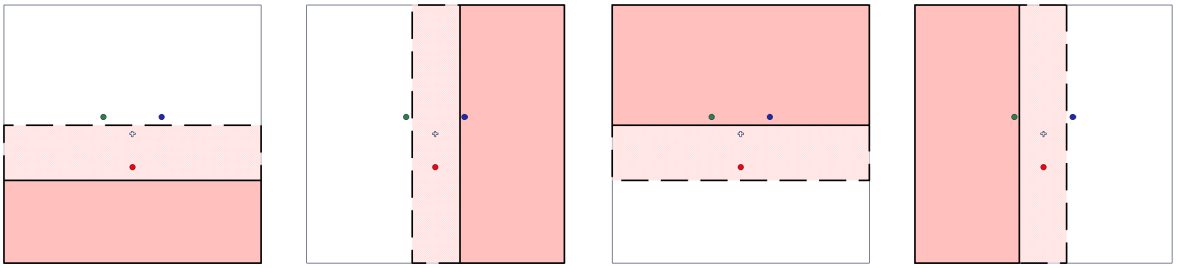

Figure 9.3: The ranges where a change in RGB value can be measured with 0 and 90-degree object orientation movements relative to the red LED.

9.2. Detection object edge

This section describes what the possibilities are in object edge detection when the green and blue LEDs have the same transition range as the red LED illustrated in Figure 9.3. Also, a model will be made on what will happen with the measurement ranges when the object does not travel perpendicular. The transition ranges can be interpolated in a way that results in all ranges under whatever angle the object is positioned. When that is done, an example will be given of how an RGB value of the receiving fibre can be translated into an object position.

9.2.1. Expectations

Say the green and blue LED gives the same light intensity course and thus the same transition ranges, like the red light intensity course shown in Figure 9.1 and Figure 9.2. This was also the desired result and was schematically illustrated in Figure 6.1. The green and blue LEDs are positioned differently with respect to the red LED, so the object edges of the transition ranges will be rotated. In that way, they are the same way aligned to the green and blue LED as they are for the red LED. The resulting transition ranges for the green LED can be seen in Figure 9.4 and the transition range for the blue LED can be seen in Figure 9.5.

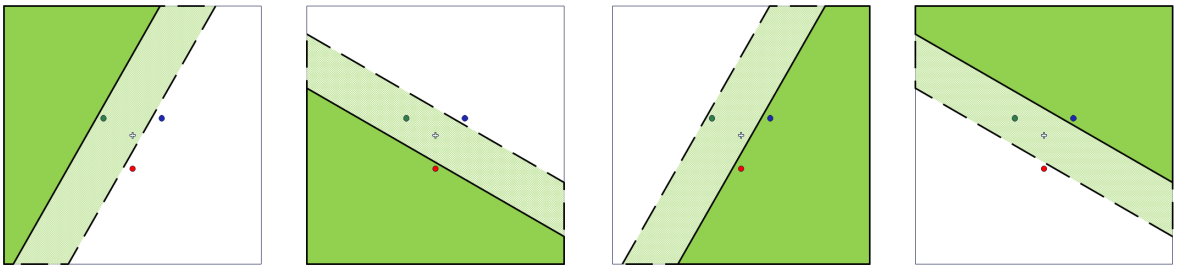

Figure 9.4: The ranges where a change in RGB value can be measured with 0 and 90-degree object orientation movements relative to the green LED.

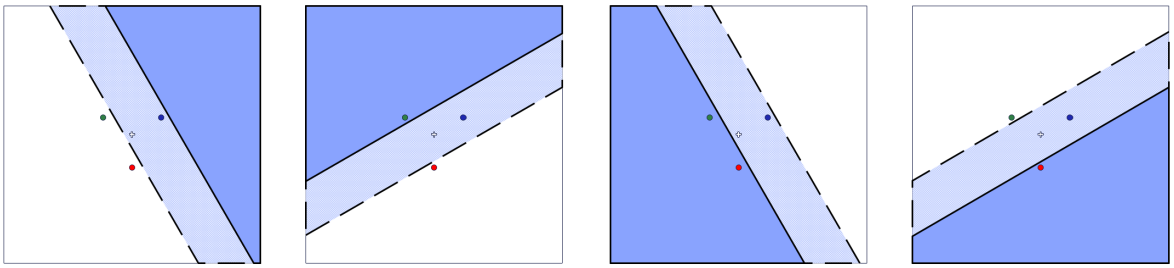

Figure 9.5: The ranges where a change in RGB value can be measured with 0 and 90-degree object orientation movements relative to the blue LED.

The difficulty of the information that now is known is that the ranges of, for example, the green and blue LEDs are not known for the object edge movements as seen in Figure 9.3. The solution is to make an expectation of what will happen to the transition range when it rotates at 90 degrees. Let's take the red measurement ranges from Figure 9.3 as an example. The first square illustrates the measurement range of a 0-degree object orientation. The second square illustrates the measurement range of a 90-degree object orientation. What happens between 0 and 90 degrees is not known for sure, but an expectation can be made because the starting point and the endpoint are known. Figure 9.6 illustrates the rotation of the transition range. The arrows indicate the coordinate system with respect to the object. The transition range of square number one lies between -7 and 2. When it is rotated 90 degrees, it has a transition range between -4 and 4. Through looking at the coordinate system, it can be seen that the -7 becomes -4 and that 2 becomes 4. The transition ranges for the angles between those transition ranges will be interpolated like in Equation 9.1

$$r_\theta = (r_{new} - r_{old}) \cdot \frac{\theta}{90} + r_{old} \tag{9.1}$$

With r_θ the desired range with an object orientation angle of θ between 0 and 90 degrees. The values r_{old} and r_{new} are respectively the transition range at 0 and 90 degrees. The coordinate system will rotate with the same angle θ. The calculated transition range lies in this new rotated coordinate system. This interpolation of the transition range can also be executed for the green and blue LEDs. Say it is desired to know the red, green and blue measurement range when an object is travelling from left to right. The red measurement range is already known, as illustrated in the fourth square from Figure 9.3. The green and blue transition ranges can be interpolated using Equation 9.1. The green transition range has to rotate 30 degrees counterclockwise, and the blue transition range has to rotate 30 degrees clockwise. Using the original coordinate system, the transition range for green lies between $x = -6$ and $x = 2.67$ and for blue between, $x = -2.67$ and $x = 6$. Figure 9.7 shows the transition ranges for the green and blue light. Now, all transition ranges for every colour are known when the object travels from the left to the right. It shows a different combination between the R-, G- and B-value. When this combination is extracted from the receiving fibre, it can tell something about the object's edge position. In the next subsection, an example is given of how an RGB value can be translated into an object edge position. It is explained why the interpolations of the measurement ranges are necessary for the calculation of the object edge position.

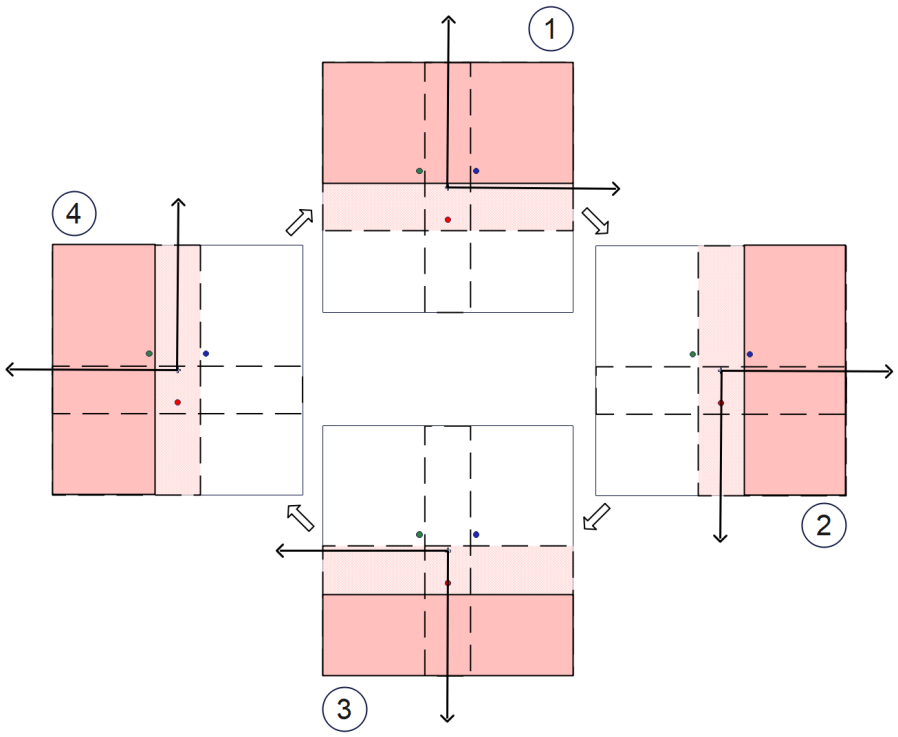

Figure 9.6: Schematic illustration of how the transition range can be rotated with 90 degrees to get the new transition range.

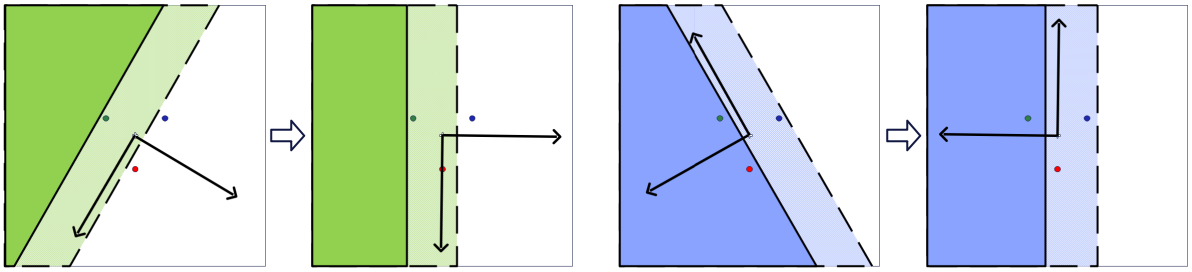

Figure 9.7: Schematic illustration example of how the green and blue ranges can be turned to get their ranges when travelling from left to right.

9.2.2. Example translating RGB-value into object position

An example will give a better image of how the end concept of the use of the primary light colours can be used for detecting the object's edge position with all the information that has been provided. For this example, there will be looked at object edge movements and positions that are perpendicular to the measurement plane. So the movements are going from bottom to top, right to left, top to bottom and left to right. The transition ranges for all three colours have to be known for all four movements. The red transition ranges are already known and can be seen in Figure 9.3. The green and blue transition ranges have to be interpolated to give their transition ranges for the desired movements. The transition ranges are interpolated with the use of Equation 9.1. The results are shown in Figure 9.8. The problem before was that an RGB value received from the receiving fibre could result in multiple object edge positions. Let's see if this also holds if every LED sent only its own colour of light. To make it easy, the transition ranges from Figures 9.1 and 9.2 will be rounded. The transition range lies between 40 and 70.

Say for example the R-value from the RGB value received from the receiving fibre gives a value of 55, which would be in the middle of the transition ranges as could be seen in the red light intensity graphs. With only the four movements taken into account, there are four possibilities where the object edge can be positioned by just knowing the R-value. Only with the combination of the G- and B-value the exact object edge position can be known. In Figure 9.8 the orange line illustrates the edge of the object when the R-value of the receiving fibre will give 55. The corresponding object edge positions are also illustrated in the green and blue transition ranges. The RGB values are listed in Table 9.1 for clearance. It can be seen that they are all different. So if the receiving fibre gives an RGB value of, for example, $[R \quad G \quad B] = [55 \quad 40 \quad 40]$. The object edge is positioned as illustrated with the orange line in Figure 9.8a.

Moving direction	**RGB value receiving fibre (0-255)**		
Bottom → Top Figure 9.8a	55	40	40
Right → Left Figure 9.8b	55	45	65
Top →Bottom Figure 9.8c	55	70	70
Left → Right Figure 9.8d	55	65	45

Table 9.1: The RGB value possibilities the receiving fibre can give when the R-value is 55.

The total range can be calculated where the object edge can be measured. What are the two values that are the farthest from the centre. For this example, the total range lies between $y = -7$ and $y = 5$ for the vertical movement and between $x = -6$ and $x = 6$ for the horizontal movement. These ranges can also be calculated for the green and blue light in the same way. All ranges are shown in Figure 9.9. The part that is overlapped by all ranges is the total measurement range. The object's edge can be detected if it goes through the grey part.

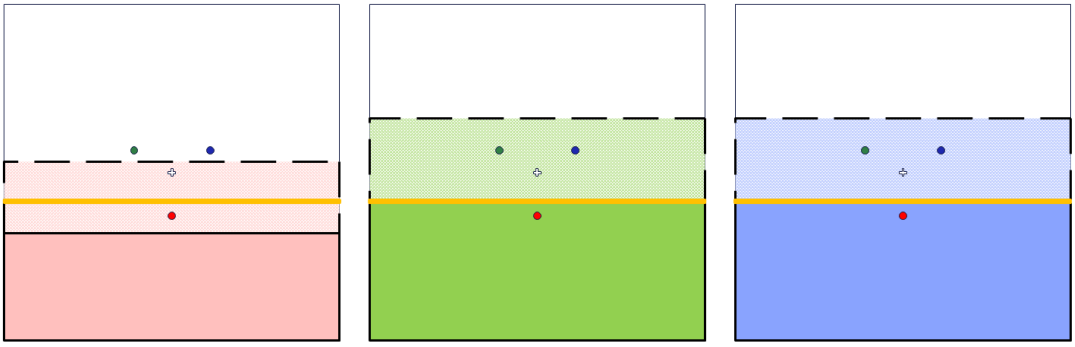

(a) The measurement range from each colour when travelling from bottom to top.

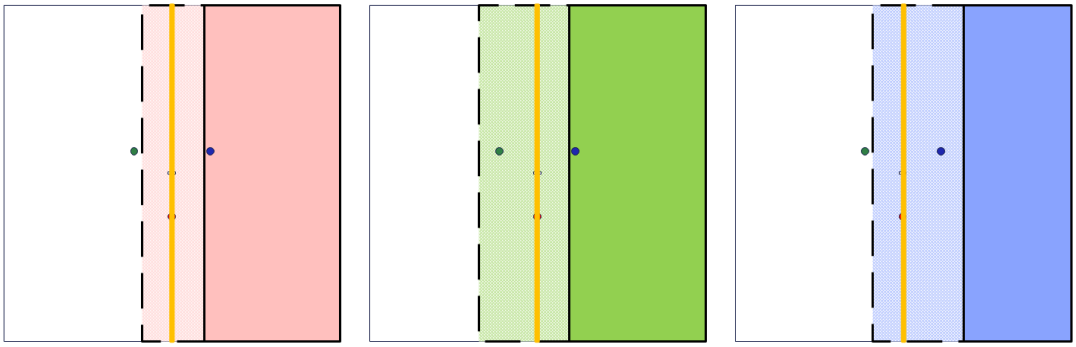

(b) The measurement range from each colour when travelling from right to left.

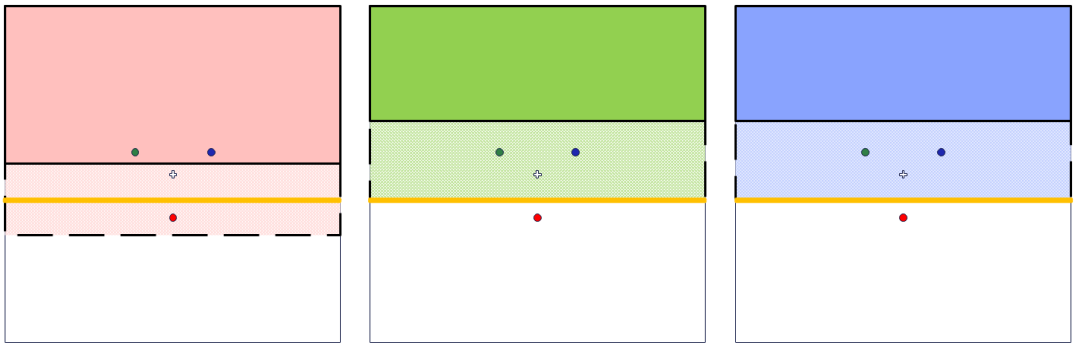

(c) The measurement range from each colour when travelling from top to bottom.

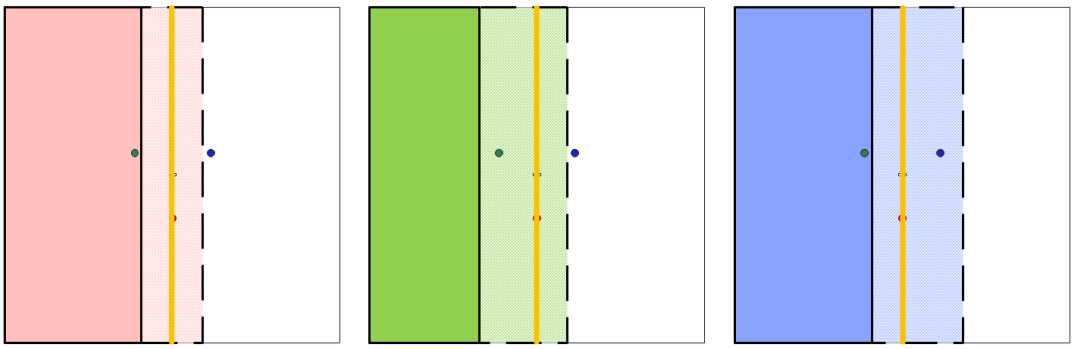

(d) The measurement range from each colour when travelling from left to right.

Figure 9.8: The measurement ranges for all perpendicular object orientation movements, with an example object edge location indicated with an orange line

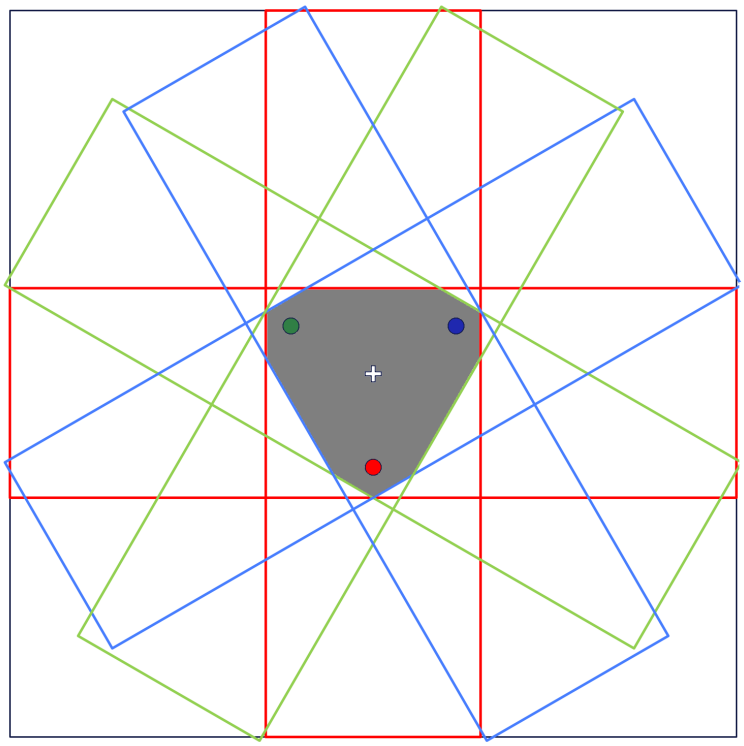

Figure 9.9: The area where the object edge can be measured when going through the grey part.

9.3. Conclusion

This chapter investigated the influence of object movement on the light intensity value of the receiving fibre when LEDs are used that each only emits one light colour. An experiment is executed that looked at the light intensity of the red LED. The green and blue transmitting fibres were covered by a thin non-transparent material to eliminate the light coming from those fibres. Two light-intensity graphs were made from the vertical and horizontal movements over the measurement plane. There were some green and blue distortions in the light intensity graphs. The green and blue distortions were set to zero because it is desired that a LED sent only one colour of light. Two transition ranges for the red LED appeared for the vertical and horizontal movement. The transition ranges can be translated into the green and blue transition ranges if the green and blue LEDs sent the same light intensity course as the red LED. The transition ranges from the red LED are rotated to get the green and blue transition ranges. Now, for every colour, two transition ranges are known. A model is made that interpolates the transition ranges of one colour in such a way that the transition range is known for every angle the object edge has. An example is given that illustrated that for vertical and horizontal movements with respect to the red LED. The example shows that a received RGB value from the receiving fibre can be translated to an object edge position. The total range, when combining all transition ranges, lies between $y = -7$ and $y = 5$ for the vertical movement and between $x = -6$ and $x = 6$ for the horizontal movement. This can also be done for the green and blue directions. When combining the ranges in a figure, the overlapping part is the total measurement range. That means that the object edge has to pass through that range in order to be detected. The assumption that the object edge can be measured by using this method is true. The only thing that can be improved is to make the transition range larger. In that way, it is easier to distinguish all possible object orientations.

10

Discussion

This research aimed to design an edge detection sensor with the use of optical fibres and the three primary light colours red, green and blue. The sensor can be implemented in an air-bearing table where a thin reflective object is being transported with air. Some research on this topic has been done. A group of bachelor students started by looking at if optical fibres can be used as a detection sensor at all. Fritz continued the research and looked in his master's thesis at if the vision of each optical fibre can be extended. This was possible by placing a volume diffuser over the optical fibres. This research continued by not only using one transmitting fibre and one receiving fibre, but using three transmitting fibres with one receiving fibre in the centre. Each transmitting fibre sent ideally their own light colour. This research validated experimentally how the edge of a floating object or a displacement of this object's edge could be detected. This chapter will give the important discussions hatched from this research.

10.1. Theoretical analysis

The vision of the optical fibres is broadened with the use of a volume diffuser. The theoretical analysis showed that it is really difficult to obtain a light intensity distribution after being diffused by a volume diffuser. A Gaussian shaped light intensity graph is assumed because a surface diffuser shows such a shape as well. This assumption turned out to be true. A lot of experiments were executed in the literature that supported this assumption. All experiments from the found literature showed a light intensity profile with a Gaussian shape after it travels through a volume diffuser.

The fact that three transmitting fibres will be used is decided based on that there are three primary light colours. So three transmitting fibres each sending their own colour. Only the fibre placement was important. The layout of the air bearings was important for making the fibre placement choice. The so-called Flowerbed air bearing table uses hexagonal-shaped air bearings. It showed great potential, so these shapes were used for determining fibre placement. Each corner of each hexagon is used for placing transmitting and receiving fibres alternately. The chosen orientation resulted that this research looked at one receiving fibre surrounded by three transmitting fibres 60 degrees apart from each other. This was decided to be one building block of the system

How much the light gets diffused depends on the diffuser type. The diffuser type choice in this research is done by testing various diffusers. This is done through an experiment. The Setacryl diffuser was chosen because this showed the best results. It was the most diffuse and did not show high-intensity spots in the middle of the light circles. If this diffuser is eventually the best choice is arguable. In later experiments, it was found that backscattering played an important role. The diffuser itself acted as a reflector. Using another diffuser did not show any improvements. Further research can investigate if other diffusers show the same results.

10.2. Experimental discussions

The ideal and premeditated working principle that each LED emits its own wavelength turned out not to be possible. It has been shown that it is really difficult to send one singular colour from a LED. The red transmitting fibre for instance has some of the other primary colours, green and blue, in its light intensity profile. This made it difficult to measure a position or orientation because first it was thought that when the object covers the red LED for instance that the receiving fibre only sees the colour red and not green and blue. In practice, this does not hold because the red LED also emits green and blue.

The material that was chosen is 50 micrometres thick brass foil paper. A thin reflecting material was needed in one experiment and a non-reflecting material was needed in the other experiment. The brass foil paper is used for both experiments, but in the experiment where no reflection is desired, the brass foil paper is sprayed black to eliminate the reflection properties.

Two experiments were executed that should be the opposite of each other. At least that was the assumption. That is because one experiment used no reflection and looked with a camera from the top downwards at the receiving fibre location, and the other experiment includes reflection and looked at the end of the receiving fibre. The measurement plane where the diffuser and the pieces of material were placed was a square of 44 by 44 millimetres. Squares of 50 micrometres thick brass foil were cut. Those squares were again cut with a specific angle. One piece of material, after being sprayed black, was used in the experiment without using reflection and the opposite piece in the other experiment with using reflection. The RGB values were not comparable to each other because in the experiment where reflection was included a thing occurred that was not expected. Despite that the setup was sealed off from external light sources, the receiving fibre still saw a relatively high RGB intensity value even when no object was covering the fibres. As mentioned before, this was due to the light that got reflected backwards inside the diffuser layer. It was hard to distinguish the multiple-angle orientations. The vertical and horizontal object displacements showed a better result. A range was found where an object displacement can be noticed by looking at the RGB value difference in the receiving fibre.

It has been seen that in the first experiments one building block, which includes one receiving fibre and three transmitting fibres, is not enough to detect the angular movement of an object looking only at the RGB value from that receiving fibre. This is because a 0 and 90-degree object orientation movements could result in the same RGB value in the receiving fibre. The reason was the disruptions the LEDs gave. To see if the final concept will work at all, chapter 9 discussed what happens when the three transmitting fibres each sent one light colour. The model made it clear that the concept works and the object edge can be measured if the object goes through a specific measurement range. The ranges that came out of this model were different from the ones measured before, but they were also more logical. The range for the horizontal object displacements has the same range to the left as to the right of the receiving fibre. This is logical because the receiving fibre and red transmitting fibre are lying on the same vertical line. The difference that it now works as expected is because of a change in, for example, R-value in the received RGB value from the receiving fibre now definitely comes from the red transmitting fibre and not the two other transmitting fibres. So it is easier to distinguish where the change in RGB value is coming from.

The model made in chapter 3 is partly true. In that chapter, it was said that the R- and G-value give a maximum value when the object is above both transmitting fibres. Chapter 9 made it clear that the transition area from a minimum to a maximum value includes the corresponding transmitting fibre and the receiving fibre. So the maximum value is not achieved immediately when the transmitting fibre is covered.

This research has proved that it is possible to use the three different primary light colours for observing an object's edge position. The light intensity transition ranges are not very wide, so it can be hard to distinguish all different object orientations. Further research can be done on the light sources and the volume diffuser that has been used. The LEDs need to send light without disruptions of other light colours in their light intensity profile. The volume diffuser can be investigated more to see what the limits are with backscattering. If backscattering will be minimized, the transition ranges can be made wider which results in more precise object edge positions. The first experiments can be executed again to see what the changes will be in those measurement results. More about the recommendations is found in chapter 12.

11

Conclusion

This chapter will discuss the most important results and conclusions that came out of this research. Most importantly, this chapter will investigate again the research objective that was stated at the beginning of this research.

11.1. Theoretical conclusions

This research started with a theoretical analysis. It showed that it was very difficult to come up with presumptions because it was hard to know what will happen to the light rays after being diffused by a volume diffuser. Literature showed, together with some thoughts, the following important conclusions:

⇒ The light intensity profile of a light circle can be assumed to have a Gaussian shape. High intensity in the middle, with decreasing intensity towards the edges.

⇒ Hexagonal air bearings showed the most potential. The fibre placement was based on the layout of the hexagonal air bearings. The experiments were executed with the emerged setup.

11.2. Experimental conclusions

Some of the four experiments executed in this research showed some results that were also assumed beforehand, but some experiments also showed something that was not assumed and not desired as well. Below are the four experiments, with key findings from the corresponding experiment:

1. Experiment 1
   The first experiment showed a valid way to calculate the centre pixel coordinates of the three transmitting fibres and the receiving fibre in the centre. The assumption was made that a small offset could occur in the scale due to some inaccuracy in, for example, the 3D-printed objects. This was as aspected minimal and would not have an enormous effect on the later experiments.

2. Experiment 2
   The second experiment tested various diffusers. The Setacryl diffuser was chosen because of its high diffusivity and minimal blooming. At the beginning of the research, an assumption was made that if the object would float above one transmitting fibre, the receiving fibre would emit the colour from that transmitting fibre. This assumption was found not to be true. What can be concluded from the second experiment is that, for example, the red transmitting fibre not only emits red light but also green and blue light. In reality, when an object is floating above one transmitting fibre, all three primary light colours could be received in the receiving fibre.

3. Experiment 3
   The third experiment investigated object displacements without light reflection. Two diffuser layers with a piece of material between them imitated the end concept. A decrease in RGB value was found after being constant for a certain distance. The decrease started at $y = -8$ for vertical movements and started at $x = -10$ for horizontal movements. A wider range was expected beforehand, but from the

results, it turned out not to be true.

4. Experiment 4
   The fourth and last experiment investigated the final concept, where reflection was included. This was the opposite of the third experiment. The same results were expected, but the opposite turned out to be true. This was due to a large amount of backscattering that occurred in the volume diffuser itself. Another diffuser that was investigated showed the same result, so the Setacryl diffuser was chosen to continue with. A range was found where the RGB value changed. This range lies for the 0-degree movement between the lines $y = -2$ and $y = 4$ and for the 90-degree movement between the lines $x = -8$ and $x = 2$.

This research aimed to execute the following research objective:

"Design and experimental validate an edge detection sensing surface with the use of optical fibres and the three primary light colours"

The four experiments tried to get the desired result to succeed in the research objective, but it turned out to be harder than expected. The disruptions in the light sources cause unwanted results. For that reason, the last chapter took a closer look at the concept itself and what will happen if the LEDs sent each only their own colour of light. What can be concluded from that last chapter was that the concept will work. The transition range for the red LED lies between the lines $y = -7$ and $y = 2$ and between $x = -4$ and $x = 4$. These ranges make much more sense. These transition ranges were also found for the green and blue transmitting fibres. A model was found that could interpolate the transition ranges in such a way that for every object's edge angle position, the three transition ranges for the three light colours are known. When an object is moving over an air-bearing table, the measurement range lies between $y = -7$ and $y = 5$ for the vertical movement and between $x = -6$ and $x = 6$ for the horizontal movement. These ranges were also found when looking at the green and blue LEDs. The part where all measurement ranges overlapped, as illustrated in Figure 11.1, is the total measurement range. That means that the object's edge position can be detected when it goes through the grey part. The RGB transition range is not that wide, so all the different object angle orientations will be hard to distinguish.

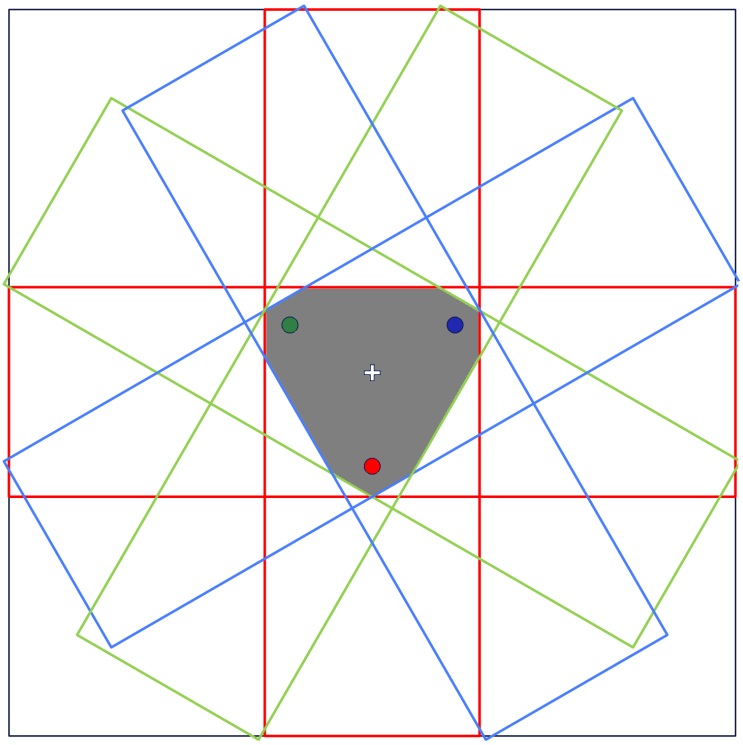

Figure 11.1: The area where the object edge can be measured when going through the grey part.

12

Recommendations

This research showed a nice way to use the three primary light colours red, green and blue for the detection of a straight object edge. Not everything was perfect, and some downsides were found. This research can be extended by looking at the following points:

⇒ *Use a light source which emits pure light.*
The experiments executed in chapter 6, chapter 7 and chapter 8 showed a lot of noise. The red LED for example did not send only the colour red. Some of the other primary light colours, green and blue, were observed. These disruptions were also found in the green and blue LED. Chapter 9 showed a model that if the LEDs sent each only one pure light colour that the object edge can be measured, way more easily. If from the start of the research LEDs were used that emit one colour, the measurements could give better and more desired results.

⇒ *Look into using a different volume diffuser*
The concept of backscattering was known beforehand, but that this plays a significant role was not expected. The volume diffuser used was good at diffusing the light evenly. The downside was that a lot of the light scattered back within the volume diffuser itself. The backscattered light was received by the receiving fibre. This causes a small transition area of the light intensity. In that way, the object angles are hard to distinguish because the RGB values will be close to each other. If the light intensity range will be wider, it will be easier to know under which angle the object is positioned. A wider light intensity range can be achieved by investigating the volume diffuser more in-depth and choosing one based on other criteria.

⇒ *Investigate round objects*
This research investigated only straight objects, but not all objects that are transported on an air-bearing table are straight. Wafers, for example, are round and are often used in the photovoltaic industry. Future research can be done by investigating round objects and their influence on RGB value. It is also possible to look at the use of different radii for the objects.

⇒ *Fibres that are not limited in how diffuse the light may be*
A restriction in this research was that each transmitting fibre may not reach adjacent receiving fibres. This research only used one receiving fibre, but the imaginary other receiving fibres from possible adjacent other building blocks did not receive light from the transmitting fibres used in this research. It was chosen not to do so, but maybe it does not matter. Maybe there will be positive advantages, or there will be no difference. The light can be more diffused and the transmitting fibres can be placed further away from each other.

⇒ *Extend the setup with more building blocks connected*
This research looked into one building block that consists of one receiving fibre surrounded by three transmitting fibres. The end concept is a full table that consists of multiple building blocks connected. The influence of more building blocks has to be investigated.

A

Tables and figures

A.1. Chapter 7

A.1.1. Perpendicular object movements without light reflection

Angle (degrees)	RGB value receiving fibre (0-255)			RGB value difference (0-255)			Absolute displacement in comparison with previous piece (mm)
	R	G	B	R	G	B	
0	111	142	147		N/A		N/A
	111	140	142	0	-2	-5	~2.0
	114	139	142	+3	-1	0	~1.8
	113	140	141	-1	+1	-1	~2.2
	116	139	142	+3	-1	+1	~2.0
	112	141	142	-4	+2	0	~1.6
	115	141	142	+3	0	0	~2.3
	110	140	143	-5	-1	+1	~2.0
	100	140	142	-10	0	-1	~2.1
	73	137	138	-27	-3	-4	~ 2.0
	36	134	134	-37	-3	-4	~ 1.9
90	111	142	147		N/A		N/A
	115	140	143	+4	-2	-4	~ 2.0
	120	140	142	+5	0	-1	~ 1.8
	113	141	143	-7	+1	+1	~2.2
	119	138	139	+6	-3	-4	~2.0
	113	141	140	-6	+3	+1	~1.6
	113	141	139	0	0	-1	~2.3
	113	139	133	0	-2	-6	~2.0
	113	135	120	0	-4	-13	~2.1
	87	117	88	-26	-18	-32	~2.0
	57	84	59	-30	-33	-29	~ 1.9

Table A.1: The object movement angles with the corresponding RGB value of the receiving fibre location.

A.2. Chapter 8

A.2.1. Object movement 0 degree orientation with light reflection

Angle (degrees)	RGB value receiving fibre (0-255)			Object edge y-coordinate (mm)	Absolute displacement (mm)
	R	G	B		
0	104	92	91	22	N/A
	103	92	89	20	~2.0
	103	92	89	18.2	~1.8
	104	92	88	16	~2.2
	103	92	89	14	~2.0
	102	92	88	12.4	~1.6
	102	91	85	10.1	~2.3
	103	91	88	8.1	~2.0
	105	93	89	6	~2.1
	101	93	89	3.9	~ 2.1
	103	97	93	3.2	~0.7
	112	102	98	2	~1.2
	113	108	103	1	~1.0
	114	110	105	0	~1.0
	119	118	112	-1	~1.0
	127	121	115	-2.1	~1.1
	123	119	113	-4	~ 1.9
	126	121	115	-6	~2.0
	127	121	116	-8	~2.0
	127	121	116	-10	~2.0
	125	118	114	-12	~2.0
	125	118	112	-14	~2.0
	127	122	117	-16	~2.0
	125	121	116	-18	~2.0
	128	122	116	-20	~ 2.0
	130	124	119	-22	~2.0

Table A.2: 0 degrees object orientation displacement with the corresponding RGB value of the receiving fibre.

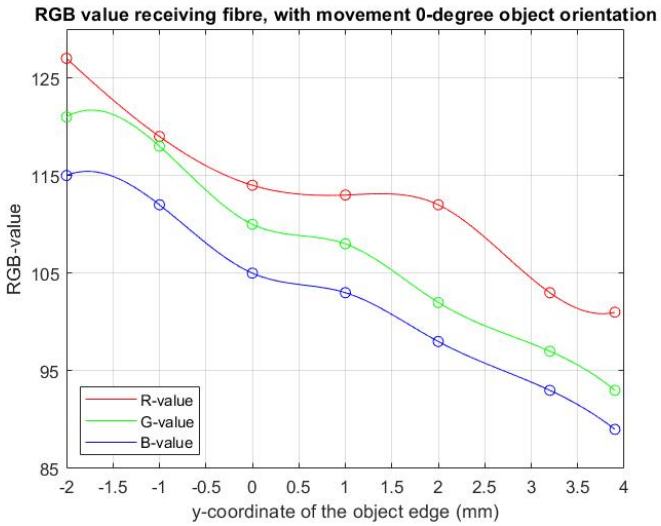

Figure A.1: More in depth graph of the RGB value course when a piece of material is travelling over the diffuser layer with a 0-degree angle.

A.2.2. Object movement 90 degree orientation with light reflection

Angle (degrees)	RGB value receiving fibre (0-255)			Object edge x-coordinate (mm)	Absolute displacement (mm)
	R	G	B		
90	104	92	91	22	N/A
	104	92	89	20	~2.0
	104	92	87	18.2	~1.8
	104	92	87	16	~2.2
	103	92	90	14	~2.0
	103	92	89	12.4	~1.6
	104	92	88	10.1	~2.3
	103	92	89	8.1	~2.0
	104	92	89	6	~2.1
	104	92	89	3.9	~ 2.1
	103	95	91	2	~ 1.9
	106	95	91	1	~1.0
	107	96	94	0	~1.0
	112	104	100	-1	~1.0
	115	105	102	-2.1	~1.1
	119	111	107	-3	~0.9
	120	111	106	-4	~1.0
	126	121	115	-5	~1.0
	125	119	113	-6	~1.0
	128	123	117	-7	~1.0
	129	123	118	-8	~1.0
	128	122	116	-10	~2.0
	125	118	114	-12	~2.0
	124	117	113	-14	~2.0
	127	123	117	-16	~2.0
	126	120	114	-18	~2.0
	127	121	115	-20	~ 2.0
	130	124	119	-22	~2.0

Table A.3: 90 degrees object orientation displacement with the corresponding RGB value of the receiving fibre.

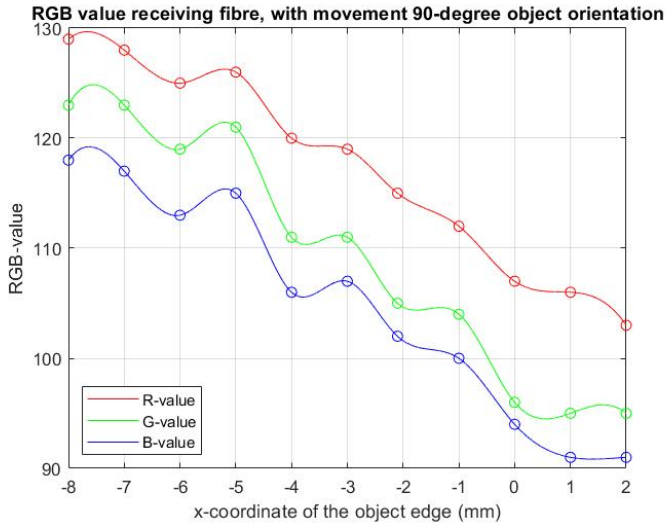

Figure A.2: More in depth graph of the RGB value course between 20 and 30

A.3. Chapter 9

A.3.1. R-value for 0- and 90-degree object orientation movement

Angle (degrees)	R-value (0-255)	Angle (degrees)	R-value (0-255)	Object edge x/y-coordinate (mm)	Absolute displacement (mm)
0	41	90	41	22	N/A
	40		41	20	~2.0
	40		41	18.2	~1.8
	40		40	16	~2.2
	40		40	14	~2.0
	40		41	12.4	~1.6
	40		41	10.1	~2.3
	41		41	8.1	~2.0
	40		41	6	~2.1
	39		40	3.9	~ 2.1
	41		41	3.2	~0.7
	41		43	2	~1.2
	42		45	1	~1.0
	44		49	0	~1.0
	46		61	-1	~1.0
	51		64	-2.1	~1.1
	53		65	-3	~ 0.9
	55		66	-4	~ 1.0
	61		66	-5	~ 1.0
	63		66	-6	~1.0
	68		66	-7	~ 1.0
	66		66	-8	~1.0
	68		68	-10	~2.0
	68		68	-12	~2.0
	66		67	-14	~2.0
	69		69	-16	~2.0
	70		70	-18	~2.0
	68		69	-20	~ 2.0
	71		71	-22	~2.0

Table A.4: 0 degrees object orientation displacement with the corresponding RGB value of the receiving fibre.

B

MATLAB codes

B.1. Chapter 5

B.1.1. Find centre coordinates of all the fibres

```
%% Finding centre coordinates of the fibres
clc; clear all; close all
%% Begin making figure
theta = 0 : 0.01 : 2*pi;
radius = 20;

% Read the image
img = imread('.jpg');            % Insert picture file between brackets
figure(1)
imshow(img)
title('Centrepositions three transmitting fibers and centreposition receiving fiber')
xlabel('Distance along profile column/width (pixels)')
ylabel('Distance along profile row/height (pixels)')
xticks(0:200:1920)
yticks(0:200:1080)
xlim([650 1250])
ylim([300 800])
ax = gca;
ax.GridLineStyle = '--';
ax.GridColor = [0.75, 0.75, 0.75];
grid on
hold on
axis on

%% Find the centre of RED fibre
% Filter the low RGB values
for c = 1:1920
    for r = 1:1080
        if img(r, c, 1) < 230
            imgR(r, c, 1) = 0;
        else
            imgR(r, c, 1) = img(r, c, 1);
        end
    end
end
imgR(:, :, 2) = 0;
imgR(:, :, 3) = 0;

% Find the unique rows and columns where in this case the R-values are located
[Rrows, Rcolumns] = find(imgR(:, :, 1) > 0);
Rrows = single(unique(Rrows));
Rcolumns = single(unique(Rcolumns));

% Seperate the rows in the different peaks
```

```
for i = 1:(size(Rrows,1)-1)
    if Rrows(i+1,1)-Rrows(i,1) ≥ 0 && Rrows(i+1,1)-Rrows(i,1) < 10
        Rrow(i,1) = 1;
    else
        Rrow(i,1) = 0;
    end
end
Rrow = single(Rrow);

Y=[0; find(Rrow == 0)];
if size(Y,1) == 1
        Rrow1 = Rrows(1:end);
        Rrowpeak1 = round((Rrow1(end)+Rrow1(1))/2); %round(mean(Rrow1));
    elseif size(Y,1) == 2
        Rrow1 = Rrows(1:Y(2));
        Rrowpeak1 = round(mean(Rrow1));
        Rrow2 = Rrows((Y(2)+1):end);
        Rrowpeak2 = round(mean(Rrow2));
    elseif size(Y,1) == 3
        Rrow1 = Rrows(1:Y(2));
        Rrowpeak1 = round(mean(Rrow1));
        Rrow2 = Rrows(Y(2)+1:Y(3));
        Rrowpeak2 = round(mean(Rrow2));
        Rrow3 = Rrows(Y(3)+1:end);
        Rrowpeak3 = round(mean(Rrow3));
end

% Seperate the columns in the different peaks
for i = 1:(size(Rcolumns,1)-1)
    if Rcolumns(i+1,1)-Rcolumns(i,1) ≥ 0 && Rcolumns(i+1,1)-Rcolumns(i,1) < 10
        Rcolumn(i,1) = 1;
    else
        Rcolumn(i,1) = 0;
    end
end
Rcolumn = single(Rcolumn);

X=[0; find(Rcolumn == 0)];
if size(X,1) == 1
        Rcolumn1 = Rcolumns(1:end);
        Rcolumnpeak1 = round((Rcolumn1(end)+Rcolumn1(1))/2); %round(mean(Rcolumn1));
    elseif size(X,1) == 2
        Rcolumn1 = Rcolumns(1:X(2));
        Rcolumnpeak1 = round(mean(Rcolumn1));
        Rcolumn2 = Rcolumns((X(2)+1):end);
        Rcolumnpeak2 = round(mean(Rcolumn2));
    elseif size(X,1) == 3
        Rcolumn1 = Rcolumns(1:X(2));
        Rcolumnpeak1 = round(mean(Rcolumn1));
        Rcolumn2 = Rcolumns(X(2)+1:X(3));
        Rcolumnpeak2 = round(mean(Rcolumn2));
        Rcolumn3 = Rcolumns(X(3)+1:end);
        Rcolumnpeak3 = round(mean(Rcolumn3));
end

if size(Y,1) == 1
     Rxx1 = Rcolumnpeak1;
     Ryy1 = Rrowpeak1;
     figure(1)
     x1 = radius * cos(theta) + Rxx1;
     y1 = radius * sin(theta) + Ryy1;
     plot(x1, y1, 'Color',[1 1 1]);
    elseif size(Y,1) == 2
       if img(Rrowpeak1, Rcolumnpeak1, 1) ≥ 230
           Rxx1 = Rcolumnpeak1;
           Ryy1 = Rrowpeak1;
           Rxx2 = Rcolumnpeak2;
           Ryy2 = Rrowpeak2;
       else
           Rxx1 = Rcolumnpeak1;
           Ryy1 = Rrowpeak2;
```

```
116             Rxx2 = Rcolumnpeak2;
117             Ryy2 = Rrowpeak1;
118         end
119       figure(1)
120       x1 = radius * cos(theta) + Rxx1;
121       y1 = radius * sin(theta) + Ryy1;
122       x2 = radius * cos(theta) + Rxx2;
123       y2 = radius * sin(theta) + Ryy2;
124       plot(x1, y1, 'Color',[1 1 1]);
125       plot(x2, y2, 'Color',[1 1 1]);
126     elseif size(Y,1) == 3
127         if img(Rrowpeak1, Rcolumnpeak1, 1) ≥ 230 && img(Rrowpeak2, Rcolumnpeak2, 1) ≥ 230
128             Rxx1 = Rcolumnpeak1;
129             Ryy1 = Rrowpeak1;
130             Rxx2 = Rcolumnpeak2;
131             Ryy2 = Rrowpeak2;
132             Rxx3 = Rcolumnpeak3;
133             Ryy3 = Rrowpeak3;
134         elseif img(Rrowpeak1, Rcolumnpeak1, 1) ≥ 230 && img(Rrowpeak3, Rcolumnpeak2, ...
                1) ≥ 230
135             Rxx1 = Rcolumnpeak1;
136             Ryy1 = Rrowpeak1;
137             Rxx2 = Rcolumnpeak2;
138             Ryy2 = Rrowpeak3;
139             Rxx3 = Rcolumnpeak3;
140             Ryy3 = Rrowpeak2;
141         elseif  img(Rrowpeak2, Rcolumnpeak1, 1) ≥ 230 && img(Rrowpeak1, Rcolumnpeak2, ...
                1) ≥ 230
142             Rxx1 = Rcolumnpeak1;
143             Ryy1 = Rrowpeak2;
144             Rxx2 = Rcolumnpeak2;
145             Ryy2 = Rrowpeak1;
146             Rxx3 = Rcolumnpeak3;
147             Ryy3 = Rrowpeak3;
148         elseif  img(Rrowpeak2, Rcolumnpeak1, 1) ≥ 230 && img(Rrowpeak3, Rcolumnpeak2, ...
                1) ≥ 230
149             Rxx1 = Rcolumnpeak1;
150             Ryy1 = Rrowpeak2;
151             Rxx2 = Rcolumnpeak2;
152             Ryy2 = Rrowpeak3;
153             Rxx3 = Rcolumnpeak3;
154             Ryy3 = Rrowpeak1;
155         elseif  img(Rrowpeak3, Rcolumnpeak1, 1) ≥ 230 && img(Rrowpeak1, Rcolumnpeak2, ...
                1) ≥ 230
156             Rxx1 = Rcolumnpeak1;
157             Ryy1 = Rrowpeak3;
158             Rxx2 = Rcolumnpeak2;
159             Ryy2 = Rrowpeak1;
160             Rxx3 = Rcolumnpeak3;
161             Ryy3 = Rrowpeak2;
162         else
163             Rxx1 = Rcolumnpeak1;
164             Ryy1 = Rrowpeak3;
165             Rxx2 = Rcolumnpeak2;
166             Ryy2 = Rrowpeak2;
167             Rxx3 = Rcolumnpeak3;
168             Ryy3 = Rrowpeak1;
169         end
170       figure(1)
171       x1 = radius * cos(theta) + Rxx1;
172       y1 = radius * sin(theta) + Ryy1;
173       x2 = radius * cos(theta) + Rxx2;
174       y2 = radius * sin(theta) + Ryy2;
175       x3 = radius * cos(theta) + Rxx3;
176       y3 = radius * sin(theta) + Ryy3;
177       plot(x1, y1, 'Color',[1 1 1]);
178       plot(x2, y2, 'Color',[1 1 1]);
179       plot(x3, y3, 'Color',[1 1 1]);
180   end
181
182   %% Find the centre of GREEN fibre
```

```
% Filter the low RGB values
for c = 1:1920
    for r = 1:1080
        if img(r, c, 2) < 230
            imgG(r, c, 2) = 0;
        else
            imgG(r, c, 2) = img(r, c, 2);
        end
    end
end
imgG(:, :, 1) = 0;
imgG(:, :, 3) = 0;

% Find the unique rows and columns where in this case the R-values are located
[Grows, Gcolumns] = find(imgG(:, :, 2) > 0);
Grows = single(unique(Grows));
Gcolumns = single(unique(Gcolumns));

% Seperate the rows in the different peaks
for i = 1:(size(Grows,1)-1)
    if Grows(i+1,1)-Grows(i,1) ≥ 0 && Grows(i+1,1)-Grows(i,1) < 10
        Grow(i,1) = 1;
    else
        Grow(i,1) = 0;
    end
end
Grow = single(Grow);

Y=[0; find(Grow == 0)];
if size(Y,1) == 1
        Grow1 = Grows(1:end);
        Growpeak1 = round((Grow1(end)+Grow1(1))/2); %round(mean(Grow1));
    elseif size(Y,1) == 2
        Grow1 = Grows(1:Y(2));
        Growpeak1 = round(mean(Grow1));
        Grow2 = Grows((Y(2)+1):end);
        Growpeak2 = round(mean(Grow2));
    elseif size(Y,1) == 3
        Grow1 = Grows(1:Y(2));
        Growpeak1 = round(mean(Grow1));
        Grow2 = Grows(Y(2)+1:Y(3));
        Growpeak2 = round(mean(Grow2));
        Grow3 = Grows(Y(3)+1:end);
        Growpeak3 = round(mean(Grow3));
end

% Seperate the columns in the different peaks
for i = 1:(size(Gcolumns,1)-1)
    if Gcolumns(i+1,1)-Gcolumns(i,1) ≥ 0 && Gcolumns(i+1,1)-Gcolumns(i,1) < 10
        Gcolumn(i,1) = 1;
    else
        Gcolumn(i,1) = 0;
    end
end
Gcolumn = single(Gcolumn);

X=[0; find(Gcolumn == 0)];
if size(X,1) == 1
        Gcolumn1 = Gcolumns(1:end);
        Gcolumnpeak1 = round((Gcolumn1(end)+Gcolumn1(1))/2); %round(mean(Gcolumn1));
    elseif size(X,1) == 2
        Gcolumn1 = Gcolumns(1:X(2));
        Gcolumnpeak1 = round(mean(Gcolumn1));
        Gcolumn2 = Gcolumns((X(2)+1):end);
        Gcolumnpeak2 = round(mean(Gcolumn2));
    elseif size(X,1) == 3
        Gcolumn1 = Gcolumns(1:X(2));
        Gcolumnpeak1 = round(mean(Gcolumn1));
        Gcolumn2 = Gcolumns(X(2)+1:X(3));
        Gcolumnpeak2 = round(mean(Gcolumn2));
        Gcolumn3 = Gcolumns(X(3)+1:end);
```

```
        Gcolumnpeak3 = round(mean(Gcolumn3));
end

if size(Y,1) == 1
     Gxx1 = Gcolumnpeak1;
     Gyy1 = Growpeak1;
     figure(1)
     x1 = radius * cos(theta) + Gxx1;
     y1 = radius * sin(theta) + Gyy1;
     plot(x1, y1, 'Color',[1 1 1]);
    elseif size(Y,1) == 2
       if img(Growpeak1, Gcolumnpeak1, 2) ≥ 230
           Gxx1 = Gcolumnpeak1;
           Gyy1 = Growpeak1;
           Gxx2 = Gcolumnpeak2;
           Gyy2 = Growpeak2;
       else
           Gxx1 = Gcolumnpeak1;
           Gyy1 = Growpeak2;
           Gxx2 = Gcolumnpeak2;
           Gyy2 = Growpeak1;
       end
     figure(1)
     x1 = radius * cos(theta) + Gxx1;
     y1 = radius * sin(theta) + Gyy1;
     x2 = radius * cos(theta) + Gxx2;
     y2 = radius * sin(theta) + Gyy2;
     plot(x1, y1, 'Color',[1 1 1]);
     plot(x2, y2, 'Color',[1 1 1]);
    elseif size(Y,1) == 3
        if img(Growpeak1, Gcolumnpeak1, 2) ≥ 230 && img(Growpeak2, Gcolumnpeak2, 2) ≥ 230
           Gxx1 = Gcolumnpeak1;
           Gyy1 = Growpeak1;
           Gxx2 = Gcolumnpeak2;
           Gyy2 = Growpeak2;
           Gxx3 = Gcolumnpeak3;
           Gyy3 = Growpeak3;
        elseif img(Growpeak1, Gcolumnpeak1, 2) ≥ 230 && img(Growpeak3, Gcolumnpeak2, ...
            2) ≥ 230
           Gxx1 = Gcolumnpeak1;
           Gyy1 = Growpeak1;
           Gxx2 = Gcolumnpeak2;
           Gyy2 = Growpeak3;
           Gxx3 = Gcolumnpeak3;
           Gyy3 = Growpeak2;
        elseif  img(Growpeak2, Gcolumnpeak1, 2) ≥ 230 && img(Growpeak1, Gcolumnpeak2, ...
            2) ≥ 230
           Gxx1 = Gcolumnpeak1;
           Gyy1 = Growpeak2;
           Gxx2 = Gcolumnpeak2;
           Gyy2 = Growpeak1;
           Gxx3 = Gcolumnpeak3;
           Gyy3 = Growpeak3;
        elseif  img(Growpeak2, Gcolumnpeak1, 2) ≥ 230 && img(Growpeak3, Gcolumnpeak2, ...
            2) ≥ 230
           Gxx1 = Gcolumnpeak1;
           Gyy1 = Growpeak2;
           Gxx2 = Gcolumnpeak2;
           Gyy2 = Growpeak3;
           Gxx3 = Gcolumnpeak3;
           Gyy3 = Growpeak1;
        elseif  img(Growpeak3, Gcolumnpeak1, 2) ≥ 230 && img(Growpeak1, Gcolumnpeak2, ...
            2) ≥ 230
           Gxx1 = Gcolumnpeak1;
           Gyy1 = Growpeak3;
           Gxx2 = Gcolumnpeak2;
           Gyy2 = Growpeak1;
           Gxx3 = Gcolumnpeak3;
           Gyy3 = Growpeak2;
        else
           Gxx1 = Gcolumnpeak1;
```

```
            Gyy1 = Growpeak3;
            Gxx2 = Gcolumnpeak2;
            Gyy2 = Growpeak2;
            Gxx3 = Gcolumnpeak3;
            Gyy3 = Growpeak1;
        end
     figure(1)
     x1 = radius * cos(theta) + Gxx1;
     y1 = radius * sin(theta) + Gyy1;
     x2 = radius * cos(theta) + Gxx2;
     y2 = radius * sin(theta) + Gyy2;
     x3 = radius * cos(theta) + Gxx3;
     y3 = radius * sin(theta) + Gyy3;
     plot(x1, y1, 'Color',[1 1 1]);
     plot(x2, y2, 'Color',[1 1 1]);
     plot(x3, y3, 'Color',[1 1 1]);
end

%% Find the centre of BLUE fibre
% Filter the low RGB values
for c = 1:1920
    for r = 1:1080
        if img(r, c, 3) < 230
            imgB(r, c, 3) = 0;
        else
            imgB(r, c, 3) = img(r, c, 3);
        end
    end
end
imgB(:, :, 1) = 0;
imgB(:, :, 2) = 0;

% Find the unique rows and columns where in this case the R-values are located
[Brows, Bcolumns] = find(imgB(:, :, 3) > 0);
Brows = single(unique(Brows));
Bcolumns = single(unique(Bcolumns));

% Seperate the rows in the different peaks
for i = 1:(size(Brows,1)-1)
    if Brows(i+1,1)-Brows(i,1) ≥ 0 && Brows(i+1,1)-Brows(i,1) < 10
        Brow(i,1) = 1;
    else
        Brow(i,1) = 0;
    end
end
Brow = single(Brow);

Y=[0; find(Brow == 0)];
if size(Y,1) == 1
        Brow1 = Brows(1:end);
        Browpeak1 = round((Brow1(end)+Brow1(1))/2); %round(mean(Brow1));
    elseif size(Y,1) == 2
        Brow1 = Brows(1:Y(2));
        Browpeak1 = round(mean(Brow1));
        Brow2 = Brows((Y(2)+1):end);
        Browpeak2 = round(mean(Brow2));
    elseif size(Y,1) == 3
        Brow1 = Brows(1:Y(2));
        Browpeak1 = round(mean(Brow1));
        Brow2 = Brows(Y(2)+1:Y(3));
        Browpeak2 = round(mean(Brow2));
        Brow3 = Brows(Y(3)+1:end);
        Browpeak3 = round(mean(Brow3));
end

% Seperate the columns in the different peaks
for i = 1:(size(Bcolumns,1)-1)
    if Bcolumns(i+1,1)-Bcolumns(i,1) ≥ 0 && Bcolumns(i+1,1)-Bcolumns(i,1) < 10
        Bcolumn(i,1) = 1;
    else
        Bcolumn(i,1) = 0;
```

```
392     end
393 end
394 Bcolumn = single(Bcolumn);
395
396 X=[0; find(Bcolumn == 0)];
397 if size(X,1) == 1
398         Bcolumn1 = Bcolumns(1:end);
399         Bcolumnpeak1 = round((Bcolumn1(end)+Bcolumn1(1))/2); %round(mean(Bcolumn1));
400     elseif size(X,1) == 2
401         Bcolumn1 = Bcolumns(1:X(2));
402         Bcolumnpeak1 = round(mean(Bcolumn1));
403         Bcolumn2 = Bcolumns((X(2)+1):end);
404         Bcolumnpeak2 = round(mean(Bcolumn2));
405     elseif size(X,1) == 3
406         Bcolumn1 = Bcolumns(1:X(2));
407         Bcolumnpeak1 = round(mean(Bcolumn1));
408         Bcolumn2 = Bcolumns(X(2)+1:X(3));
409         Bcolumnpeak2 = round(mean(Bcolumn2));
410         Bcolumn3 = Bcolumns(X(3)+1:end);
411         Bcolumnpeak3 = round(mean(Bcolumn3));
412 end
413
414 if size(Y,1) == 1
415      Bxx1 = Bcolumnpeak1;
416      Byy1 = Browpeak1;
417      figure(1)
418      x1 = radius * cos(theta) + Bxx1;
419      y1 = radius * sin(theta) + Byy1;
420      plot(x1, y1, 'Color',[1 1 1]);
421     elseif size(Y,1) == 2
422        if img(Browpeak1, Bcolumnpeak1, 3) ≥ 230
423            Bxx1 = Bcolumnpeak1;
424            Byy1 = Browpeak1;
425            Bxx2 = Bcolumnpeak2;
426            Byy2 = Browpeak2;
427        else
428            Bxx1 = Bcolumnpeak1;
429            Byy1 = Browpeak2;
430            Bxx2 = Bcolumnpeak2;
431            Byy2 = Browpeak1;
432        end
433      figure(1)
434      x1 = radius * cos(theta) + Bxx1;
435      y1 = radius * sin(theta) + Byy1;
436      x2 = radius * cos(theta) + Bxx2;
437      y2 = radius * sin(theta) + Byy2;
438      plot(x1, y1, 'Color',[1 1 1]);
439      plot(x2, y2, 'Color',[1 1 1]);
440     elseif size(Y,1) == 3
441         if img(Browpeak1, Bcolumnpeak1, 3) ≥ 230 && img(Browpeak2, Bcolumnpeak2, 3) ≥ 230
442            Bxx1 = Bcolumnpeak1;
443            Byy1 = Browpeak1;
444            Bxx2 = Bcolumnpeak2;
445            Byy2 = Browpeak2;
446            Bxx3 = Bcolumnpeak3;
447            Byy3 = Browpeak3;
448         elseif img(Browpeak1, Bcolumnpeak1, 3) ≥ 230 && img(Browpeak3, Bcolumnpeak2, ...
                3) ≥ 230
449            Bxx1 = Bcolumnpeak1;
450            Byy1 = Browpeak1;
451            Bxx2 = Bcolumnpeak2;
452            Byy2 = Browpeak3;
453            Bxx3 = Bcolumnpeak3;
454            Byy3 = Browpeak2;
455         elseif  img(Browpeak2, Bcolumnpeak1, 3) ≥ 230 && img(Browpeak1, Bcolumnpeak2, ...
                3) ≥ 230
456            Bxx1 = Bcolumnpeak1;
457            Byy1 = Browpeak2;
458            Bxx2 = Bcolumnpeak2;
459            Byy2 = Browpeak1;
460            Bxx3 = Bcolumnpeak3;
```

```
461             Byy3 = Browpeak3;
462         elseif  img(Browpeak2, Bcolumnpeak1, 3) ≥ 230 && img(Browpeak3, Bcolumnpeak2, ...
                3) ≥ 230
463             Bxx1 = Bcolumnpeak1;
464             Byy1 = Browpeak2;
465             Bxx2 = Bcolumnpeak2;
466             Byy2 = Browpeak3;
467             Bxx3 = Bcolumnpeak3;
468             Byy3 = Browpeak1;
469         elseif  img(Browpeak3, Bcolumnpeak1, 3) ≥ 230 && img(Browpeak1, Bcolumnpeak2, ...
                3) ≥ 230
470             Bxx1 = Bcolumnpeak1;
471             Byy1 = Browpeak3;
472             Bxx2 = Bcolumnpeak2;
473             Byy2 = Browpeak1;
474             Bxx3 = Bcolumnpeak3;
475             Byy3 = Browpeak2;
476         else
477             Bxx1 = Bcolumnpeak1;
478             Byy1 = Browpeak3;
479             Bxx2 = Bcolumnpeak2;
480             Byy2 = Browpeak2;
481             Bxx3 = Bcolumnpeak3;
482             Byy3 = Browpeak1;
483         end
484       figure(1)
485       x1 = radius * cos(theta) + Bxx1;
486       y1 = radius * sin(theta) + Byy1;
487       x2 = radius * cos(theta) + Bxx2;
488       y2 = radius * sin(theta) + Byy2;
489       x3 = radius * cos(theta) + Bxx3;
490       y3 = radius * sin(theta) + Byy3;
491       plot(x1, y1, 'Color',[1 1 1]);
492       plot(x2, y2, 'Color',[1 1 1]);
493       plot(x3, y3, 'Color',[1 1 1]);
494 end
495
496 %% Compute centreposition receiving fibre
497 R = [Rxx1, Ryy1];
498 G = [Gxx1, Gyy1];
499 B = [Bxx1, Byy1];
500
501 Check1 = sqrt(imabsdiff(Rxx1,Gxx1)^2+imabsdiff(Ryy1,Gyy1)^2);
502 Check2 = sqrt(imabsdiff(Rxx1,Bxx1)^2+imabsdiff(Ryy1,Byy1)^2);
503 Check3 = sqrt(imabsdiff(Gxx1,Bxx1)^2+imabsdiff(Gyy1,Byy1)^2);
504
505 Distance = mean([Check1; Check2; Check3]);
506 Scale_1mm = Distance/10;
507 Scale_1pix = 10/Distance;
508
509 Mid1 = [imabsdiff(Rxx1,Gxx1)/2+min([Rxx1,Gxx1]), ...
        imabsdiff(Ryy1,Gyy1)/2+min([Ryy1,Gyy1])];
510 Mid2 = [imabsdiff(Rxx1,Bxx1)/2+min([Rxx1,Bxx1]), ...
        imabsdiff(Ryy1,Byy1)/2+min([Ryy1,Byy1])];
511 Mid3 = [imabsdiff(Gxx1,Bxx1)/2+min([Gxx1,Bxx1]), ...
        imabsdiff(Gyy1,Byy1)/2+min([Gyy1,Byy1])];
512
513 Midpoint1 = [Mid1(:,1)+(Bxx1-Mid1(:,1))/3, Mid1(:,2)+(Byy1-Mid1(:,2))/3];
514 Midpoint2 = [Mid2(:,1)+(Gxx1-Mid2(:,1))/3, Mid2(:,2)+(Gyy1-Mid2(:,2))/3];
515 Midpoint3 = [Mid3(:,1)+(Rxx1-Mid3(:,1))/3, Mid3(:,2)+(Ryy1-Mid3(:,2))/3];
516
517 Measurepoint_x = radius/2 * cos(theta) + Midpoint1(:,1);
518 Measurepoint_y = radius/2 * sin(theta) + Midpoint1(:,2);
519
520 figure(1)
521 hold on
522 plot(Measurepoint_x, Measurepoint_y, 'Color',[1 1 1])
523 plot([Rxx1 Gxx1], [Ryy1 Gyy1], 'Color', [1 1 1])
524 plot([Rxx1 Bxx1], [Ryy1 Byy1], 'Color', [1 1 1])
525 plot([Gxx1 Bxx1], [Gyy1 Byy1], 'Color', [1 1 1])
```

B.2. Chapter 6

B.2.1. Making RGB graphs from diffuser pictures

```
%% Making RGB graphs from the different diffusers
clc
clear all
close all

%% Begin making figure
% Read the image
img = imread('.jpg');             % Insert picture file between brackets

R = [688, 965];
G = [425, 812];
B = [425, 1122];
Mid = [513, 966];

Mid_rows = 503:1:523;
Mid_colums = 956:1:976;

imgR = img(R(1,1), R(1,2), :);
imgG = img(G(1,1), G(1,2), :);
imgB = img(B(1,1), B(1,2), :);
imgMid = img(Mid_rows, Mid_colums, :);
R_value = round(mean(imgMid(:,:,1),'all'));
G_value = round(mean(imgMid(:,:,2),'all'));
B_value = round(mean(imgMid(:,:,3),'all'));

xr = [G(1,2) B(1,2)];
yr = [R(1,1) R(1,1)];

%%
figure(1)
improfile(img,xr,yr)
title('Light intensity graph going through the red LED')
xlabel('Distance along profile (pixels)')
ylabel('RGB-value')
grid on
xlim([0 310])
ylim([0 300])
legend('R-value','G-value','B-value')

%%
theta = 0 : 0.01 : 2*pi;
radius = 10;
Measurepoint_rx1 = radius/2 * cos(theta) + xr(1,2);
Measurepoint_ry1 = radius/2 * sin(theta) + yr(1,2);
Measurepoint_rx2 = radius/2 * cos(theta) + xr(1,1);
Measurepoint_ry2 = radius/2 * sin(theta) + yr(1,1);

figure(2)
imshow(img)
hold on
plot(Measurepoint_rx1, Measurepoint_ry1, 'Color',[1 1 1])
plot(Measurepoint_rx2, Measurepoint_ry2, 'Color',[1 1 1])
plot(xr, yr, 'Color', [1 1 1])
```

B.3. Chapter 7

B.3.1. Computing RGB value receiving fibre location

```
%% Computing RGB value receiving fibre location
clc; clear all; close all
%% Read the images
img1 = imread('.jpg');                      % Load picture 1
img2 = imread('.jpg');                      % Load picture 2
img3 = imread('.jpg');                      % Load picture 3
img4 = imread('.jpg');                      % Load picture 4
img = (double(img1) + double(img2) ...
       + double(img3) + double(img4))/4;    % Make average picture

R = [688, 965];
G = [425, 812];
B = [425, 1122];
Mid = [513, 966];

Mid_rows = 493:1:533;                       % Take an area around the pixel
Mid_colums = 946:1:986;

imgMid = img(Mid_rows, Mid_colums, :);
R_value = round(mean(imgMid(:,:,1),'all'));
G_value = round(mean(imgMid(:,:,2),'all'));
B_value = round(mean(imgMid(:,:,3),'all'));
```

B.3.2. Making graphs of object displacement vs RGB value

```
%% Graph of displacement versus RGB values
clc; clear all; close all
%%
% 0 degree object orientation movement
x0 = [-22 -20 -18.2 -16 -14 -12.4 -10.1 -8.1 -6 -4 -2.1];
R0 = [111 111 114 113 116 112 115 110 100 73 36];
G0 = [142 140 139 140 139 141 141 140 140 137 134];
B0 = [147 142 142 141 142 142 142 143 142 138 134];

% 90 degree object orientation movement
x90 = [-22 -20 -18.2 -16 -14 -12.4 -10.1 -8.1 -6 -4 -2.1];
R90 = [111 115 120 113 119 113 113 113 113 87 57];
G90 = [142 140 140 141 138 141 141 139 135 117 84];
B90 = [147 143 142 143 139 140 139 133 120 88 59];

xi = x0(1):0.001:x0(end);
vidR=interp1(x0,R0,xi,'spline');
vidG=interp1(x0,G0,xi,'spline');
vidB=interp1(x0,B0,xi,'spline');
%%
figure(1)
plot(xi,vidR,'r')
hold on
plot(xi,vidG,'g')
plot(xi,vidB,'b')
plot(x0, R0, 'o', 'Color', [1 0 0])
plot(x0, G0, 'o', 'Color', [0 1 0])
plot(x0, B0, 'o', 'Color', [0 0 1])
xline(-8, '--', 'LineWidth', 1)
title('RGB value receiving fibre, with movement 0-degree object orientation')
xlabel('y-coordinate of the object edge (mm)')
ylabel('RGB-value')
grid on
xticks([-22:2:-2])
yticks([30:10:150])
xlim([-22 -2])
ylim([30 150])
legend('R-value','G-value','B-value', 'Location','southwest')
```

B.4. Chapter 8

B.4.1. Find receiving fibre coordinates and average RGB value

```
%% Find the receiving fibre end and the average colour emitted by the fibre end
clc
clear all
close all

%% Begin making figure
theta = 0 : 0.01 : 2*pi;
radius = 20;

% Read the image
img1 = imread('0grad_18mm_1.jpg');
img2 = imread('0grad_18mm_2.jpg');
img3 = imread('0grad_18mm_3.jpg');
img4 = imread('0grad_18mm_4.jpg');

img = (double(img1) + double(img2) + double(img3) + double(img4)) / 4;

%% Find middle fibre
% Filter the low RGB values
for c = 1:1600
    for r = 1:1200
        if img(r, c, 1) < 20
            imgR(r, c, 1) = 0;
        else
            imgR(r, c, 1) = img(r, c, 1);
        end
    end
end
imgR(:, :, 2) = 0;
imgR(:, :, 3) = 0;

% Find the unique rows and columns where in this case the R-values are located
[rows, columns] = find(imgR(:, :, 1) > 0);
rows = single(unique(rows));
columns = single(unique(columns));

for i = 1:(size(rows,1)-3)
    if rows(i+1,1)-rows(i,1) == 1 && rows(i+2,1)-rows(i,1) == 2 && ...
        rows(i+3,1)-rows(i,1) == 3
        row(i,1) = rows(i,1);
    else
        row(i,1) = 0;
    end
end

for j = 1:(size(columns,1)-3)
    if columns(j+1,1)-columns(j,1) == 1 && columns(j+2,1)-columns(j,1) == 2 && ...
        columns(j+3,1)-columns(j,1) == 3
        column(j,1) = columns(j,1);
    else
        column(j,1) = 0;
    end
end

AllRows = nonzeros(row);
AllColumns = nonzeros(column);

Mid_rows = AllRows(1+10,1):1:AllRows(end-10,1);
Mid_colums = AllColumns(1+10,1):1:AllColumns(end-10,1);

imgMid = img(Mid_rows, Mid_colums, :);
R_value = round(mean(imgMid(:,:,1),'all'));
G_value = round(mean(imgMid(:,:,2),'all'));
B_value = round(mean(imgMid(:,:,3),'all'));
```

Bibliography

[1] Fiber Optic Basics. URL https://www.newport.com/t/fiber-optic-basics.

[2] light - Total internal reflection | Britannica. URL https://www.britannica.com/science/light/Total-internal-reflection.

[3] Multimode vs. Single-mode Fibre. URL https://www.black-box.eu/en-int/page/28542/Resources/technical/Black-Box-Explains/fibre-optic-cable/multimode-vs-singlemode-fibre.

[4] Snell's law | Definition, Formula, & Facts | Britannica. URL https://www.britannica.com/science/Snells-law.

[5] Specialty Fibers for Medical Laser Systems. URL https://www.heraeus.com/en/hca/industries_and_applications_hca/medical_laser_systems/medical_laser_systems_hca.html#carousel-929131-3.

[6] The basics of microchips | ASML. URL https://www.asml.com/en/technology/all-about-microchips/microchip-basics.

[7] Tribotronics. URL https://www.tudelft.nl/3me/over/afdelingen/precision-and-microsystems-engineering-pme/research/mechatronic-system-design-msd/msd-research/tribotronics.

[8] Fraunhofer ISE. Technical report, 2014. URL http://citeseerx.ist.psu.edu/viewdoc/download?doi=10.1.1.692.880&rep=rep1&type=pdf.

[9] Plastic Optical Fiber vs. Glass Optical Fiber, 2015. URL https://www.fiberopticshare.com/plastic-optical-fiber-vs-glass-optical-fiber.html.

[10] International Technology Roadmap for Photovoltaic (ITRPV) 2015 Results Seventh Edition, March , 3 2016.

[11] Optical Fiber Tutorial - Optic Fiber - Communication Fiber – Fosco Connect, 2 2016. URL https://www.fiberoptics4sale.com/blogs/archive-posts/95146054-optical-fiber-tutorial-optic-fiber-communication-fiber.

[12] A Brief History of Fiber Optics - Muth Technology, 5 2017. URL https://www.muthtechnology.com/a-brief-history-of-fiber-optics/.

[13] Fiber optics and its applications, 5 2017. URL https://www.ukessays.com/essays/physics/fiber-optics-and-its-applications.php.

[14] Difference Between CMOS & CCD and Why CMOS Sensors Are Preferred for Machine Vision Cameras | Machine Vision Blog, 12 2019. URL https://www.phase1vision.com/blog/difference-between-cmos-and-ccd.

[15] Photovoltaic Equipment International Technology Roadmap for Photovoltaic (ITRPV) 2019 Results. 2019.

[16] Single Mode vs. Multimode Fiber Optic Cables - Cleerline SSF Fiber, 3 2019. URL https://cleerlinefiber.com/2019/03/19/singlemode-vs-multimode-fiber-optic-cables/.

[17] Satish Addanki, I. S. Amiri, and P. Yupapin. Review of optical fibers-introduction and applications in fiber lasers. *Results in Physics*, 10:743–750, 9 2018. ISSN 2211-3797. doi: 10.1016/J.RINP.2018.07.028.

[18] Lucio Claudio Andreani, Angelo Bozzola, Piotr Kowalczewski, Marco Liscidini, and Lisa Redorici. Silicon solar cells: toward the efficiency limits. *https://doi.org/10.1080/23746149.2018.1548305*, 4(1):1548305, 1 2018. ISSN 23746149. doi: 10.1080/23746149.2018.1548305. URL https://www.tandfonline.com/doi/abs/10.1080/23746149.2018.1548305.

[19] Svetlana Avramov-Zamurovic, Jae Myung Yoo, and Nicholas G Dagalakis. Capacitive displacement sensor for detecting planar submicrometer motion. *Review of Scientific Instruments*, 87:65001, 2016. doi: 10.1063/1.4952585. URL http://dx.doi.org/10.1063/1.4952585http://scitation.aip.org/content/aip/journal/rsi/87/6?ver=pdfcov.

[20] Monika Bahl. Structured Light Fields in Optical Fibers. *Fiber Optics - From Fundamentals to Industrial Applications*, 9 2019. doi: 10.5772/INTECHOPEN.85958.

[21] Johannes Bernreuter. Polysilicon Price: Chart, Forecast, History | Bernreuter Research, 2021. URL https://www.bernreuter.com/polysilicon/price-trend/.

[22] Xavier F. Brun and Shreyes N. Melkote. Analysis of stresses and breakage of crystalline silicon wafers during handling and transport. *Solar Energy Materials and Solar Cells*, 93(8):1238–1247, 8 2009. ISSN 0927-0248. doi: 10.1016/J.SOLMAT.2009.01.016.

[23] Roderick Burnett. Understanding How Ultrasonic Sensors Work , 3 2020. URL https://www.maxbotix.com/articles/how-ultrasonic-sensors-work.htm.

[24] Stephen Carey, D Martin Knotter, Eric Ooms, Johannes Boersma, Elfried Van Der Sar, Robbert Cop, Wim Gerritzen, Hans Van Zadelhoff, and Henk Bouma. Yield Impact of Backside Metal-ion contamination. 2012. doi: 10.4028/www.scientific.net/SSP.187.287. URL www.scientific.net.

[25] Tyler Cooper. Fiber-Optic Internet in the United States, 9 2020. URL https://broadbandnow.com/Fiber.

[26] Bassem Dahroug, Guillaume J. Laurent, Valérian Guelpa, and Nadine Le Fort-Piat. Design, modeling and control of a modular contactless wafer handling system. *Proceedings - IEEE International Conference on Robotics and Automation*, 2015-June(June):976–981, 6 2015. doi: 10.1109/ICRA.2015.7139295.

[27] J. Elfferich, F. van Melis, T. Neeft, and A. Tiktak. *The simulation and design of a one-sided distributed optical sensor for wafer tracking (BSc thesis)*. 2019.

[28] Zachary Favors, Wei Wang, Hamed Hosseini Bay, Zafer Mutlu, Kazi Ahmed, Chueh Liu, Mihrimah Ozkan, and Cengiz S. Ozkan. Scalable Synthesis of Nano-Silicon from Beach Sand for Long Cycle Life Li-ion Batteries. *Scientific Reports 2014 4:1*, 4(1):1–7, 7 2014. ISSN 2045-2322. doi: 10.1038/srep05623. URL https://www.nature.com/articles/srep05623.

[29] Craig Freudenrich. Physics of Total Internal Reflection - How Fiber Optics Work | HowStuffWorks. URL https://computer.howstuffworks.com/fiber-optic6.htm.

[30] Arnout Fritz. *Distributed optical sensor surface concept for planar object detection: Using optical fibers as a vision distributor (MSc thesis)*. 2021.

[31] RJ Hagler and Carolyn Guzik. Optical Fiber Technology: When to Choose Glass vs. Plastic Fiber, 12 2018. URL https://www.lumitex.com/blog/optical-fiber-technology.

[32] Jeff Hecht. *Optics : light for a new age*. Scribner, New York, 1st ed. edition, 1987. ISBN 9780684188799.

[33] Rico Hooijschuur, Niranjan Saikumar, S Hassan Hosseinnia, Ron A J Van Ostayen, Terenziano Raparelli, Federico Colombo, Andrea Trivella, and Luigi Lentini. Air-Based Contactless Wafer Precision Positioning System. *Applied Sciences 2021, Vol. 11, Page 7588*, 11(16):7588, 8 2021. ISSN 20763417. doi: 10.3390/APP11167588. URL https://www.mdpi.com/2076-3417/11/16/7588/htmhttps://www.mdpi.com/2076-3417/11/16/7588.

[34] Jingang Hu, Yuming Zhou, Man He, and Xiaoming Yang. Novel multifunctional microspheres of polysiloxane@CeO2-PMMA: Optical properties and their application in optical diffusers. *Optical Materials*, 36(2):271–277, 2013. ISSN 09253467. doi: 10.1016/J.OPTMAT.2013.09.007. URL http://dx.doi.org/10.1016/j.optmat.2013.09.007.

[35] Jingang Hu, Yuming Zhou, and Tao Zhang. The novel optical diffusers based on the fillers of boehmite hollow microspheres. *Materials Letters*, 136:114–117, 12 2014. ISSN 0167577X. doi: 10.1016/J.MATLET.2014.08.018. URL http://dx.doi.org/10.1016/j.matlet.2014.08.018.

[36] Jingang Hu, Yuming Zhou, and Xiaoli Sheng. Optical diffusers with enhanced properties based on novel polysiloxane@CeO2@PMMA fillers. *Journal of Materials Chemistry C*, 3(10):2223–2230, 2 2015. ISSN 2050-7534. doi: 10.1039/C4TC02287D. URL https://pubs.rsc.org/en/content/articlehtml/2015/tc/c4tc02287dhttps://pubs.rsc.org/en/content/articlelanding/2015/tc/c4tc02287d.

[37] Jingang Hu, Yuming Zhou, Muhua Wang, Minghua Yang, and Guobing Yan. Optical diffusers based on the novel fillers of polysiloxane@boehmite core–shell microspheres. *Materials Letters*, 165:107–110, 2 2016. ISSN 0167-577X. doi: 10.1016/J.MATLET.2015.11.121.

[38] Len Jelinek. Global Semiconductor Market Trends Opportunities and Challenges Facing the Semiconductor Industry. 2018.

[39] Len Jelinek, Chief Analyst, and Chris Welch. TECHNOLOGY, MEDIA & TELECOMMUNICATION ABSTRACT Semiconductor Silicon Demand Forecast Tool. 2020.

[40] Pawan Kalyani. An Empirical Study on Internet to Home Through Optical Fibre in Indian Internet Service Provider Market with Special Reference to Customer Switching Pattern with the Introduction of Reliance Jio "GigaFiber" and other Players like BSNL, Airtel,Tata Sky Broadband etc. 10 2019. doi: 10.5281/zenodo.3523848.

[41] C. Langens, C. Petsch, D. Robijns, and M. Wiersma. *Wafer tracking using an integrated and distributed system (BSc thesis)*. 2018.

[42] Alex Milne. Multi-Mode vs. Single-Mode Fiber-Optic Cable: Debates and Differences. URL https://www.rfvenue.com/blog/2016/03/16/multi-mode-vs-single-mode.

[43] Manish Pandey and Gaurav Mishra. Types of Sensor and Their Applications, Advantages, and Disadvantages. *Advances in Intelligent Systems and Computing*, 814:791–804, 2019. ISSN 21945357. doi: 10.1007/978-981-13-1501-5{_}69. URL https://link.springer.com/chapter/10.1007/978-981-13-1501-5_69.

[44] Hyoung Ghi Park and Dahl Young Khang. High-performance light diffuser films by hierarchical buckling-based surface texturing combined with internal pores generated from physical gelation induced phase separation of binary polymer solution. *Polymer*, 99:1–6, 9 2016. ISSN 00323861. doi: 10.1016/j.polymer.2016.06.060.

[45] Courtney Peterson. JYI Issue Three Features: Charged-Coupled Devices (CCDs). URL http://www.if.ufrgs.br/~marcia/ccd.html.

[46] Kees Pijnenburg. *Development of a novel manufacturing method for a contactless handling system using a variable outlet restriction (MSc Thesis)*. 2022. URL https://repository.tudelft.nl/islandora/object/uuid:ec02b866-79c4-417b-8d32-50323a262e9f?collection=education.

[47] Paul Polishuk. Plastic optical fibers branch out. *IEEE Communications Magazine*, 44(9):140–148, 9 2006. ISSN 01636804. doi: 10.1109/MCOM.2006.1705991.

[48] P.J. Ribeyron, C. Roux, J. Gaume, J.P. Rakotoniaina, D. Muñoz, A. Danel, O. Nos, and S. Harrison. How to Deal with Thin Wafers in a Heterojunction Solar Cells Industrial Pilot Line: First Analysis of the Integration of Cells Down to 70µm Thick in Production Mode. *32nd European Photovoltaic Solar Energy Conference and Exhibition*, pages 358–362, 7 2016. doi: 10.4229/EUPVSEC20162016-2BO.9.2. URL http://www.eupvsec-proceedings.com/proceedings?paper=37461.

[49] Hannah Ritchie and Max Roser. Energy Production and Consumption, 2020. URL https://ourworldindata.org/energy-production-consumption.

[50] Jelle Snieder. *Development of an Air-Based Contactless Transport Demonstrator (MSc thesis)*. Delft, 2017. URL https://repository.tudelft.nl/islandora/object/uuid%3A870adc6e-2f78-468c-a6c2-079eaec49226?collection=education.

[51] W. Suthabanditpong, M. Tani, C. Takai, M. Fuji, R. Buntem, and T. Shirai. Facile fabrication of light diffuser films based on hollow silica nanoparticles as fillers. *Advanced Powder Technology*, 27(2):454–460, 3 2016. ISSN 0921-8831. doi: 10.1016/J.APT.2016.01.028.

[52] T. ter Horst, J. Kuijper, V. Tsan, and A. Versluis. *Levitating wafer tracking using an integrated sensor system (BSc thesis)*. 2017.

[53] Ash Turner. How Many People Have Smartphones Worldwide (Dec 2021). URL https://www.bankmycell.com/blog/how-many-phones-are-in-the-world.

[54] J. van Rij, J. Wesselingh, R. A.J. van Ostayen, J. W. Spronck, R. H. Munnig Schmidt, and J. van Eijk. Planar wafer transport and positioning on an air film using a viscous traction principle. *Tribology International*, 42(11-12):1542–1549, 12 2009. ISSN 0301-679X. doi: 10.1016/J.TRIBOINT.2009.03.013.

[55] Vincent Vandaele, Pierre Lambert, and Alain Delchambre. Non-contact handling in microassembly: Acoustical levitation. *Precision Engineering*, 29(4):491–505, 10 2005. ISSN 0141-6359. doi: 10.1016/J.PRECISIONENG.2005.03.003.

[56] Yvonne Voorrips. *The design of a distributed sensing system for contactless substrate transport (MSc thesis)*. 2017.

[57] H.P. Vuong. Air-based contactless actuation system for thin substrates: The concept of using a controlled deformable surface (PhD thesis). 2016. doi: 10.4233/UUID:2D375F1B-3857-4C03-87E8-CB0FC45F3F13. URL https://repository.tudelft.nl/islandora/object/uuid%3A2d375f1b-3857-4c03-87e8-cb0fc45f3f13.

[58] Joseba Zubia and Jon Arrue. Plastic Optical Fibers: An Introduction to Their Technological Processes and Applications. *Optical Fiber Technology*, 7(2):101–140, 4 2001. ISSN 1068-5200. doi: 10.1006/OFTE.2000.0355.